AUTOMATED RAPID PARTICLE INVESTIGATION USING SCANNING ELECTRON MICROSCOPY

By

JEROD LAURENCE WILKINS

Bachelor of Science in Civil Engineering

Oklahoma State University

Stillwater, Oklahoma

2011

Submitted to the Faculty of the
Graduate College of the
Oklahoma State University
in partial fulfillment of
the requirements for
the Degree of
MASTER OF SCIENCE
December, 2013

AUTOMATED RAPID PARTICLE INVESTIGATION

USING SCANNING ELECTRON MICROSCOPY

Thesis Approved:

Dr. Tyler Ley

Thesis Adviser

Dr. Bruce Russell

Dr. Stephen Cross

ACKNOWLEDGEMENTS

My advisor, Dr. Tyler Ley, deserves my unconditional gratitude for his support, encouragement, wisdom, and guidance. His passion and knowledge in the field of Civil Engineering is the source of my inspiration to forever learn and grow as a Civil Engineer. His teachings far exceed that of the class room as he has set an example for what one can achieve through hard work.

I am forever grateful to have had the support of such a knowledgeable research team. Mohammed Aboustait and Qinang Hu were always willing to provide support in the areas of their expertise. Their actions were truly selfless and their friendship will never be forgotten.

I would like to thank my mother, father, brother, and sister for their continuous words of encouragement. When times were stressful they were always there to lift my spirits. My wife and daughter, Britney and Breanna, deserve my most heartfelt gratitude as they were continuously understanding and supportive. My wife spent many hours waiting on my return from work and school and always welcomed me home with love. My one year old daughter never ceased to remind me of the most important things in this life……..God, family, and love.

Name: JEROD WILKINS

Date of Degree: DECEMBER, 2013

Title of Study: AUTOMATED RAPID PARTICLE INVESTIGATION USING SCANNING ELECTRON MICROSCOPY

Major Field: CIVIL ENGINEERING

Abstract: The chemical composition of fly ash particles has been known to vary significantly depending on a number of factors. Current bulk methods of investigation including X-Ray Fluorescence and X-Ray Diffraction are thought to be inadequate in determining the performance of fly ash in concrete. It is the goal of this research to develop a method of Automated Rapid Particle Investigation that will not look at fly ash as a bulk material but as individual particles. By examining each particle individually scientists and engineers will have the ability to study the variation in chemical composition by comparing the chemistry present in each particle. The method of investigation developed by this research provides a practical technique that will allow the automated chemical analysis of hundreds, or even thousands, of fly ash particles in a matter of minutes upon completion of sample preparation and automated scanning electron microscope (ASEM) scanning. This research does not examine the significance of the chemical compounds discovered; rather, only the investigation methodology is discussed. Further research will be done to examine the importance of the chemistry discovered with this automated rapid particle investigation technique.

TABLE OF CONTENTS

LIST OF TABLES

Table Page

LIST OF FIGURES

Figure Page

CHAPTER I

INTRODUCTION

CONCRETE

Concrete is the most widely used construction material in the world due to its durability, versatility, availability, and economy (Kosmatka, Kerkhoff, & Panarese, 2008) (Mehta & Monteiro, 2006). It is estimated that the present annual consumption of concrete in the world is around 11 billion metric tons (Mehta & Monteiro, 2006). Concrete is neither as strong nor as tough as steel but is still the most widely used material for construction. Three primary reasons concrete is chosen over steel include its resistance to water, the ability to mold plastic concrete into desired shapes, and its relatively low cost and high availability (Mehta & Monteiro, 2006). Although concrete has proven to be an excellent construction material its abundant use has raised a concern. The major concern with the high volume of use of concrete is the impact that the production of portland cement, the primary binder in concrete, has on the environment.

ENVIRONMENTAL CONCERNS

Portland cement is manufactured by introducing materials containing calcium and silica into a rotary kiln where these ingredients are burned at temperatures reaching approximately 1500°C (Mehta & Monteiro, 2006). During this burning within the kiln the chemical reactions involved in the formation of clinker, the primary component in the production of portland cement, are completed. Once the clinker has been produced it is pulverized into a fine powder and a small

amount of gypsum is mixed with the pulverized clinker resulting in the production of portland cement. The production of clinker is said to generate approximately 7% of the world's total carbon dioxide emissions (Malhotra, 2001) (Mehta & Monteiro, 2006). If the demand for portland cement could be reduced then the negative effects that its production has on the environment could also be reduced. The use of supplementary cementing materials (SCM) has shown to be an excellent alternative to portland cement in concrete and are commonly used to decrease the demand for portland cement.

FLY ASH AS A SCM

Fly ash is presently one of the most common SCMs used in concrete due to its satisfactory performance in many applications. Depending on the class of fly ash used it will exhibit either pozzolanic (ASTM C618 Class F) or pozzolanic and self-cementing (ASTM C618 Class C) properties and contribute to the strength and many other properties of concrete (Thomas, 2007). A self-cementing material requires only water to produce cementitious hydration product where as a pozzolanic material requires water and calcium hydroxide to produce cementitious hydration product; therefore, when fly ash is mixed with portland cement and water it will produce calcium silica hydrate which is the primary binding reaction product in concrete (Helmuth, 1987) (Malhotra & Ramezanianpour, 1994).

Fly ash is a byproduct of the combustion of coal in coal-fired power plants and when used in unison with portland cement can improve many of the properties of concrete including strength and resistance towards aggressive chemicals (Kosmatka et al., 2008) (Malhotra, 2004) (Thomas, 2007). When pulverized coal is burned there is a certain amount of incombustible matter in the coal (Malhotra & Ramezanianpour, 1994). This incombustible matter cools and forms spherical glass particles known as fly ash that are collected in dust collection systems (Helmuth, 1987) (Malhotra & Ramezanianpour, 1994). By utilizing byproducts, such as fly ash,

in construction materials the amount of waste being disposed of in landfills can be reduced, however; since fly ash is a byproduct of another process it is often inconsistent in its chemical phases and produces variable performance in concrete (Helmuth, 1987) (Malhotra, 1989).

According to the American Coal Ash Association's "Production and Use Survey" only 43.50% of the 130.1 million tons of coal ash produced in 2011 was beneficially used. The substitution level of fly ash for portland cement in concrete is often limited to 20% since it is a byproduct of burning coal and shows variable performance in concrete (Hu et al., 2013). If fly ash was better understood then the demand for clinker, CO_2 emissions, and the cost of concrete could be reduced by replacing larger portions of portland cement with fly ash to alter the performance of concrete (Malhotra, 2004).

Over the years there have been persistent problems concerning the variability of fly ash and the difficulty of characterizing it for predictable performance in concrete (Helmuth, 1987). Despite the extensive research and literature on the chemical properties of concrete made with cement and fly ash the essential chemistry and physics of these systems are not well defined (Helmuth, 1987). There are current procedures for classifying fly ash as related to its bulk chemical composition, but these techniques are unable to determine what chemical phases are present within an individual fly ash particle (Malhotra, 1989). This information could have a significant impact on the performance of concrete. The development of an improved investigation technique that will rapidly characterize individual fly ash particles will be the focus of this research.

RESEARCH OBJECTIVE

The research presented in this paper focuses on a technique of rapid fly ash particle characterization. **A**utomated **S**canning **E**lectron **M**icroscopy or **ASEM** was used in unison with **Segmented EDS** and **image analysis** to create a method of rapid particle investigation. ASEM

uses a laboratory SEM that has an image analysis based operating system built into the microscope. This allows the user to program the microscope to find areas with certain characteristics and complete a more detailed analysis. This technique can analyze numerous particles in one scan and gather useful information. The challenge with this method is that the actual phase distribution of a fly ash particle is still unknown to researchers. This causes the information that ASEM provides to be somewhat difficult to interpret. However, if ASEM and Segmented EDS Analysis are both used on a single particle to create chemical phase thresholds it becomes possible to use the information gathered by ASEM to directly evaluate the particles of interest.

The goal of this research is to provide improved methods of chemical investigation and analysis to identify certain key chemical phases within fly ash so that they may be properly classified and their impact on the performance of concrete be quantified. This would further reduce the demand for clinker and contribute to the efforts of creating a more environmentally safe construction and engineering industry while also creating a more economical construction material. Previous research on Segmented EDS Analysis was conducted at the National Institute of Standards and Technology (NIST) and the results from that research are used in the development of this rapid investigation technique.

CHAPTER II

RESEARCH SIGNIFICANCE

CURRENT INVESTIGATION TECHNIQUES

The chemical composition of fly ash particles is commonly determined through bulk chemical analysis such as X-ray fluorescence (XRF) or X-ray diffraction (XRD) (Helmuth, 1987) (Malhotra & Ramezanianpour, 1994). When using these techniques the fly ash material under investigation is usually ground into a fine powder and made into a bulk sample by placing a certain amount of the material into a pellet or some sort of mold (ASTM C114). These methods reveal the bulk chemical composition present in the sample under investigation but do not give any insight into the characteristics of individual particles. In fact, the current testing and specifications used to classify fly ash do not predict the performance of fly ash with hydraulic cement in concrete (ASTM C618). The need for further research for improved characterization of fly ashes for use in concrete is widely recognized, but there is less agreement on what needs to be done (Helmuth, 1987). There is a special need for rapid test methods that can be used with confidence to predict long-term performance of fly ash in concrete (Helmuth, 1987).

AUTOMATED RAPID PARTICLE INVESTIGATION

The method developed by the research discussed in this paper uses artificial intelligence and mathematical modeling to identify fly ash particles of interest and analyze the individual particles through automated techniques. This technique will be referred to as Automated Rapid

Particle Investigation (ARPI). Upon completion of the initial sample preparation and Automated Scanning Electron Microsope (ASEM) scan hundreds, or even thousands, of particles can be analyzed by an image analysis program developed in this research. With the use of this image analysis program the individual chemical composition of these particles will become known in a matter of minutes. Automated Rapid Particle Investigation is intended to rapidly gather as much useable information concerning individual fly ash particles as possible.

There is a current procedure for investigating individual fly ash particles known as **T**omography **A**ssisted **C**hemical **Co**rrelation (TACCo) but this technique is able to examine just one particle per analysis and each analysis requires a significant amount of time to complete. TACCo is able to show three dimensional chemical composition of an individual fly ash particle in detail. Although Automated Rapid Particle Investigation only provides two dimensional data, the quantity of data gathered is increased significantly when compared with TACCo.

Automated Rapid Particle Investigation is intended to significantly increase the number of particles investigated per analysis while decreasing the analysis time. The data gathered using this technique is intended to be used to aid in the effectiveness of fly ash as a supplementary cementing material. The benefits of using fly ash in concrete mixtures as a SCM are often significant from a strength, durability, and construction perspective; however, one must be aware that not all of the effects of using fly ash in concrete mixtures are positive. It is the goal of this research to present a rapid method of particle investigation that will produce useable data concerning fly ash so that a better understanding of fly ash can be achieved and higher substitution levels can be used in concrete mixtures.

CHAPTER III

FLY ASH INVESTIGATION TECHNIQUES

CURRENT ASTM SPECIFICATIONS

It is widely recognized that there is a need for further research to improve characterization techniques for fly ash used in concrete. As mentioned previously the current techniques for investigating fly ash give no insight into the chemical composition of individual particles; rather, only a bulk chemical analysis is performed. X-ray fluorescence has been used to classify fly ash into two categories, Class C or Class F, depending on the percentage of silica, aluminum, and iron oxide present in the ash (ASTM C618). This classification technique is commonly thought to provide an incomplete description of the potential effects fly ash will have on fresh and hardened concrete (Malhotra & Ramezanianpour, 1994).

The American Society for Testing and Materials (ASTM), Committee C09, has developed ASTM C618 which specifies chemical and physical properties for classifying fly ash as either Class C or Class F ash. ASTM C618 examines the bulk oxide content of the ash under investigation. The use of XRF is widely used to examine the bulk oxide content of fly ash. ASTM C618 defines Class C fly ash as having a sum of SiO_2, Al_2O_3, and Fe_2O_3 contents equal to or greater than 50% and Class F fly ash as having a sum of SiO_2, Al_2O_3, and Fe_2O_3 contents equal to or greater than 70%. Class C and Class F fly ash must contain 5% or less of SO_3 and 1.5% or less of available alkalis. This classification technique has been believed to

inadequately describe the potential effects that fly ash will have on concrete (Malhotra & Ramezanianpour, 1994). .

PREVIOUS WORK ON FLY ASH INVESTIGATION

In an effort to advance the understanding of the chemical compounds present in fly ash and to refine microanalysis techniques Ryan Chancey, of the University of Texas, explored a new investigation technique. In Chancey's research x-ray diffraction, scanning electron microscopy (SEM), energy-dispersive spectroscopy (EDS), and multispectral image analysis (MSIA) were used to accurately characterize the crystalline and amorphous compounds present in fly ash. In this technique of investigation the fly ash being examined was investigated as a bulk sample. This technique did not examine the properties of individual fly ash particles.

X-ray diffraction was used in Chancey's research to quantitatively and qualitatively classify the crystalline phases present in fly ash. When x-rays pass through a sample the radiation is scattered by the interaction with the atoms that are present in the sample. The ordered structure of a crystal produces a scattered pattern that is characteristic to the phases present in the sample under investigation. Rietveld quantitative x-ray diffraction (RQXRD) was used to quantify the chemical phases present in the sample through a least square curve fitting procedure. The quantitative analysis of crystal phases in the sample required lengthy scan times due to the high amorphous phase composition of the fly ash.

Scanning electron microscopy (SEM), energy-dispersive spectroscopy (EDS), and multispectral image analysis (MSIA) techniques were used in the qualitative and quantitative analysis of amorphous phases present in fly ash. Raw elemental maps were created of bulk samples through the use of the SEM/EDS system. Each elemental map was processed and then different maps were overlaid through the use of MSIA, three at a time using red, green, and blue to represent three different elements. Each resulting color in the overlaid image was determined

to be a phase containing each element in the raw map. For example if a particle contained orange then it would be comprised of green and blue and would therefore be a phase containing whatever elements were assigned these colors in their raw elemental map. This technique is called multispectral overlaying. Once this MSIA technique is completed the resulting overlaid images are inspected and a rough estimate of the phases present are determined and used in the MultiSpec program to iteratively calculate the number of individual phases present in the sample. EDS was used to investigate the composition of these phases. Following qualitative analysis of the amorphous phases the quantity of these phases were investigated using a clustering analysis function of MultiSpec. Each pixel in the multispectral overlaid image was assigned to a phase and the relative proportions of each phase were determined.

This technique provided useful information regarding the qualitative and quantitative properties of fly ash; however, it proved to be a fairly complex and time consuming process. The qualitative analysis of crystalline phases was perhaps the only straight forward procedure in this analysis technique. The quantitative analysis of crystalline phases as well as the qualitative and quantitative analysis of amorphous phases showed to be subject to procedural details and analytical assumptions (Chancey, 2008).

TACCo

Research was conducted at Oklahoma State University and a novel technique of chemical investigation of fly ash particles was developed. This technique, known as Tomography Assisted Chemical Correlation (TACCo), is a method of chemical investigation that fuses the 3D results from a micro X-ray computed tomography (CT) scan with 2D electron probe microanalysis (EPMA) to create three dimensional chemical maps of particles (Hu et al., 2013). The research showed that accurate and repeatable results are obtained when using this technique (Hu et al., 2013).

In order to produce 3D chemical maps of particles using TACCo an individual particle must me embedded in epoxy and scanned using μCT (Figure 1a). Once a 3D scan has been obtained from μCT the sample is polished so that a cross section of the particle is exposed (Figure 1b). The polished section is then investigated by EPMA and the results are processed using an unsupervised clustering analysis known as ISO Means to reveal the distinct constituents of the cross-section (Figure 1c). These distinct constituents are represented through color segmentation. Next an algorithm is used to find the matching section of the particle in the 3D μCT data (Figure 1d & 1e). The matching section found from running the algorithm on the μCT data is then compared to the same section from EPMA and a correlation in made that allows the user to determine what gray scale values represent the different chemical constituent of the section (Figure 1f). Once the gray scale thresholds for each chemical phase have been determined the data from μCT can be used with these thresholds to determine the 3D distribution of chemical phases in the particle (Figure 2). Each color in Figure 2 represents a different chemical phase.

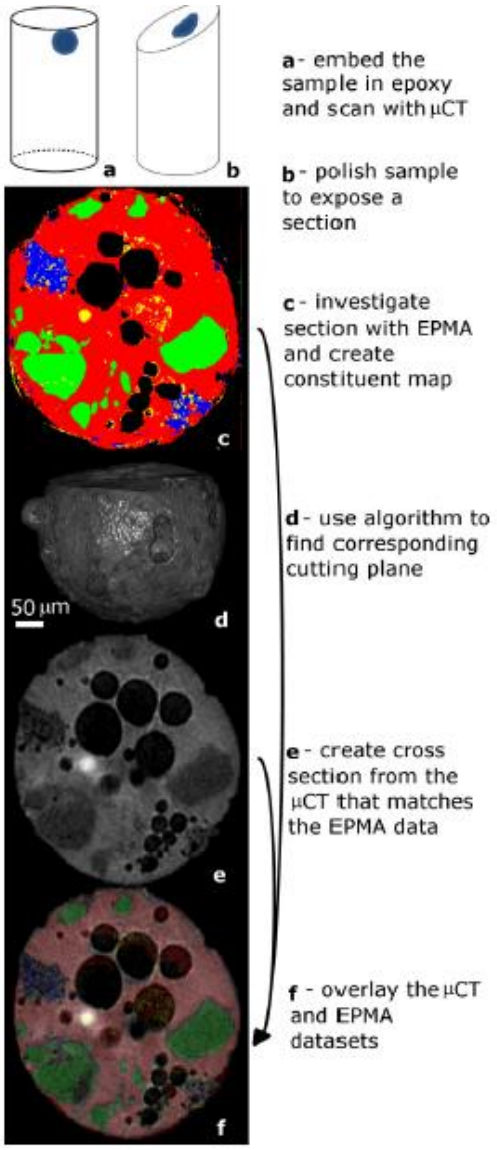

Figure 4: Process of fusing microCT with EPMA data in TACCo (Hu et al., 2013).

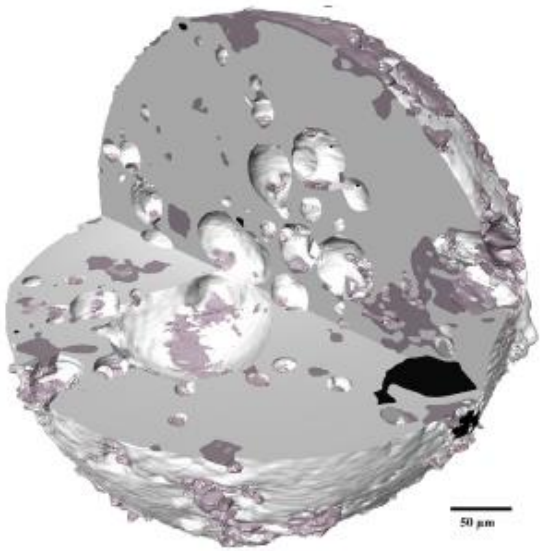

Figure 5: 3D chemical map of a fly ash particle using TACCo (Hu et al., 2013).

TACCo has shown to produce accurate and repeatable results that give insight into the chemical phases present and their distribution in fly ash particles. It is without question that TACCo is a powerful technique and has the potential to revolutionize the way particles are investigated; however, it requires a significant amount of manual analysis and time to produces one 3D chemical map. Since the variability of the properties of fly ash depends on a number of factors it is necessary to investigate the properties of fly ash frequently for the use in concrete mixtures. A rapid technique that requires less manual analysis time is the goal of this research.

CHAPTER IV

SCANNING ELECTRON MICROSCOPY, AFA, AND SEGMENTED EDS ANALYSIS

SCANNING ELECTRON MICROSCOPY

In the development of Automated Rapid Particle Investigation information from a scanning electron microscope (SEM) is used in unison with information from Segmented EDS Analysis to rapidly reveal the primary constituents of the particles under investigation. A SEM permits the observation of the topographic and chemical features of materials on a nanometer to micrometer scale through the use of gray-scale images (Goldstein et al., 2003). In a SEM the area of interest on a sample is bombarded with a finely focused electron beam. This bombardment results is a variety of signals emitting from the sample including backscattered electrons, secondary electrons, characteristic x-rays, and other photons of various energies. These signals can be analyzed and many of the characteristics of the sample can be determined. The SEM is composed of an electron gun, lenses, detectors, sample stage, and a control console. The majority of these components will be briefly described in this chapter.

The electron gun provides a stable electron beam of variable energy (Goldstein et al., 2003). Figure 3 shows a schematic of a conventional thermionic tungsten electron gun. The electron gun consists of a tungsten filament, grid cap, and anode. The tungsten filament serves as the cathode (negative electrode) and when heated resistively by a current will produce thermionic

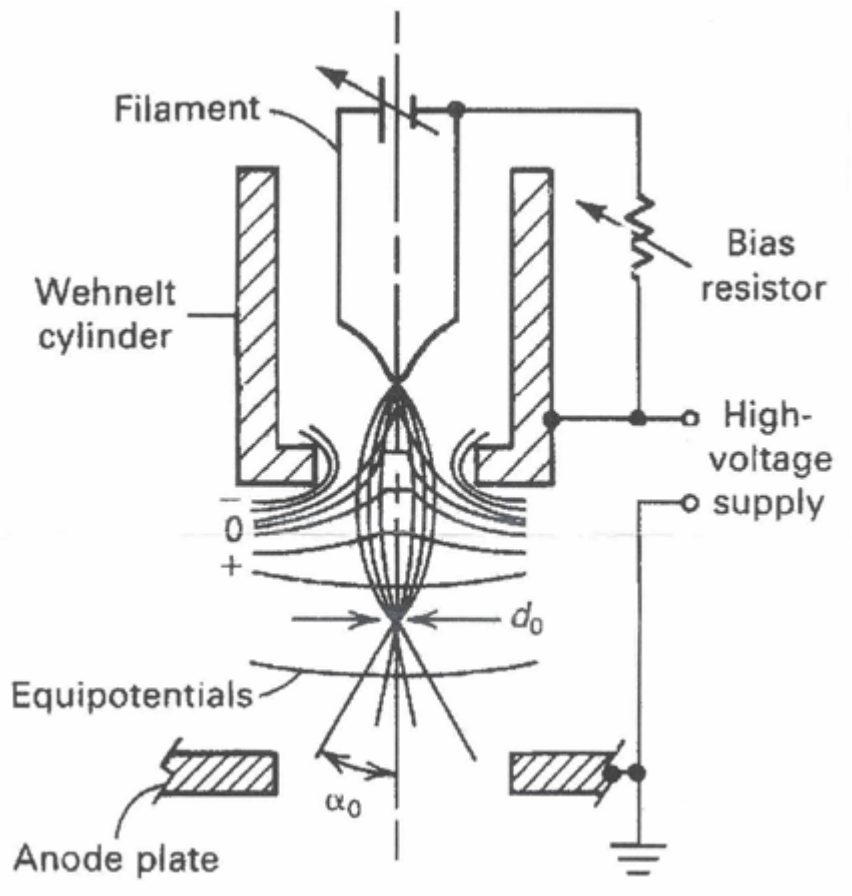

Figure 6: Tungsten Filament Electron Gun.

electron emissions. The grid cap is set to a voltage slightly more negative than the filament which causes a focusing effect of the electron beam (Goldstein et al., 2003). The anode, which is at ground potential, accelerates the electrons leaving the high negative potential filament.

As the electron beam passes through the grid cap in the electron gun the electrons are forced to a crossover diameter, $d_{0,}$ of approximately 50 µm. The electron beam passes through the anode and travels down a column containing lenses that act to focus the electrons on their path to the sample. The condenser and objective lenses act to demagnify the crossover diameter to

a final spot size of approximately 10 nm in diameter on the specimen (Goldstein et al., 2003). These lenses consist of an iron case enclosing a coil wire and when a current is passed through this coil an electromagnetic field is created. This field acts to focus off-axis electrons towards the optic axis. In a typical SEM column there are usually one to three condenser lenses and a final objective lens. The condenser lens works to demagnify the beam as it travels through the column and the objective lens (the strongest lens due to the high current applied to it) focuses the beam onto the sample providing additional demagnification (Goldstein et al., 2003).

As the electron beam travels towards the sample, which is placed on a moveable sample stage, the electron gun and lenses determine the trajectories of the electrons in the beam and will be focused on the sample in approximately parallel paths (Goldstein et al., 2003). Once the beam reaches the sample it will enter the specimen and interact with the samples atoms. Some of the beam electrons will collide with the samples atoms elastically and others inelastically producing signals used in the analysis of materials. These scattering events result in an interaction volume much larger than the original beam diameter of approximately 10 nm at the surface of the specimen (Figure 4).

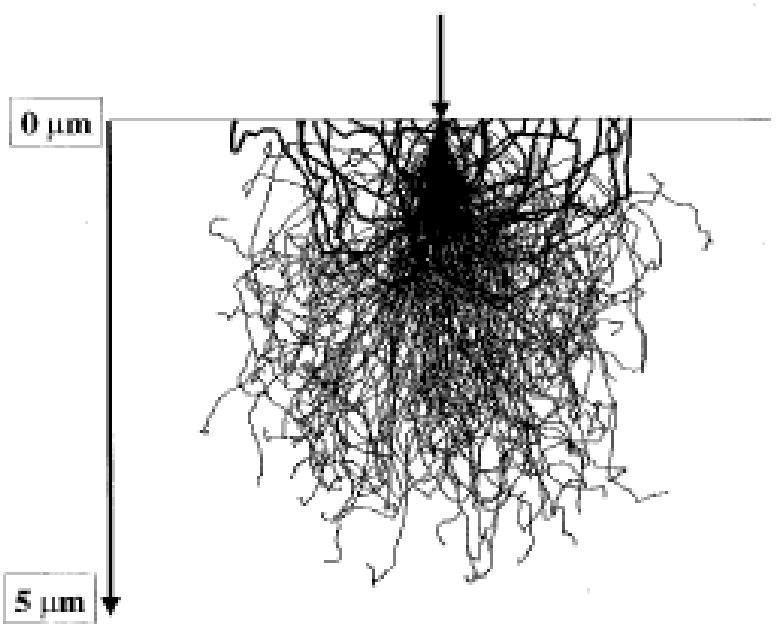

Figure 7: Interaction volume of an electron beam (Goldstein et al., 2003).

As the electron beam enters the sample a portion of the electrons in the beam will experience elastic collisions with the atoms in the sample and will eject out of the specimen. These electrons are called backscatter electrons (BSE). The degree at which beam electrons backscatter has shown to depend on the atomic number of the atom they are interacting with. As the atomic number increases so does backscattering. This shows that the signal produced by backscattering correlates to the elements present as long as all other factors are held constant. Secondary electrons (SE) are loosely bound outer shell electrons from the samples atoms that, when a sufficient amount of kinetic energy is provided by a beam electron, will eject from the atom through inelastic collisions with the beam electrons. A portion of these secondary electrons will escape from the sample.

Backscattered and secondary electrons are the primary signals used to produce images in a SEM. By recording the intensity of these signals, through the use of detectors, at locations on the sample contrast can be produced that defines the properties of the sample. When a sample is scanned with the electron beam the beam location (x-*y* coordinate) is recorded along with the

signal intensity *I* at that location. An image is formed by recording these signals in a numerical array (*x*, *y*, *I*) and representing this data by adjusting the gray values of pixels in a digital image to correspond to these intensities at the appropriate locations. Figure 5 is an example of a BSE digital image of a fly ash particle. The pixel brightness increases with increasing BSE signal.

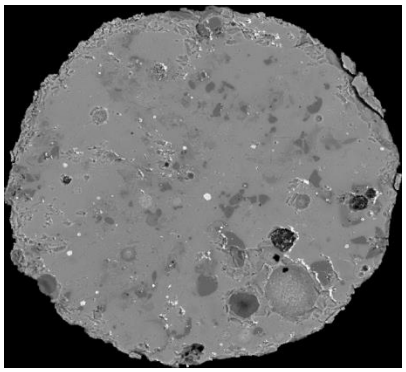

Figure 8: BSE image of a fly ash particle.

Flat polished samples create BSE images that are highly dependent on the chemical composition of the material under investigation. Higher BSE signals result in a brighter gray value for that location and as the atomic number of elements in the flat and polished specimen increase so do the BSE signals. This BSE signal contrast mechanism is referred to as "atomic number", "compositional", or "material" contrast and is a fundamental component in the rapid investigation technique developed in this research.

ENRGY-DISPERSIVE SPECTROMETRY

In addition to gathering information from a sample to create BSE and SE images a SEM, when equipped with an energy-dispersive spectrometer (EDS) or other signal collection device, is capable of gathering qualitative and quantitative chemical compositional data. When the electron beam interacts with the atoms of a sample x-ray photons are generated in addition to the BSE and SE emissions. Characteristic and bremsstrahlung radiation are both formed due to this beam-

atom interaction. When an electron enters a specimen it can undergo deceleration due to interaction with the Coulombic field of the specimen atoms. This deceleration causes a loss in energy of the electron and is emitted as a photon. This radiation is called bremsstrahlung radiation and creates a continuous spectrum of background radiation due to the fact that it can take on any energy value from zero to the beam energy as seen in Figure 6 (Goldstein et al., 2003).

Characteristic x-rays are a much more useful form of radiation as they have energies specific to the elements from which they are emitted. When the electron beam interacts with atoms in the specimen the beam electron can collide with a tightly bound inner shell electron of an atom in the sample thus emitting that electron from the atom. This ionizes the atom and leaves it in an energetic state. A series of allowed electron transitions occur from the outer shells to fill the vacancy in the inner shell allowing the excited atom to relax to its ground state. Electrons in each shell of an atom have firm defined energies as do the shells themselves for a specific element. The excess energy is released from the atom during relaxation by way of a characteristic x-radiation photon or the ejection of another outer shell electron (Goldstein et al., 2003). The latter of the two is known as the Auger process. The characteristic x-ray photon has an energy that is specific to the element from which it originated and therefore it provides information regarding the chemical composition of the sample.

Once these characteristic x-rays have been produced they can be collected by an energy-dispersive spectrometer (EDS). An EDS is typically comprised of a semiconductor that, when exposed to radiation, will create a charge pulse that is converted to a voltage pulse. This voltage pulse is proportional to the energy of the original incoming characteristic x-ray photon. Since the characteristic x-ray has an energy specific to an element and the voltage pulse is proportional to this energy, the voltage pulses can be summed together for each voltage to provide counts, number of occurrences, for a given energy. This information is used to produce an energy

spectrum for a given range of energies as shown in Figure 6. EDS allows the elemental composition of a sample to be evaluated through the use of these energy spectrums.

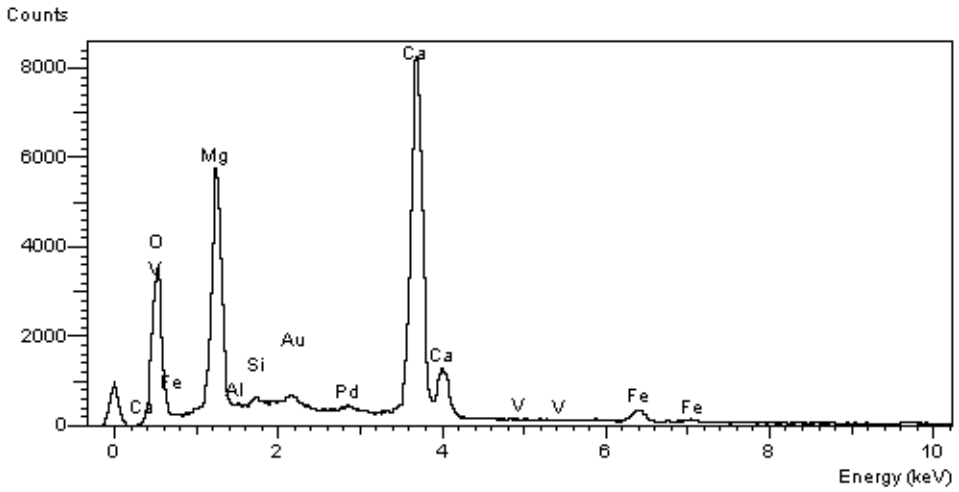

Figure 9: X-ray spectrum where energy is represented on the x-axis and intensity on the y-axis.

EDS can also be used to create raw elemental maps that are represented as gray-value images. This is done through a technique called gray-scale x-ray mapping. As mentioned previously BSE gray-scale images represent the chemical contrast of a sample through the atomic number contrast mechanism These BSE images are useful tools when examining the composition of samples but alone do not yield any specific information about the elements present (Goldstein et al., 2003). X-ray mapping is similar to BSE images as the intensity of the signal gathered dictates the brightness of the pixel at that location. The signal used in gray-scale x-ray mapping is the intensity of characteristic x-rays at a location; therefore, the only characteristic photons considered in the intensity evaluation are photons with energies specific to the element being investigated. For example, if a raw elemental map of aluminum were being created then only the characteristic x-rays of aluminum would be considered when calculating the intensity. Figure 7 shows raw elemental maps for calcium, silicon, aluminum, and iron.

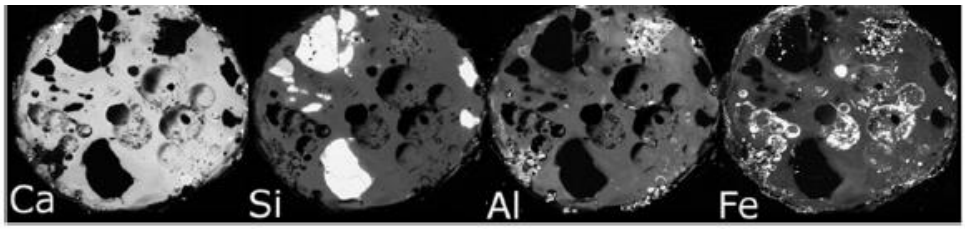

Figure 10: Raw elemental x-ray maps of calcium, silicon, aluminum, and iron (Hu et al., 2013).

SEGMENTED EDS ANALYSIS

The above described BSE images and raw elemental maps along with multivariate statistical analysis can be used in a Segmented EDS Analysis to identify and qualitatively describe the compositionally distinct areas in a sample (Hu et al., 2013). This technique identifies the areas with distinct compositional characteristics through the use of an unsupervised clustering technique known as ISO Means (Hu et al., 2013). This technique is further described in Appendix A. Upon completion of this segmentation process a color segmented chemical map is generated that shows the compositionally distinct areas in the sample. Figure 8 shows an example of the BSE image, raw elemental map images, and color segmented EDS image for fly ash particle 1C. The red, green, blue, and yellow areas represent distinct chemical phases with the composition shown in Table 1. Information derived from a Segmented EDS Analysis for fly ash particle 2C performed at NIST is a fundamental component of this research.

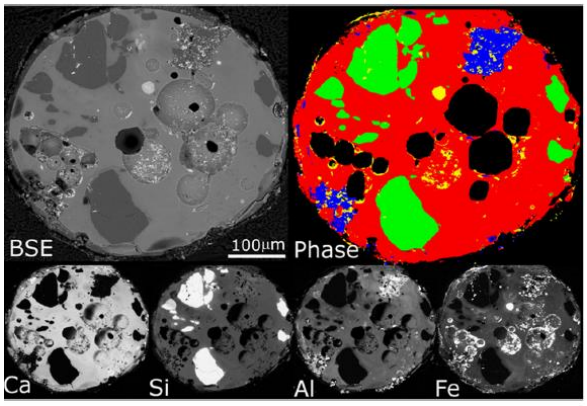

Figure 11: BSE image of particle 1C used for the NIST Segmented EDS Analysis (Top Left). Gray-scale x-ray map images for particle 1C used for Segmented EDS Analysis (Bottom). Color segmentation of particle 1C produce by Segmented EDS Analysis (Top Right) (Hu et al., 2013).

Table 1: Chemical composition of each color present in particle 1C (Hu et al., 2013).

element		Ca	Si	Al	Fe	O	K	Mg	S	Ti	area % on cross section	mass absorption* (cm^2/g)
Particle 1C - 427 µm diameter												
yellow	weight %	9.66	10.10	6.72	67.17	3.56	0.34	1.31	0.47	0.67	2.52	6.50
	1σ	7.05	6.64	4.62	12.46	6.12	0.51	1.61	0.93	0.97		
red	weight %	27.87	22.96	12.38	10.88	20.00	0.32	3.19	0.55	1.86	70.60	2.76
	1σ	6.78	5.90	3.49	7.87	9.98	0.46	1.68	0.61	1.12		
blue	weight %	4.36	29.35	31.00	14.59	19.11	0.35	0.56	0.27	0.41	5.82	2.15
	1σ	6.69	8.81	8.40	13.75	12.09	0.64	1.22	0.47	0.69		
green	weight %	1.08	65.21	0.53	1.29	31.29	0.07	0.17	0.12	0.26	21.05	1.09
	1σ	2.70	7.22	1.10	2.99	6.67	0.33	0.34	0.25	0.56		

AUTOMATED FEATURE ANALYSIS

Automated Feature Analysis (AFA) is an application that allows the SEM to automatically search a user specified region for features of interest and perform an analysis of these features. AFA is capable of locating features, calculating diameters of these features along with other geometric properties, and analyzing the elemental composition of the features of interest. Upon completion of initial setup AFA can analyze approximately 1,000 to 25,000 features in one hour while an analyst might be able to accomplish only 60 features in one hour (ASPEX, 2007). Since the sample is placed on a mobile sample stage it is possible to move this

stage under the electron beam and investigate different locations on the sample automatically through the use of AFA.

The AFA application performs a search of a user defined region which can be defined by a circle, polygon, or series of stage points. To create a search region the user must define stage points for the boundary, or the location, of the search area. For example, if the search region is a rectangle the user could define the two extreme opposite corners as show in Figure 9.

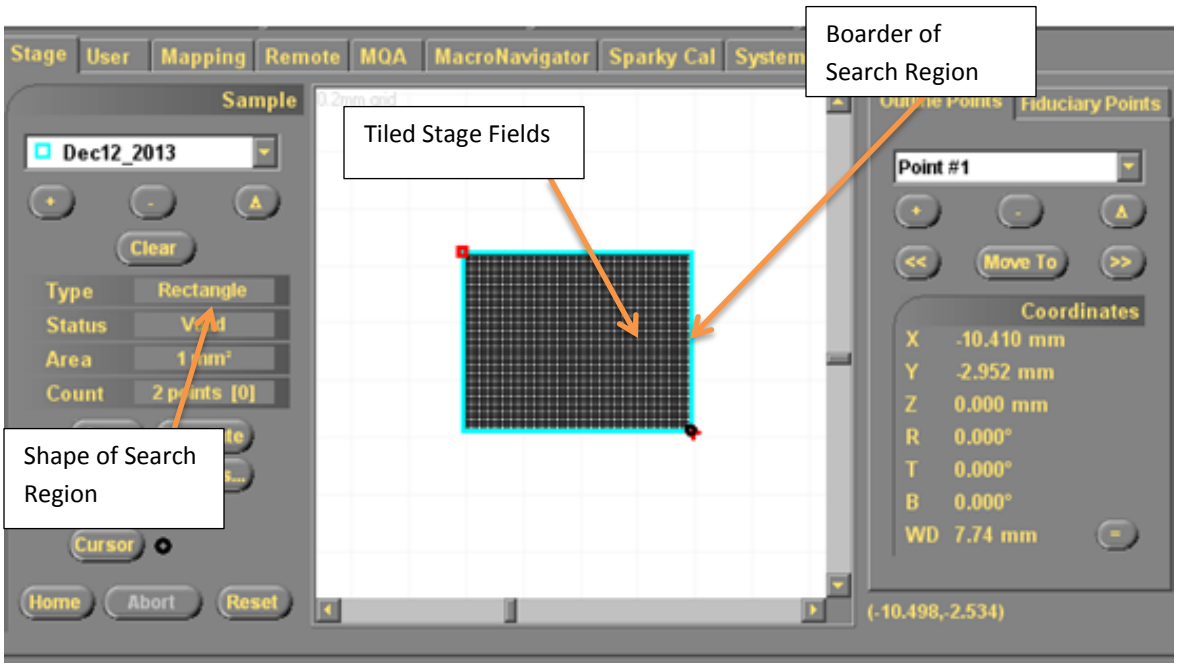

Figure 12: Rectangular search region for AFA and corresponding Stage Fields.

Once the search region is defined it is automatically divided into small square areas called "stage fields" as shown in Figure 9. These "stage fields" are individually searched for information during the AFA analysis and the images (BSE or SE) produced of each field can be saved individually. Signals from BSE or SE emissions are used to search for features of interest by comparing the intensity of the signal received to a user defined threshold on a pixel by pixel basis. The user defined threshold is a gray-scale value that determines which intensities are features and which are not. Once a feature is located a rotating cord algorithm measures the

geometric properties of the feature. Upon completion of the morphological evaluation of the feature, if desired, it can be investigated by EDS to collect information concerning its chemical composition. The beam is located at the center of the feature during EDS evaluation. This process is repeated for each feature located in AFA.

The research presented here does not use the full capabilities of AFA as they can be restrictive to the overall requirements for Automated Rapid Particle Investigation. It is desired to develop a rapid particle investigation technique and gather as much useful information as possible from each particle (feature) located in the investigation. For example, EDS produces elemental information of the feature but only at one location, the center, of the feature. This does not provide a representation of the chemical composition of the feature. Although the morphological information produced by AFA is useful it was more beneficial to determine this information post AFA, as it could be incorporated into one computer program that determines chemical and morphological information. As a result only the saved BSE images of each "stage field" created during AFA are used in Automated Rapid Particle Investigation.

CHAPTER V

METHODOLOGY

OVERVIEW

Automated Rapid Particle Investigation can be summarized into three steps which are sample preparation, ASEM scanning, and image analysis. The first step is to embed fly ash particles in an epoxy puck. This requires that a sample of fly ash be placed on a glass plate with a circular mold place around it. Epoxy is then poured over the sample of fly ash and is contained in the circular mold where it is allowed to cure and harden into a puck. The surface of the puck containing fly ash is then polished until clean cross-sections of the embedded fly ash are exposed. The second step is to coat the sectioned surface in a conductive carbon coating and investigate the sample with ASEM to obtain stage field images. In the third step of this technique the resulting BSE stage field images from the ASEM scan are analyzed with an image analysis program developed in this research. Stage fields containing fly ash particles are located and the particles are further investigated to reveal their chemical composition using the developed program. Once these stage fields have been analyzed the percent of the cross-section occupied by each chemical phase present in the particles found are presented in a table. Details of Automated Rapid Particle Investigation are presented next.

SAMPLE PREPARATION

Mix 20 milligrams of fly ash in a vial containing 25 ml of acetone and 25 ml of isopropyl. Ensure that this mixture is watertight and sonicate for 20 minutes to disperse the fly

ash particles in the mixture as shown in Figure 10. While the fly ash mixture is sonicating clean a glass plate with acetone and apply epoxy release agent to the plate and circular ring molds as shown in Figure 11. Place ring molds on glass plate and seal the mold-plate interface with plumber's putty as shown in Figure 12.

Figure 13: Vial used to mix fly ash, acetone, and isopropyl (Left). Sonicator used to reduce fly ash clumping (Right).

Figure 11: Glass plate (Left), circular ring mold (Center), and epoxy release agent (Right).

Figure 12: The use of plumbers putty to seal the mold-plate interface.

Remove the vial containing the fly ash from the sonicator and shake 30 times to further decrease the potential for clumping of particles. Use a dropper to extract solution from the vial by placing the dropper at the 5 ml line on the vial. Using the dropper, place five well-spaced drops in the circular ring mold as shown in Figure 13.

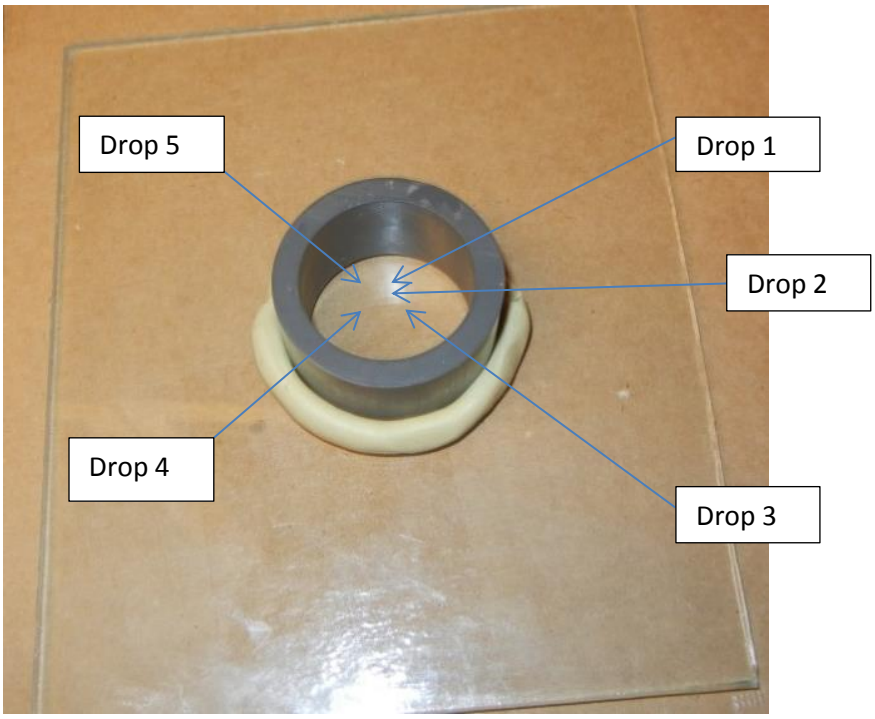

Figure 13: Fly ash mixture drops placed in circular mold.

Once the fly ash mixture has been placed in the mold allow fifteen minutes for the mixture to dry. Prepare the epoxy by mixing the resin and hardener at a 5:1 resin to hardener ratio. Mix the epoxy in a measuring bowl for two minutes using a slow circular motion to avoid entrapping air in the final resin hardener mixture. Pour a very thin layer of epoxy into the mold so that there is only enough in the mold to cover the bottom surface completely. Once the mold has been prepared with a thin lift of epoxy, place the glass plate containing the prepared mold in a vacuum chamber to cure for twelve hours (Figure 14). After the thin epoxy lift has cured for twelve hours remove it from the vacuum and apply a second lift of epoxy to the mold. Fill the mold about 2/3 of the height of the mold and replace it in the vacuum to cure for a final twelve hours. Upon completion of the final cure remove the epoxy puck form the circular mold and prepare to polish the fly ash surface.

Figure 14: Vacuum chamber.

POLISHING

Once the epoxy puck has been prepared it is polished with an Extec polisher until a clean cross-section of the embedded fly ash is exposed. Polishing was carried out manually by holding

the puck in one's hand and applying slight pressure downward onto the pad. The following describes the process of polishing the epoxy fly ash puck. Mix 1/8 µm diamond powder with isopropyl alcohol 10% by weight of diamond powder in a glass jar to create a diamond slurry used for polishing as shown in Figure 15. Load the magnetic polishing pad onto the polishing machine and place the diamond slurry in a manner to allow insertion of a tube used to extract the slurry for application to the pad as shown in Figure 15.

Figure 15: Diamond powder (Top Left), Glass jar used to mix diamond slurry (Top Center), Extec Polisher (Top Right), Magnetic polishing pad (Bottom Left), Magnetic pad loaded in polisher (Bottom Center), Slurry with extraction tube inserted (Bottom Right).

Figure 16: Extec polisher function and setting console.

Turn on the Extec polisher and program the appropriate settings into the polisher using the function keys (Figure 16). In order to ensure proper function of the polisher for the intended purposes nine settings were programed. The polisher speed was set to 100 rpm, the time was set to 30 minutes, the direction of rotation was set to contra, the coolant option was set to off to prevent the application of water to the sample, the head was turned off since polishing was carried out manually, the fingers were not allowed to drop since the automatic polishing option was not used, bottle one and two were set to pulse every 0 seconds for 0 seconds while bottle three, the bottle containing the diamond slurry, was set to pulse for 10 seconds every 30 seconds to maintain an adequate concentration of diamond slurry on the polishing pad. These setting were selected through trial and error until the desired results were obtained. Once these settings were programed and "enter" was selected the polisher began revolving and applying diamond slurry to the pad. Holding the puck firmly in one's hand it was pressed onto the pad with slight downward pressure and oscillated back and forth about its centroid as well as moved in a circular motion globally. Polishing was carried out for 30 to 45 minutes until the desired level of polishing was achieved. Examination of the level of polishing was carried out under a stereomicroscope.

ASEM INVESTIGATION

Once the epoxy puck has been polished it is scanned with a SEM automatically to create a set of AFA BSE stage field images that will be further analyzed by the image analysis program. The puck must first be coated with a conductive carbon coating to prevent charge build up from the electron beam and then placed in a holder in a manner to minimize the working distance of the sample in the SEM (Figure 17). A working distance between 7 mm and 12 mm was found to be satisfactory.

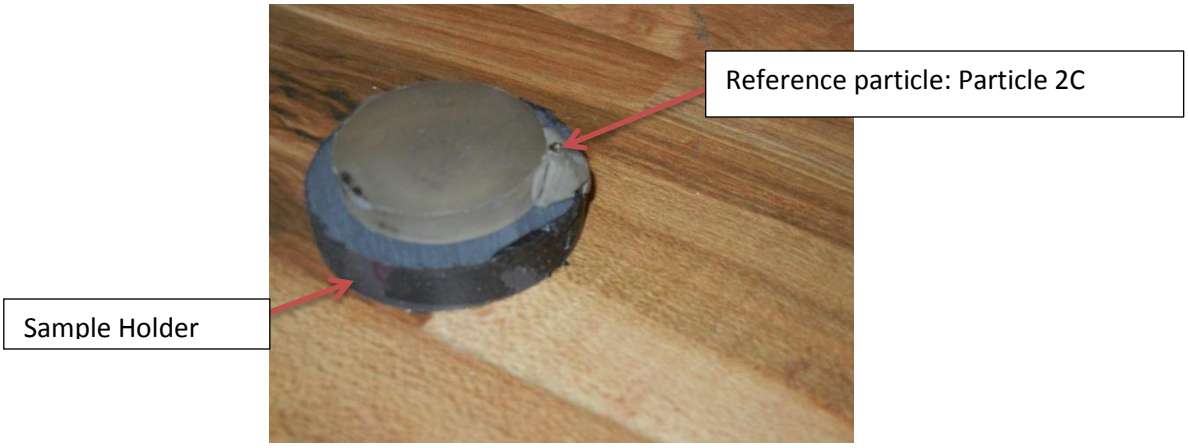

Figure 17: Epoxy puck in sample holder with particle 2C attached to the side with clay.

A reference particle that has been investigated by Segmented EDS, as described earlier, is attached to the side of the epoxy puck as shown in Figure 17. Fly ash particle 2C, an ASTM Class C fly ash, was used in this research as the reference particle. The holder, puck, and reference particle are then placed in the SEM sample chamber. The chamber is automatically placed in a vacuum when closed. The beam energy is set to 11 keV, filament drive to 70%, brightness to 3%, contrast to 100%, magnification to 15000X, and spot size to 38%. The working distance will vary depending on the placement of the sample within the sample holder. It is desired to maintain a working distance between 7 mm and 12 mm. These settings were selected through a trial and error process until satisfactory BSE images were achieved. Figure 18 shows an example of the SEM settings. Be sure that the filament is allowed 30 minutes to saturate and become stable before beginning the analysis.

Figure 18: SEM Console

Once the sample has been loaded and the SEM settings have been appropriately adjusted the Automated Feature Analysis (AFA) can be set up. Before setting up AFA take a backscatter image of the reference particle, particle 2C in this instance, as this will be used in the image analysis program to determine the chemical phases present in the particles found by AFA. Figure 19 shows a backscatter image of particle 2C with an eliminated background.

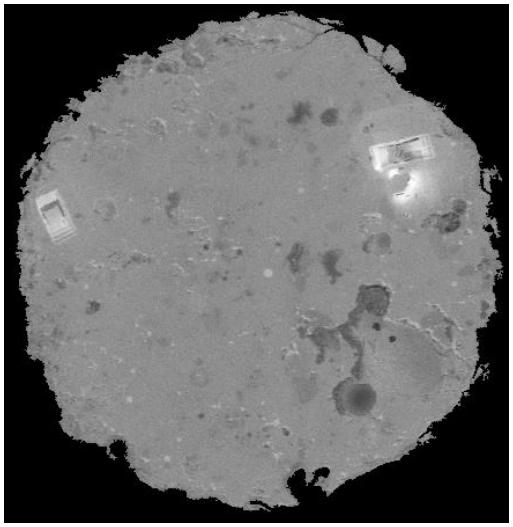

Figure 19: Backscatter Electron image of particle 2C taken at OSU.

To begin the setup for AFA the user must determine a search region for the SEM to investigate. This is done by creating a "stage area" as shown in Figure 9. The stage area is created by driving the stage to points defining the boundary of the desired search area and adding these points as "outline points". When adding the boundary points it is essential that the magnification and working distance be set to the desired values to be used during AFA as these points will allow AFA to focus the electron beam automatically. The boundary points define a perimeter of focused points and create a focused plane between these points; therefore, since the sample is polished to a flat surface all points in this plane will be focused producing quality BSE images. Once the stage area has been created AFA setup can precede by selecting this stage field for the analysis. The "video" settings should be set to the values obtained in the initial setup as shown in Figure 18. This can be done by simply selecting the "current" button. For the Detector

select “BSED”, this will allow the backscatter electron detector to be used and will create BSE stage field images. Figure 20 shows the “Video” setup tab for AFA.

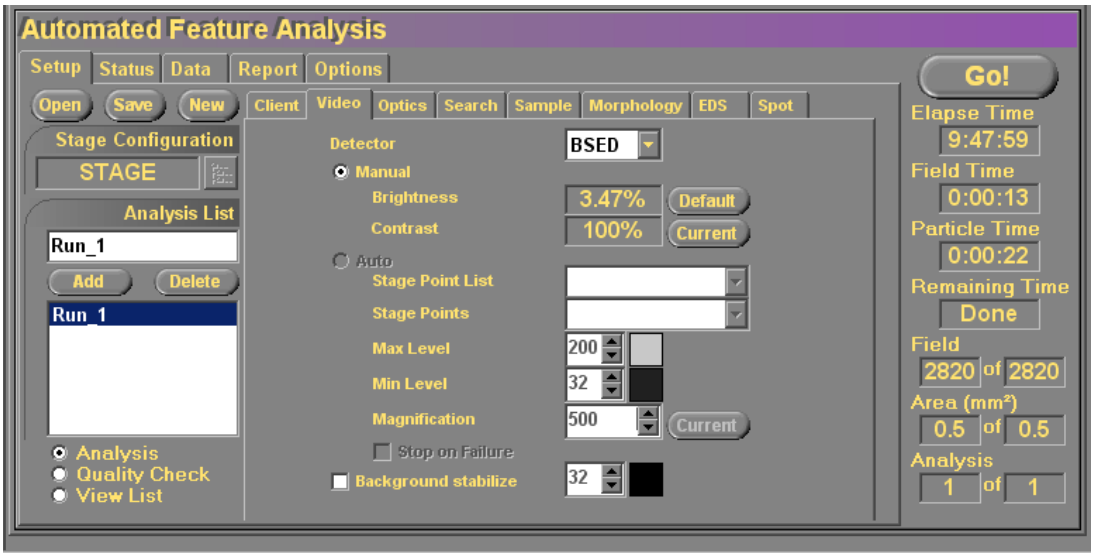

Figure 20: Video tab for AFA.

The next tab in AFA is the “Optics” tab. Under this tab the magnification and focusing are established. The magnification should be 15000x while the method for focusing should be “Use stage coordinates”. This magnification of 15000x was established so that particles as small as 1µm could be detected. The selection of the level of magnification dictates the “precision” and “field size” automatically. Using the stage coordinates, or stage points, to focus allows quality images to be generated as described previously by creating a focused plane between these points. Figure 21 illustrates the settings of the “Optics” tab.

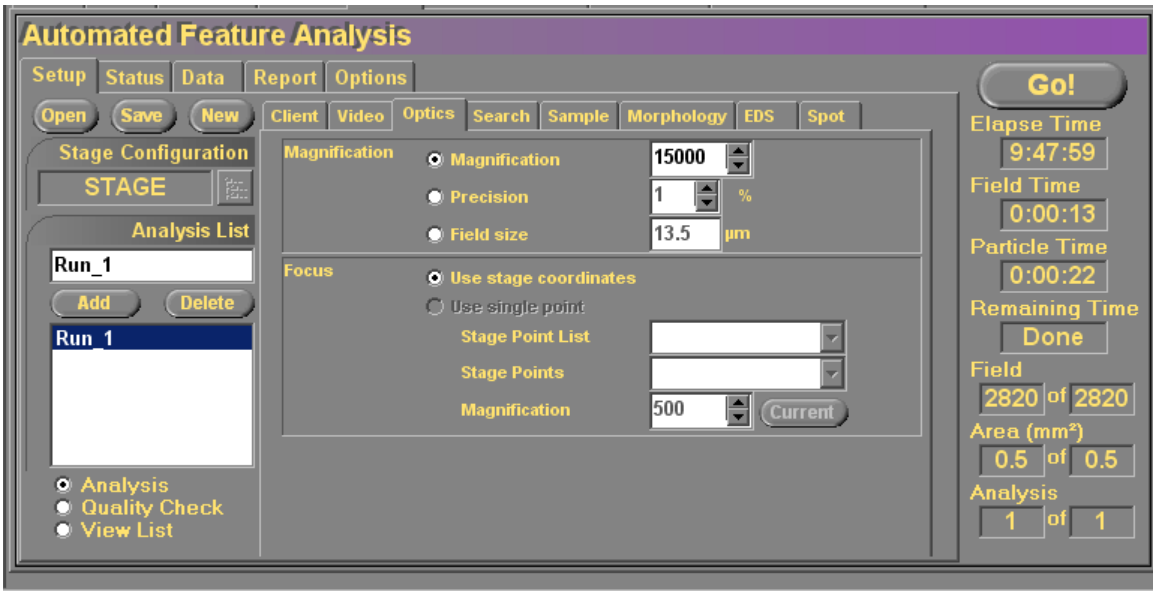

Figure 21: Optics tab in AFA.

The search tab will be the next tab to be set. Other than the "Number of electron fields" the settings under this tab are not used in the analysis since all stage fields will be saved and post processed. Each stage field can be divided into electron fields and searched according to the electron fields. By selecting 1 x 1 for the number of electron fields the stage field is searched as a solid area. The threshold under the search and measure, although not used, can be set by viewing a particle and selecting the "Thresholds" tab at the bottom of the screen and adjusting the thresholds until only the particle is viewed in the screen. The Dwell time under the search and measure options should be minimized to increase the speed of AFA. Figure 22 illustrates the "Search" tab for AFA.

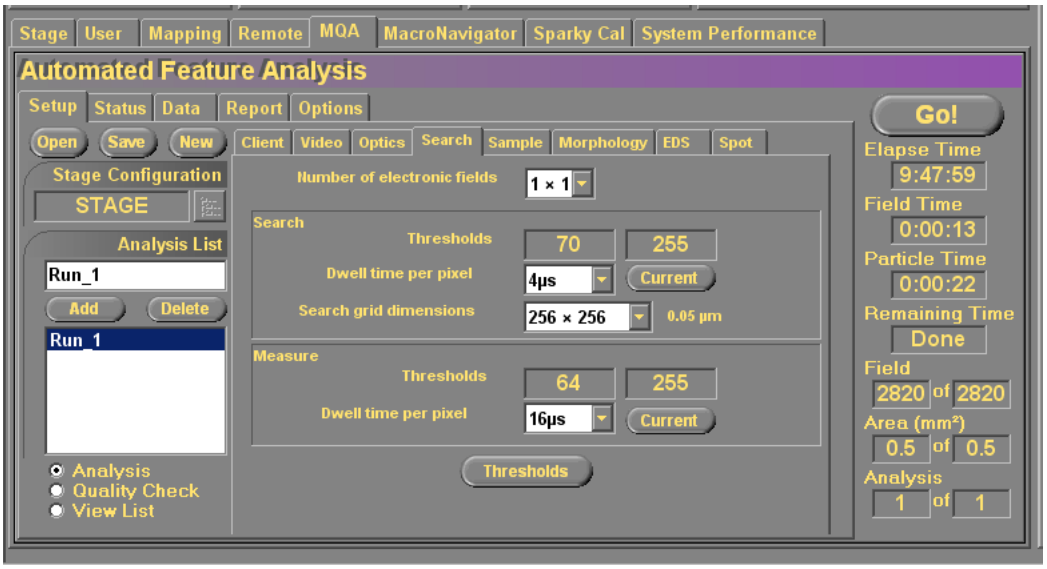

Figure 22: Search tab for AFA.

Next, the sample options are established under the "Sample" tab. These settings are subject to the requirements of the investigation. The maximum number of stage fields, particles, and analysis duration were set to 1,000, 10,000, and 600, respectively. Be sure that the "Save stage field images" option is selected as this will cause every stage field BSE image to be saved for further analysis and is the reason the search and measure options are not necessary for the analysis. Use the current settings for field image quality and 512 x 512 for the field image dimension. Figure 23 shows the "Sample" tab for AFA.

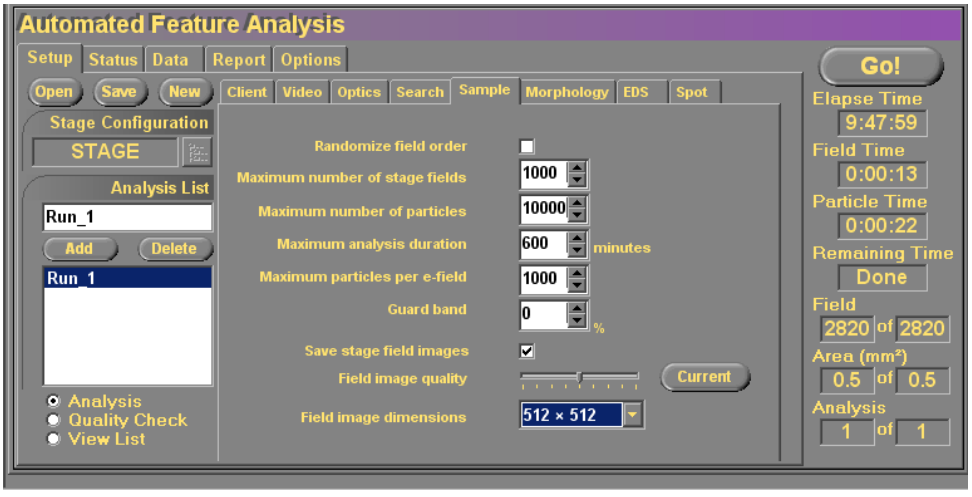

Figure 23: Sample tab for AFA.

Since every "stage field" image is saved and no EDS data is collected on the sample it is not necessary to use the "Morphology" or "EDS" tabs in AFA. The spot size should be set to manual under the "Spot" tab in AFA. This allows AFA to use the established spot size in the initial setup of the SEM settings as shown in Figure 18. Figure 24 shows an example of the "Spot" tab in AFA. Once the previous settings for AFA have been established the analysis is performed by selecting "GO!". Upon completion of AFA a set of AFA stage field BSE images will have been created and saved in a designated location. These BSE images will be further analyzed by an image analysis program created in this research to reveal the primary chemical constituents present in the particles found in each AFA stage field. An example of the resulting BSE stage field images produced by AFA is shown in Figure 25.

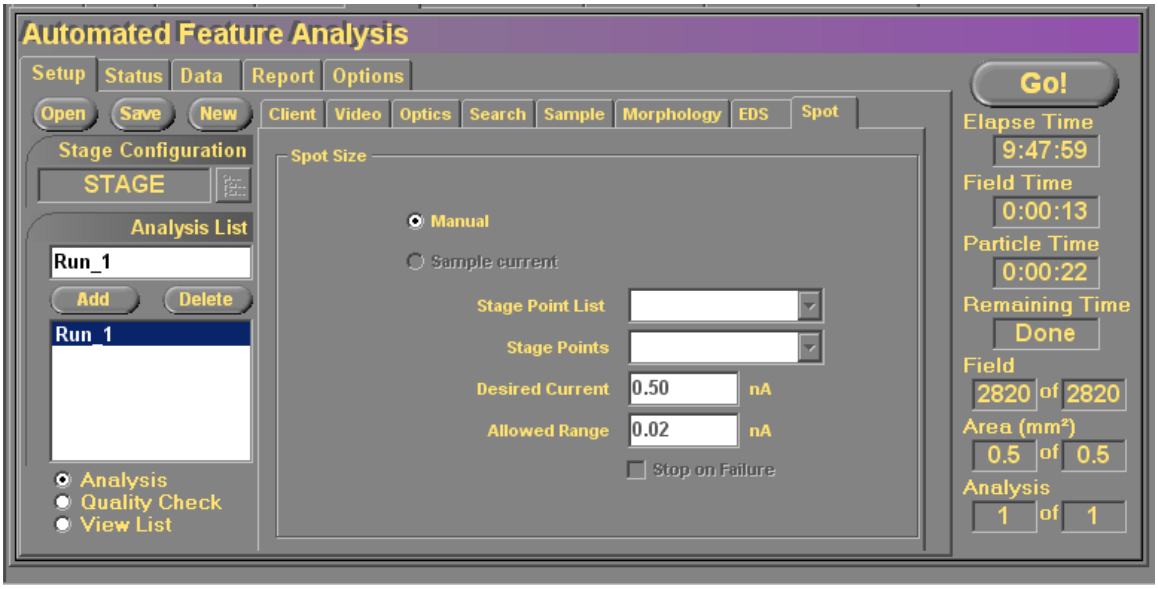

Figure 24: Spot tab for AFA.

Figure 25: Four stage field BSE images obtained through AFA.

IMAGE ANALYSIS - OVERVIEW

Once a set of BSE stage field images have been created through AFA they can then be analyzed by an image analysis Matlab program developed in this research. This program searches the set of stage field images for features that meet the user defined search criteria established in the program. Features that pass the criteria are now considered fly ash particles. After these particles have been identified they are compared to the results of the NIST Segmented EDS (SEDS) Analysis to reveal the primary chemical composition of the identified particles. This is accomplished by comparing the gray-scale values of each particle's pixels in the digital AFA stage field images to the gray-scale values of the pixels in the digital transformed BSE image from SEDS. In a digital gray-scale image each pixel is assigned a gray value. This is demonstrated in Figure 39 through Figure 45. Fly ash particle 2C was used in this research as the reference particle.

The gray-scale values of the BSE image used in the SEDS Analysis occupy regions of distinct chemical composition which are represented by a color segmented image as shown in Figure 26. Notice how different shades of gray in the BSE image reflect regions differing in color in the SEDS image (Figure 26). Since the chemical composition of each color has been determined by the NIST SEDS Analysis and the gray-scale values of the BSE image of the particle used in the SEDS Analysis correspond to these colors the chemical composition of these gray-scale values are also known. This allows the use of only the BSE gray-scale image to be used to identify the primary chemical constituents of a particle. This makes since if we recall the "atomic number" contrast mechanism discussed in Chapter 4. The "atomic number" contrast mechanism says that as the atomic number of an element increases the BSE signal also increases which creates a BSE image representing the chemical contrast of a particle. SEDS Analysis is required to reveal the chemical composition of these gray-scale values in order to establish a qualitative understanding of this contrast.

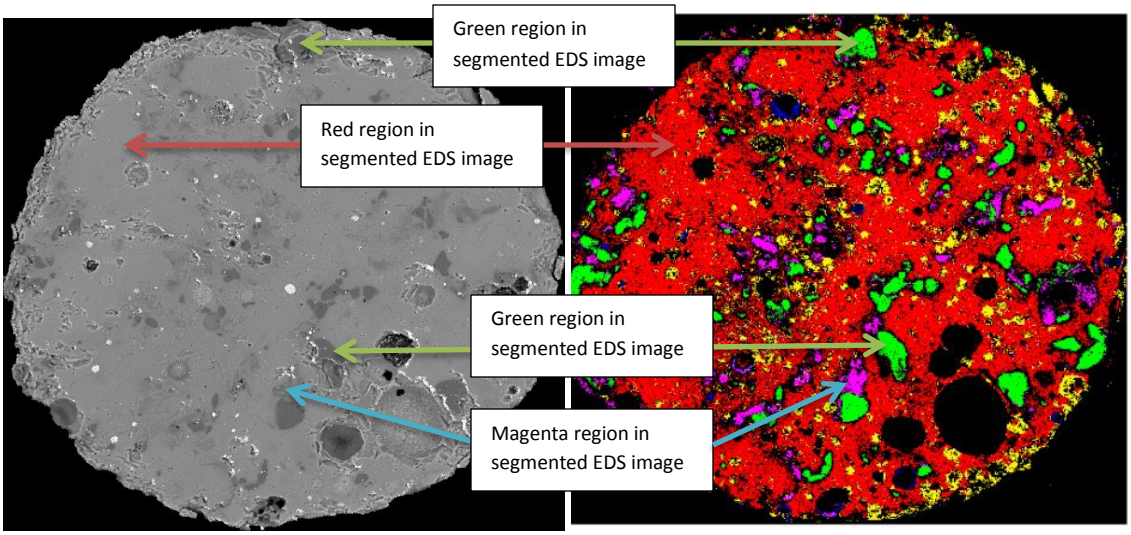

Figure 26: BSE gray-scale image of particle 2C used in the Segmented EDS Analysis (Left). Color segmented chemical map of particle 2C produce by Segmented EDS Analysis (Right).

The image analysis portion of this investigation technique is a three step process. First, a gray-scale histogram transformation of the BSE image of the reference particle used for the SEDS analysis at NIST to the gray-scale histogram of the same particle scanned at OSU is performed. Next, the color segmented chemical map is theoretically overlaid on the transformed BSE image and each color is used to define a range of gray-scale values that occupy the same space as that color. This allows the chemical composition of each range of gray-scale values corresponding to each color to become known. Last, each stage field BSE image produced by AFA is searched for particles and, once found; the gray-scale values of each particle are placed in the established ranges of gray-scale values corresponding to a distinct chemical composition found in the second step to quantify the percent area of each particle belonging to a particular chemistry. Each process in the image analysis program as well as the reason for the process will be explained next.

IMAGE ANALYSIS – TRANSFORMATION

In order to make an accurate comparison between the stage field BSE images produced with Oklahoma State Universities (OSU) ASEM and the Segmented EDS data produced with equipment at NIST a transformation of the gray-scale BSE image taken at NIST to the gray-scale

BSE image created of the reference particle at OSU is required. This transformation is required because 1) the orientation of the BSE image must be identical to the color segmented chemical image produce by Segmented EDS and 2) the gray-scale values of this identically oriented BSE image must be reflective of the gray-scale values present in the AFA stage field images. Let us first examine requirement No. 1 for the transformation.

In order to use only the stage field BSE image gray-scale values to evaluate the chemical constituents of the discovered particles from AFA we must first understand the chemical compositions represented by these gray-scale values. This is done by looking at gray-scale values in the BSE image of particle 2C that occupy the same space as the SEDS color segmented image of particle 2C. Figure 27 shows an example of making this evaluation for the green phase. The first image in Figure 27 is the complete BSE image of particle 2C taken at NIST used in SEDS Analysis. The center image in Figure 27 is a BSE image of particle 2C showing only the green regions of the particle and the right image is the SEDS color segmented image of particle 2C. The center image in Figure 27 is created by turning on only the regions in the left image of Figure 27 that occupy the exact geometric space as the green regions in the SEDS color segmented image; therefore, it is essential that the orientation of the BSE image be identical to the SEDS color segmented image. If the orientation were not exact than gray values that do not represent the chemical composition of the green phase would be labeled as having the green chemistry and would therefore be incorrect. For example if the left image in Figure 27 were inverted it would

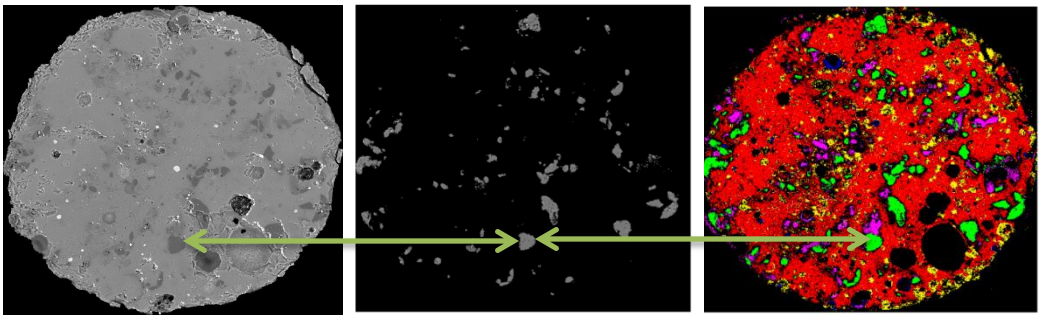

Figure 27: BSE image of particle 2C taken at NIST used in SEDS Analysis (Left). Only the regions in the BSE image of particle 2C taken at NIST that occupy the same space as the green regions in the SEDS color segmented image (Center). SEDS color segmented image (Right).

not change the appearance of the center image except that the gray-scale shades would change depending on what regions of the inverted image fell in the green regions of the SEDS color segmented image. For this reason it is required that the BSE image of particle 2C taken at NIST, and used in the SEDS Analysis, be used to define the chemistries of the gray-scale values occupying each color phase because its orientation is that of the SEDS color segmented image. This leads to requirement No. 2 for the transformation.

Requirement No. 2 for the transformation can be best explained by first examining the BSE images and corresponding gray-scale histograms of particle 2C created by equipment at OSU and NIST (Figure 28). Notice how the gray-scale histograms and BSE images differ for each scan. These histograms represent the gray-scale distribution within its corresponding BSE image. It is known that the chemistry of particle 2C at the section shown in Figure 28 is defined by the color segmented image; however, the gray-scale values are shown to differ between the two images. As mentioned in Chapter 4 the BSE image of a particle reveals the chemical contrast of the particle and gives no insight into the actual qualitative composition; therefore, the same chemistries will likely be represented by differing gray-scale values when examined with different SEMs and/or settings while the chemical contrast remains. For example, calcium may appear brighter due to a higher gray-scale value when examined with one SEM and darker when examined with another SEM. The same may be true for aluminum but the contrast between

calcium and aluminum will remain producing BSE images that represent the same chemical contrast. For this reason, since the BSE image of particle 2C taken at NIST must be used due

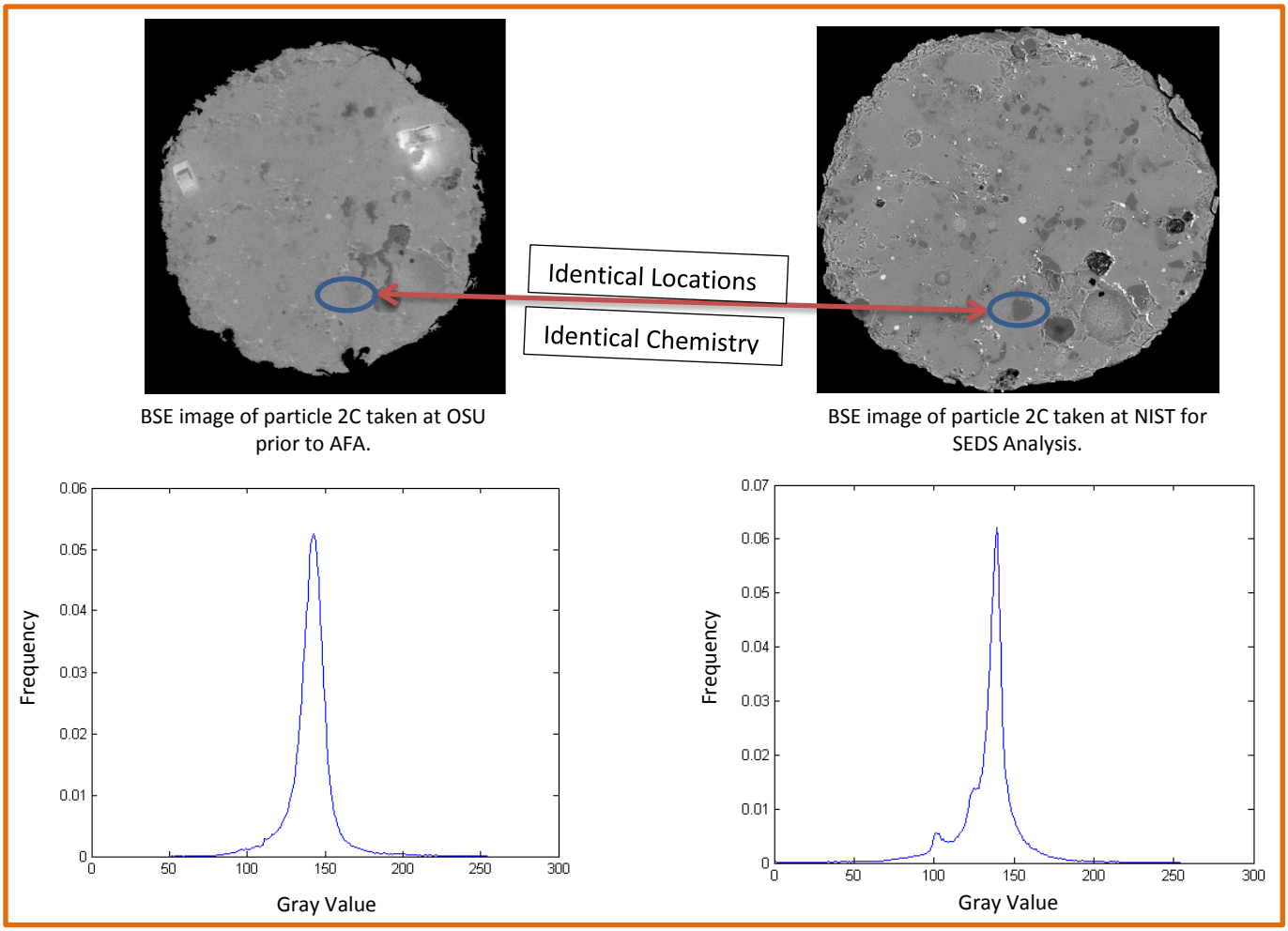

Figure 28: BSE image of particle 2C taken at OSU prior to AFA (Top Left) and corresponding gray value histogram (Bottom Left). BSE image of particle 2C taken at NIST for the SEDS Analysis (Top Right) and corresponding gray value histogram (Bottom Right).

to requirement No. 1 to reveal the chemistry for ranges of gray-values occupying each color in the color segmented image than this BSE image's gray value histogram must also be transformed so that the gray-values in this image represent the gray values produced by the equipment at OSU. This is done so that gray value thresholds can be defined for each chemical phase in the color segmented image and a percentage of each phase can be calculated in the BSE particle images produced by AFA. This explains the reason for the initial BSE scan of a reference

particle, particle 2C in this case, during the ASEM investigation portion of this research. The initial scan of the reference particle, taken before AFA at OSU, is used to transform the BSE image used in the SEDS Analysis at NIST so that the gray value thresholds defining each chemical constituent accurately represents the gray values produced during AFA at OSU. If this transformation were not performed and the BSE image of particle 2C from NIST were used than the gray value ranges for each chemical phase would be shifted to create an incorrect evaluation of each particle found during AFA at OSU. This may become more obvious once the "Color Segmentation" portion of the image analysis program has been explained in the following section Image Analysis – Color Segmentation.

Now that the reasons for the transformation have been discussed the transformation process itself can be shown. To perform the transformation the BSE scan of the reference particle, taken prior to AFA at OSU using the exact settings of AFA, is loaded into the image analysis program. The BSE scan taken at NIST of the same reference particle is also loaded into the image analysis program. Recall that the reference particle is the particle used for the SEDS Analysis and is particle 2C in this research. Before these images can be used the backgrounds of each image must be eliminated. Background elimination is necessary to alleviate background noise in the image so that only areas of interest in the image are evaluated. If the background were not deleted than the gray-scale histogram would not represent the particle of interest; rather, it would represent the whole image. By setting all background pixels to a gray value of zero the effects of the background are removed from the gray-scale histogram. An example of the effects of the background on the gray-scale histogram is shown in Figure 29 for the OSU BSE scan of the reference particle, particle 2C. A gray value of 110 was used in this example to eliminate the background. This gray value is determined iteratively until the entire background has been eliminated and all that remains is the particle of interest. Background elimination is accomplished by setting all pixels in the image with gray values less than the determined gray

value, 110 in this example, to a value of zero which is black in a gray-scale image. The largest remaining feature is then found through a labeling process. All pixels within the largest feature are returned to their original values to maintain the integrity of the particle's gray-scale values.

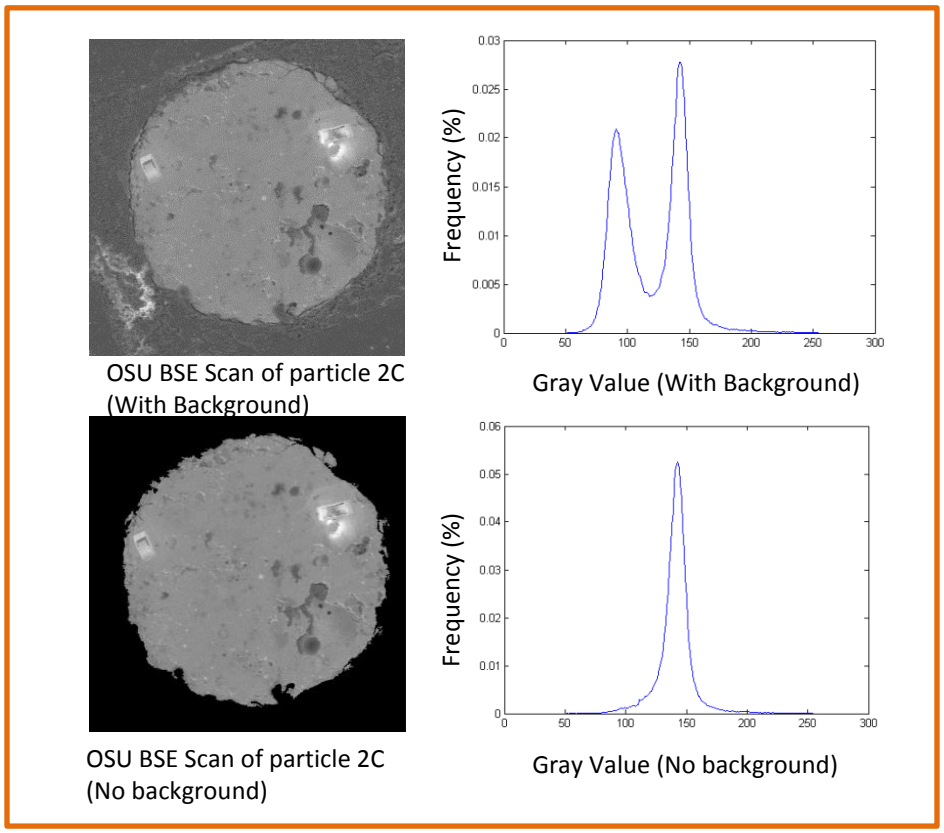

Figure 29: BSE image with background of particle 2C and corresponding gray-scale histogram (Top). BSE image without background of particle 2C and corresponding gray-scale histogram (Bottom).

Once these images of particle 2C have been loaded into Matlab and their backgrounds have been deleted the command "histeq" is used to transform the BSE image gray values developed at NIST to the BSE image gray values of the same reference particle, particle 2C, developed at OSU prior to AFA. The "histeq" command performs the following operations on the images' gray value histograms. Let us refer to the BSE image developed at NIST used in SEDS as histogram (A) and the image developed at OSU prior to AFA as histogram (B). The objective is to transform the gray-scale values of (A) to the values of (B). If a histogram is equalized using its unique equalization function it will become a histogram of constant value

(Gonzalez & Woods, 2008). This constant value histogram is independent of the original histogram (Gonzalez & Woods, 2008). Therefore all histograms equalized with their unique equalization function will become the same constant value histogram (Gonzalez & Woods, 2008). A property of the equalization function is that this process can be reversed by using the inverse of the equalization function returning the constant value histogram back to its original histogram. Using this property if histogram (A) is equalized with its own equalization function and then reversed using the inverse of the equalization function of histogram (B) then histogram (A) will be transformed from its original form to the uniform histogram and then back to the form of histogram (B). This process shifts the gray value histogram of the BSE image developed at NIST, used in SEDS, to the gray value histogram of the BSE image developed at OSU prior to AFA. Figure 30 illustrates the process of transforming the BSE image of the reference particle, particle 2C, developed at NIST to the BSE image developed at OSU.

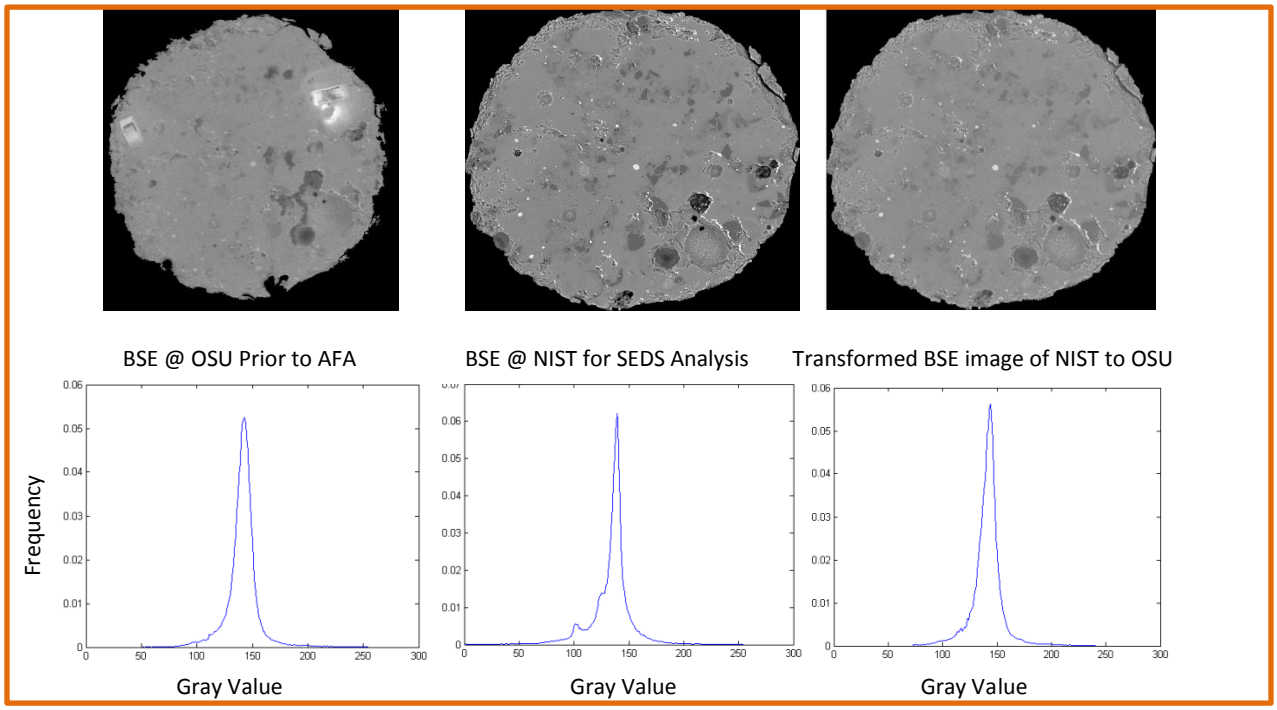

Figure 30: BSE image of the reference particle, particle 2C, taken at OSU prior to AFA analysis (Top Left) and corresponding gray value histogram (Bottom Left). BSE image of the reference particle, particle 2C, taken at NIST for SED Analysis (Top Center) and corresponding gray value histogram (Bottom Center). Transformed BSE image of particle 2C (Top Right) and corresponding gray value histogram (Bottom Right).

Figure 31 shows the histogram comparison of the BSE image of particle 2C from NIST used in the SEDS Analysis, the BSE image of particle 2C created at OSU prior to AFA, and the transformed BSE image of particle 2C from NIST. Notice that in Figure 31 there are two transformed histograms one labeled "no smoothing" and another labeled "smoothing". When a histogram of discrete integers is transformed a certain number of the transformed values are non-integer numbers and must be rounded since gray-scale values are always an integer. This can result in a jagged histogram. By using the smoothing command, which is a moving average technique, these jagged outliers are eliminated resulting in a smooth and reasonably accurate transformed histogram. Figure 32 shows the histogram comparison of the BSE image from OSU taken prior to AFA and the transformed BSE image from NIST used in SEDS Analysis. Also shown in this figure is the result of subtracting these histograms from one another. The ideal result of this subtraction would be a straight line along the value of zero on the frequency axis; however, this transformation is not exact but does yield extremely useful results as the error is significantly small.

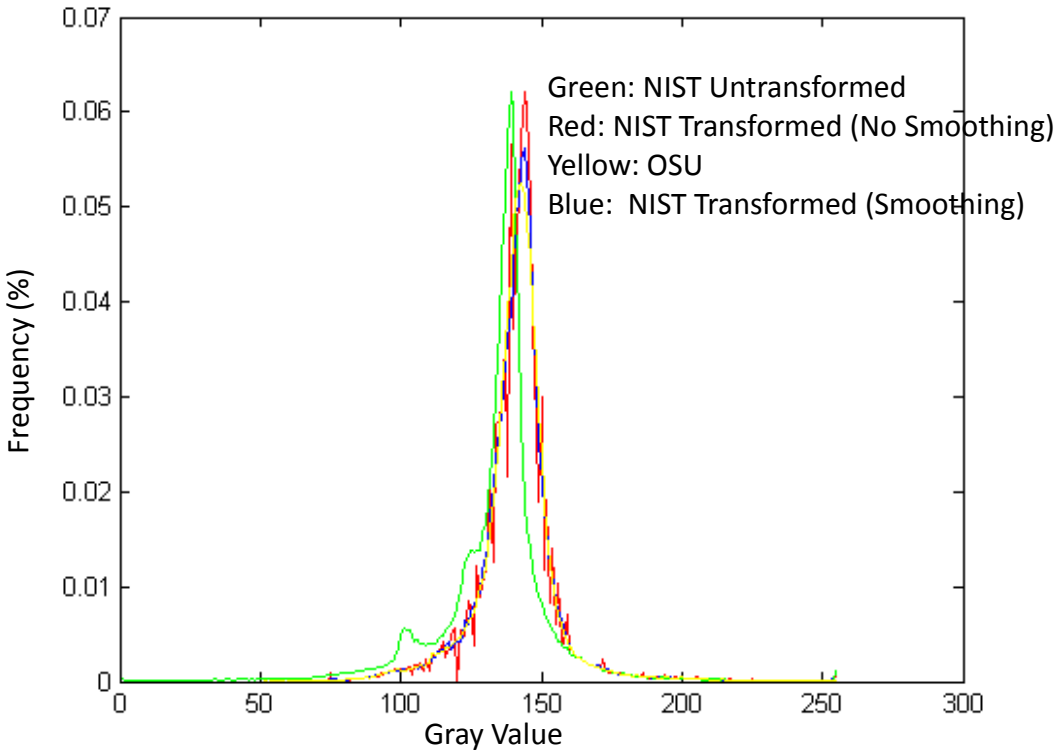

Figure 31: Histogram transformation comparison.

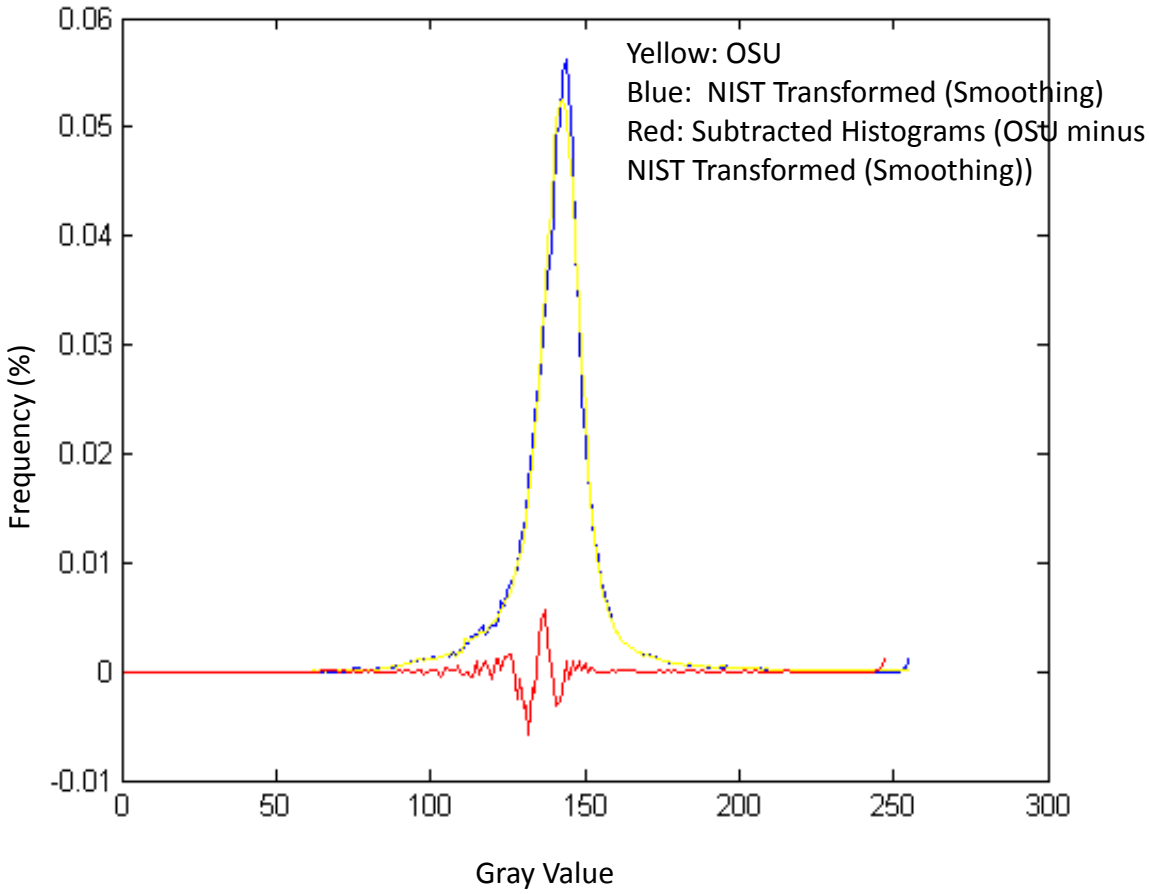

Figure 32: Histogram transformation comparison with histogram subtraction.

IMAGE ANALYSIS - COLOR SEGMENTATION

Once the transformation process has been completed and a BSE image of the reference particle has been created that accurately represents the gray values that define specific chemistries in the particles discovered by AFA, gray value threshold for these chemistries are established. Gray value thresholds are created that define a range of gray values that represent the portion of the reference particle occupied by each color in the color segmented map developed by SEDS analysis. Figure 33 shows the transformed BSE image of particle 2C and the color segmented map of the same particle. Notice how the gray-scale image has a contrast that matches the color segmented image. Since each color in the SEDS color segmented map represents a unique chemical composition in the particle and the BSE image of this same particle represents the

chemical contrast of the particle, through the "atomic number" contrast mechanism, there is a natural correlation between the color segmented map and the BSE image.

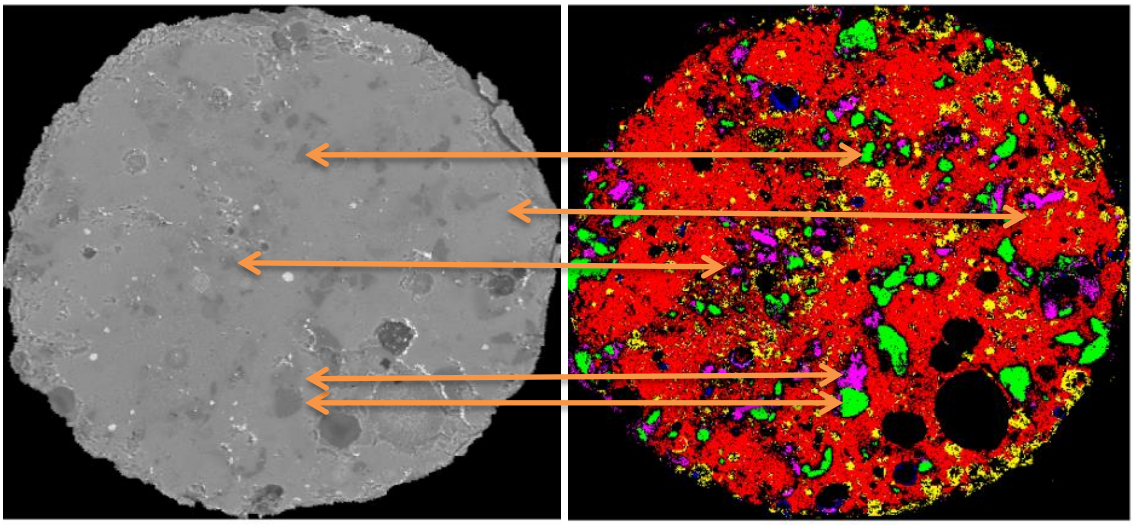

Figure 33: BSE image of particle 2C (Left). SEDS color segmented map of particle 2C (Right).

The process of defining gray-scale chemical thresholds is presented here. First, a gray-scale histogram of each color is created by viewing only the gray values occupying the same space in the BSE image as the color of interest in the color map. This requires that the orientation of the BSE image of the reference particle be identical to the color segmented map. For this reason it is essential that the BSE image of the reference particle used in SEDS at NIST be used to define the gray-scale chemical thresholds since it is guaranteed that its orientation is identical. We can't guarantee that a BSE image of the reference particle taken at OSU will have the identical orientation as the SEDS color segmented map, recall transformation requirement No.1.

In order to define gray-scale chemical thresholds the color of interest in the SEDS color segmented map is viewed exclusively. Once this color exclusive image has been created the same regions in the transformed BSE image are viewed and a gray-scale histogram is created. Figure 34 illustrates this process for the red phase. All regions in Figure 34B are turned off except the red regions. This image is illustrated in Figure 34D. Next, the regions in Figure 34A

that occupy the exact space as Figure 34D are turned on. This image is illustrated in Figure 34C. The histogram for Figure 34C is then plotted and represents the gray-scale distribution for the red phase and is the first step in establishing gray-scale chemical thresholds for this phase. This process is repeated for the green, blue, yellow, and magenta chemical phases.

The green phase required a slight modification due to its non- bell shaped curve. The gray-scale histogram for the green phase showed a shelf towards the right side of the histogram. This shelf was thought to be incorrect since none of the other phases experienced this behavior. An error in the SEDS Analysis could be the cause of this shelf. In order to eliminate this shelf a "shelf modification" factor was created. This factor acts to clip the shelf off and is developed iteratively until only the shelf is eliminated. Figure 35 illustrates the shelf modification and resulting green phase gray-scale histogram creation. Notice how once a "shelf modification" factor of 133 is applied to the histogram that the shelf becomes clipped and no longer exists. The histogram generation is shown by an arrow diagram in Figure 35, for a sample green region, starting at the color segmented chemical map developed by SEDS Analysis and ending with the clipped histogram. Notice the importance of orientation of the BSE image and the SEDS image.

Once the gray-scale histogram for each color is created they are plotted together and gray value thresholds for each color are determined. Figure 36 shows the red, green, blue, yellow, and magenta gray-scale histograms plotted together. Upon examination of the gray-scale histograms for each color it is evident that the red and green chemical phases are the only phases with gray-scale thresholds that can be evaluated. The yellow phase occupies much of the same gray value range as the red phase and the red phase has a much higher frequency over this range of gray values; therefore, the red phase is considered the dominant phase for this range of gray values. The blue and magenta phases occupy the range of gray values occupied by the red and green phases and so it is not feasible to specify gray value thresholds for the blue and magenta phases since the red and green phases have higher frequencies. It is apparent that the red and green

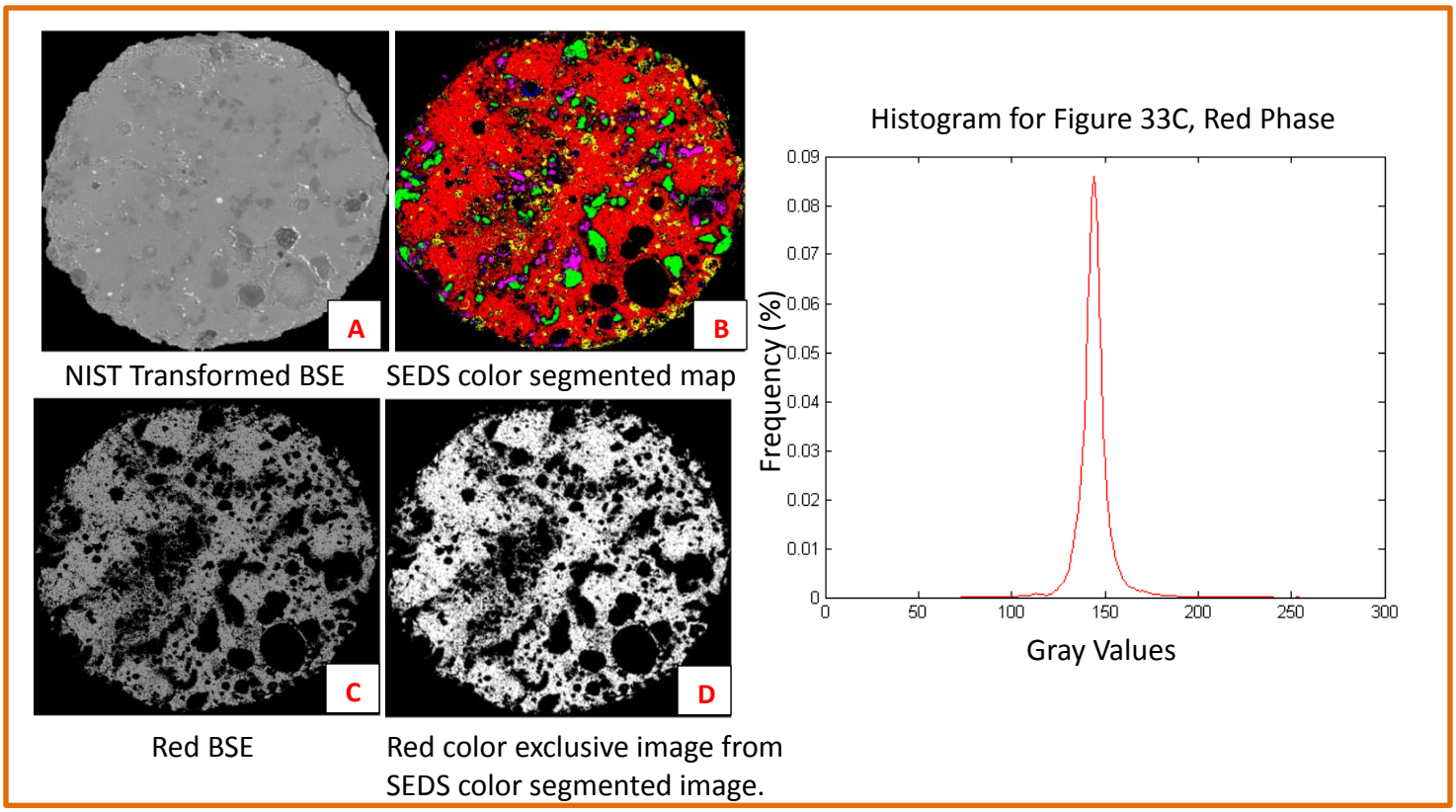

Figure 34: Color exclusive gray-scale histogram creation for the red chemical phase for particle 2C.

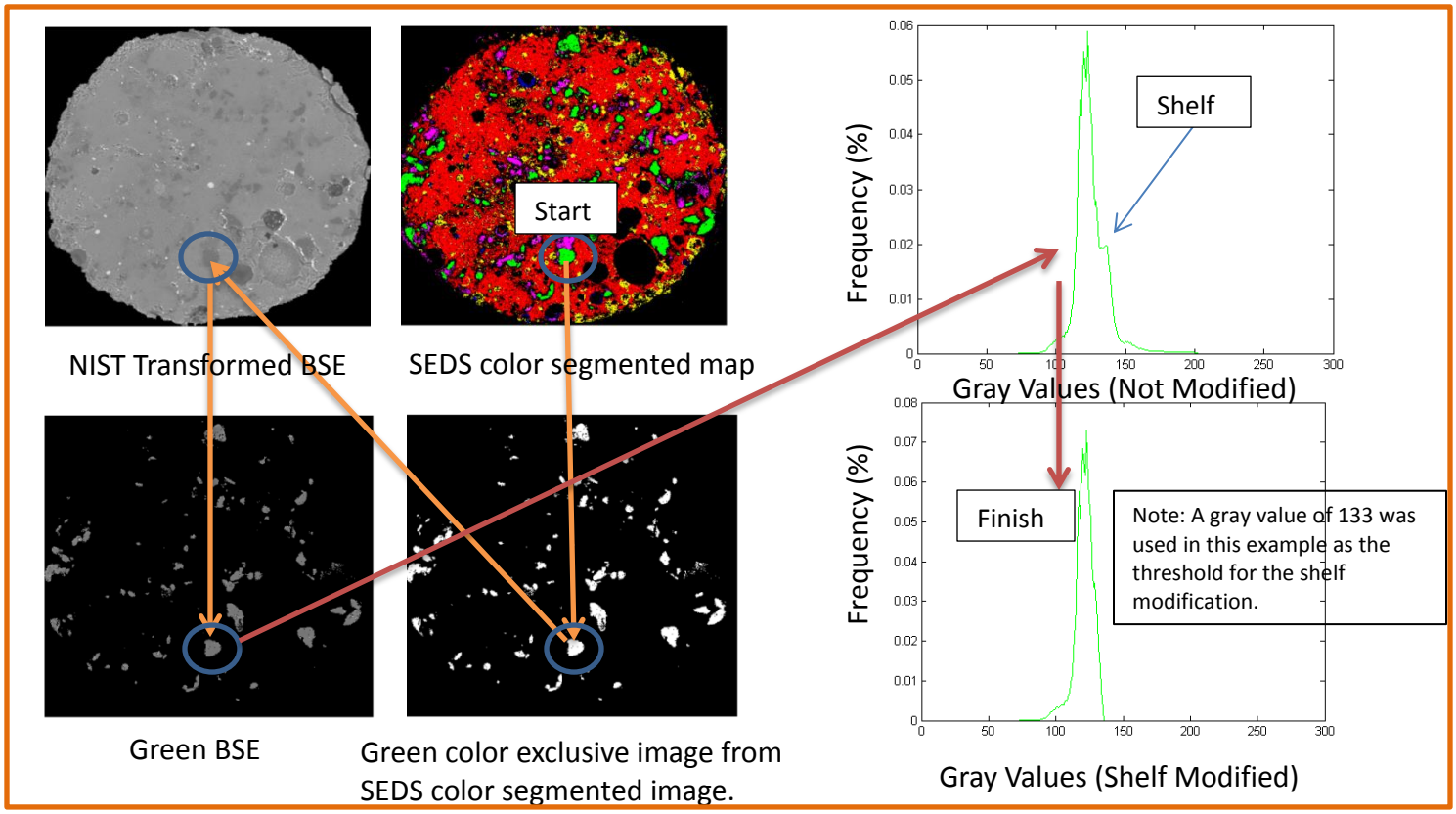

Figure 35: Color exclusive gray-scale histogram creation for the green chemical phase for particle 2C.

chemical phases are the most dominant phases present for the ranges of gray-scale values to be investigated and useful information can be obtained by classifying fly ash particles discovered in AFA as either red, green, mixture, or other.

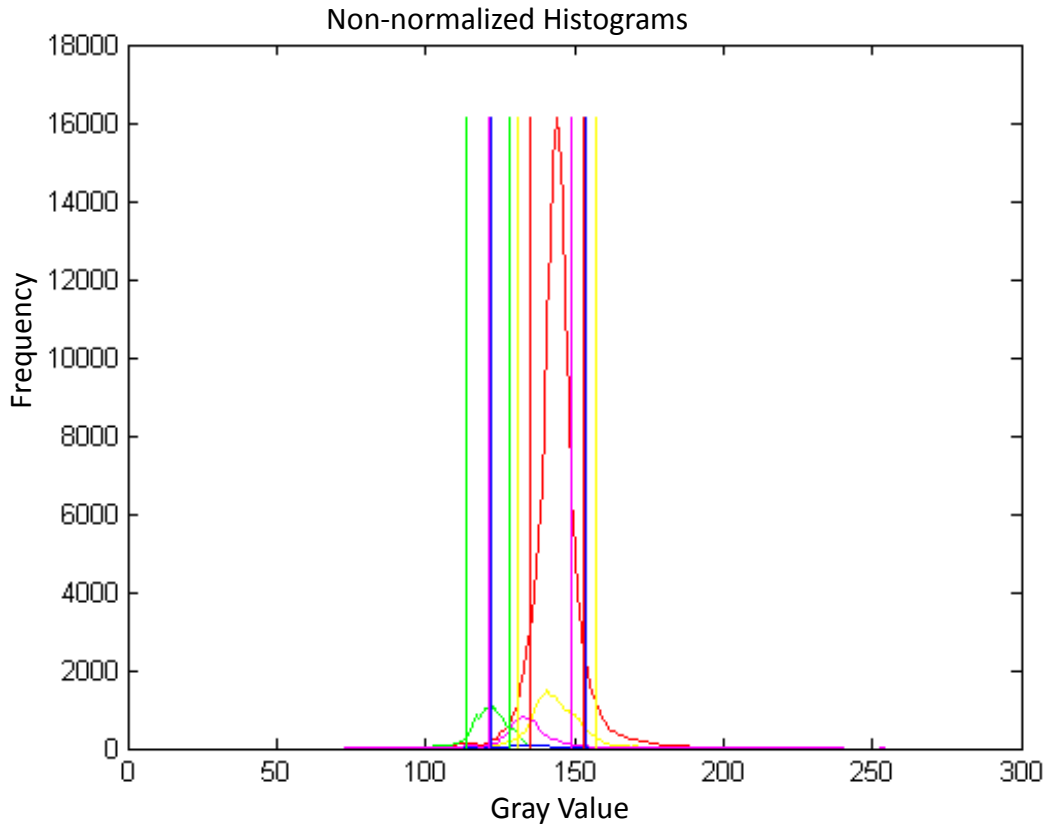

Figure 36: Color segmented gray-scale histogram comparison with vertical lines representing one standard deviation.

Since the frequency of occurrence of gray values showed to be approximately normally distributed the mean gray value for the green phase plus or minus one standard deviation and the mean gray value for the red phase minus one standard deviation and plus two standard deviations was decided to represent the gray-scale range defining the red and green chemical phases (Figure 37). This prevented overlapping of the threshold values for the lower red phase threshold and the upper green phase threshold and represented the chemical data well. The gray values with the highest frequency of occurrence in each chemical phase would probably best define that phase while the gray values with the lowest occurrence do not necessarily reflect the chemical phase

they occupy in the color segmented map from SEDS Analysis. For example, Figure 37 shows the red and green chemical phase gray-scale histograms with both containing a peak of highest occurrence of a specific gray value along with a decrease in frequency as the gray values deviate further from this peak. As the gray values increase for the green phase and decease for the red phase they eventually intersect. Clearly the gray values in this overlap are not specific to one chemical phase; therefore, it is fair to say that as the gray values progressively deviate from the peak occurrence gray value of a single phase, the red phase for instance, that their distinct representation of that single phase decreases. Using this logic it is desirable to define a gray-scale range that minimizes the deviation from the peak occurrence.

One standard deviation from the mean gray value for the green phase and one standard deviation to the left and two standard deviations to the right for the red phase was used to determine the upper and lower gray-scale thresholds for the green and red phases. This resulted in a tolerable amount of deviation from the peak value of occurrence. In this example the mean gray values for the red and green phases were 144 and 121, respectively. The standard deviations were 9 and 7 for the red and green phases, respectively. These values resulted in a range of gray values defining the red phase and green phase of 135 to 162 and 114 to 128, respectively. The range for the mixture phase is 129 to 134. The chemistry verification section in the results chapter, Chapter 6, will confirm the accuracy of this threshold determination technique. The lower range is defined as all gray-values less than the least green phase threshold and the high range is defined as all gray-values larger than the largest red phase threshold. These thresholds will be used to evaluate the chemical composition of discovered particles from BSE AFA images and will likely vary between different analyses since they are derived using the transformed BSE image of the reference particle taken prior to each analysis.

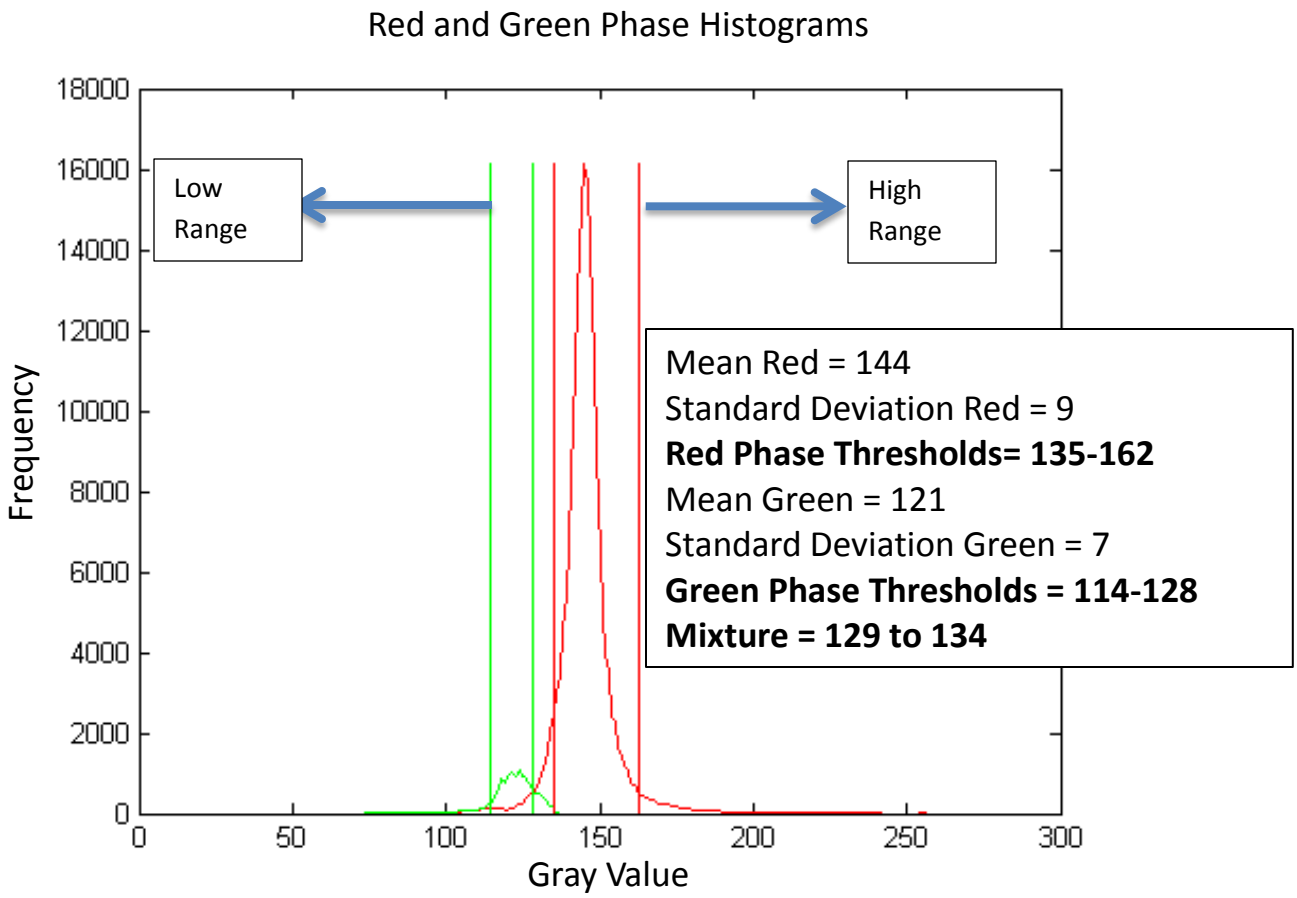

Figure 37: Red and Green chemical phase histogram comparison and corresponding thresholds, particle 2C.

IMAGE ANALYSIS – AFA STAGE FIELD EVALUATION

Now that accurate gray-scale chemical thresholds have been defined, through the use of SEDS Analysis and the transformed BSE image of the reference particle, the primary chemical composition of the particles discovered in the AFA stage field BSE images can be determined. A search and classify process is performed by opening each individual BSE stage field image found during AFA and processing each image through a set of search criteria to identify fly ash particles in these stage field images. Once particles have been identified their gray-scale histograms are compared to the gray-scale chemical threshold limits determined during the image analysis color segmentation portion of this research. The percent of each particle occupying the red and green chemical phases as well as the mixed regions are determined by the summation of the pixels

assigned gray-values within these threshold limits divided by the total number of pixels in the particle. Normalized histograms that represent the percent frequency of each gray value in a particle are used in these analyses. The process of searching the AFA stage field images and classifying each particle as a percent of red, green, or a mixture chemical phase is explained in the following section. There are six search criteria for identifying fly ash particles 1) background clipping, 2) no particle may be in contact with the AFA stage field image boarder, 3) each particle must contain at least 500 pixels, 4) particles must have a major to minor axis ratio less than 1.5, 5) each particle must occupy at least 65% of its individual image, and 6) each particle must have a particle boarder to individual image boarder ration less than 80%. These six search criteria are explained in detail in the following paragraphs.

Search Criterion 1 is the background clipping process. The background is eliminated from stage field images by selecting a gray value that clips all areas of the image with gray values less than this selected value. A gray value of 93 was used in this example for the AFA stage field images. This value was determined iteratively by choosing a value and viewing its impact on a sample of BSE AFA stage field images and may change for different BSE data sets. This value is different than the value of 110, which may also vary from one analysis to another, which was used to clip the background of the reference particle during the transformation portion of the image analysis process. The reason a different value is used in the AFA stage field images is because the process of removing the background is different for AFA images than for the reference particle. Recall that for the reference particle the largest remaining feature is found through a labeling process after initial clipping and its contents are returned to their original gray-scale values. The AFA stage field images are different in that all pixels with gray values less than the determined value, 93 in this case, are set to a gray value of zero and no gray values less than this are intentionally recovered as in the reference particle background clipping process. The reason for the difference in the background elimination procedure is that in the reference particle

image we are only concerned with obtaining a quality image of one particle, particle 2C in this case. Particle 2C is always the largest feature in the reference particle BSE image. It is easy to find the largest single feature in an image and return the contents of this feature back to its original gray-scale values; however, when searching AFA stage field images we are interested in finding all particles in the image and the number of particles could sum to more than one per image. For this reason it was determined beneficial to clip the background then perform five other search criteria on the remaining features until particles were discovered. Once the background has been eliminated the AFA stage field becomes an image containing potential particles on a black background. Figure 38 shows an example of a BSE AFA stage field image with an eliminated background. Figure 39 illustrates background clipping of a theoretical AFA stage field image.

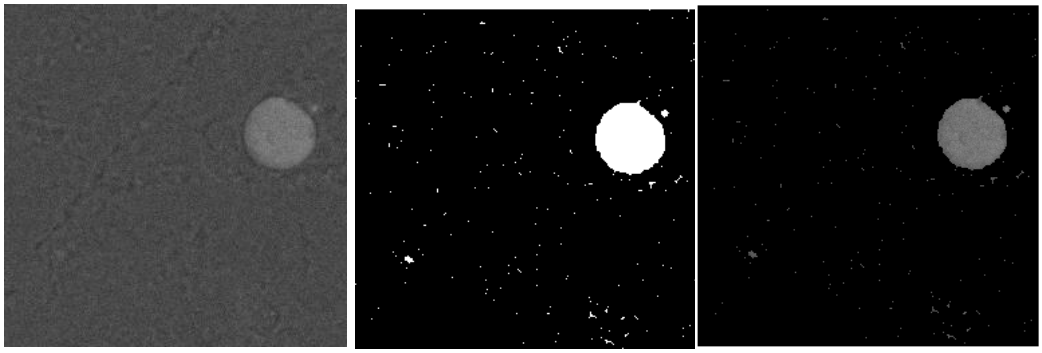

Figure 38: Original AFA stage field image (Left). Only regions in the AFA stage field image with gray values greater than 93 (Center). Gray scale image of AFA stage field with background eliminated (Right).

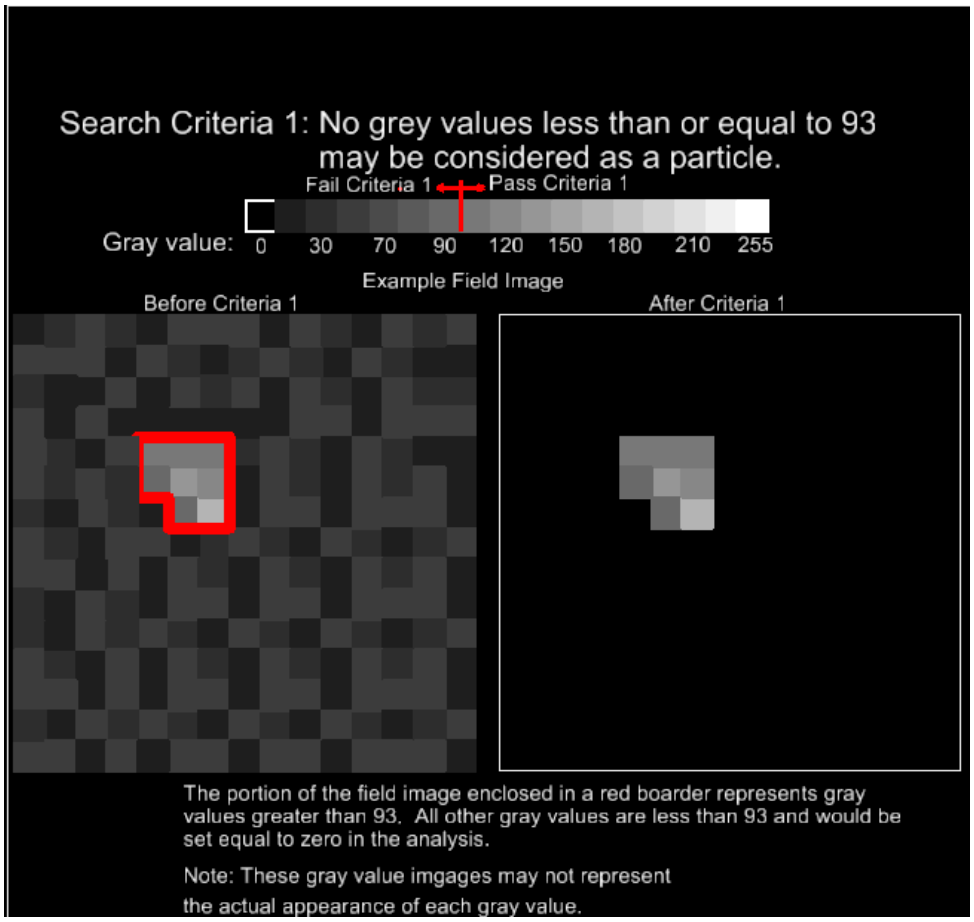

Figure 39: Illustration of Search Criterion 1, background clipping.

Once the background has been eliminated all regions in the image that are not black are classified as a specific label and are potential particles. These labels are then evaluated to reveal fly ash particles and their chemical composition. It is clear that Figure 38 contains one quality fly ash particle. It is desired to allow the Matlab program to make this same evaluation. The remaining five search criteria are performed on these labels to eliminate labels that are not considered to be fly ash particles or do not provide usable information. These criteria are 2) no particle may be in contact with the stage field image boarder, 3) each particle must contain at least 500 pixels, 4) particles must have a major to minor axis ratio less than 1.5, 5) each particle must occupy at least 65% of its individual image, and 6) each particle must have a particle boarder to individual image boarder ration less than 80%. The term particle is used loosely here

in reference to features/labels in the AFA stage field image that may or may not be a fly ash particle. Actual particles are determined upon completion of all of the search criteria. Figure 40 shows an AFA stage field image with a clipped background, using gray value 93, and the remaining features that are specified as labels to be further analyzed. The background clipped image is black and white with the white features becoming labels and the black areas background. The gray-values are restored for these labels if a feature is confirmed to be a particle.

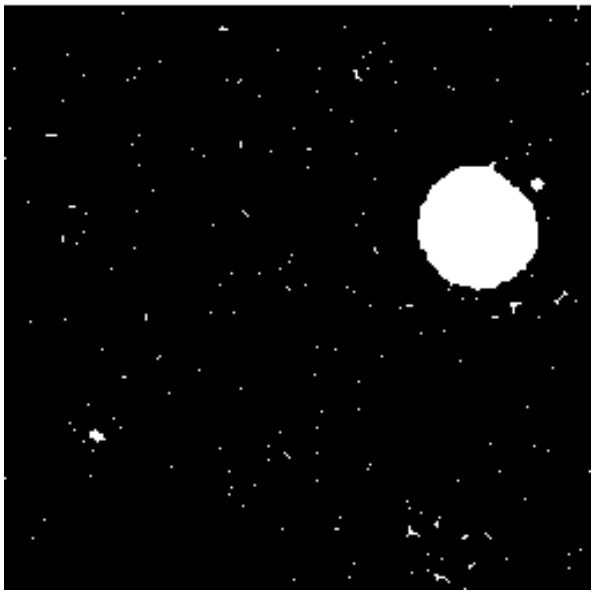

Figure 40: AFA stage field image with a clipped background. Each white feature is designated as a label and is a potential particle.

Search Criterion 2 was developed to eliminate particles that are not fully represented in a single AFA stage field image. Some features only partially occupy a stage field image and the analysis of these features would result in incomplete data for the feature/particle. Figure 41 illustrates the elimination of particles in contact with the AFA stage field image boarder. In order to perform this criterion the boarder of the image is defined and any label containing pixels that are also a part of the AFA stage field image boarder is set to a gray-value of zero, which is black, eliminating this label from the analysis.

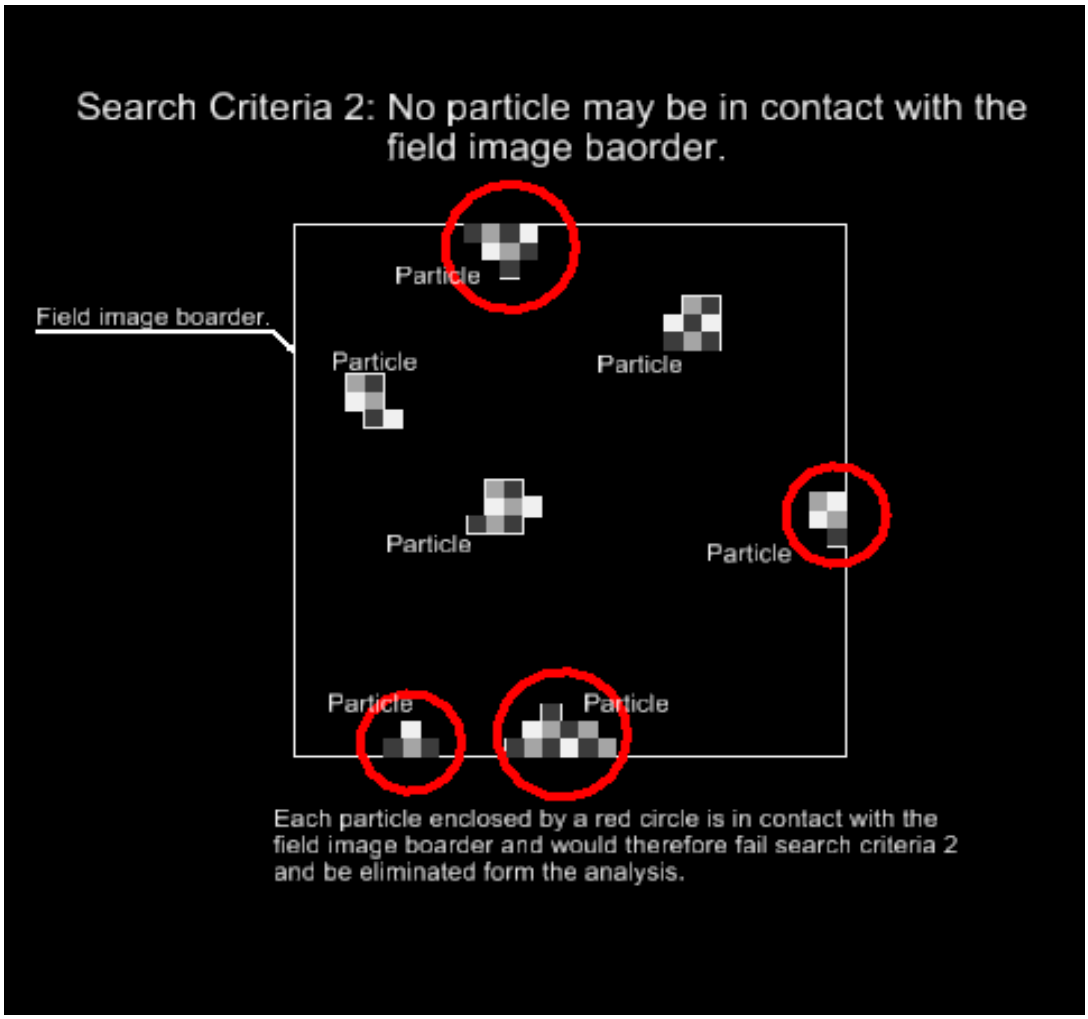

Figure 41: Search Criterion 2, elimination of particles in contact with the AFA stage field boarder.

Search Criterion 3 eliminates all particles comprised of less than 500 pixels. This criteria was thought necessary in order to discard particles that would not provide a sufficient amount of information regarding its chemistry and to eliminate features that were not particles. Particles with a small quantity of pixels produces a small quantity of information concerning the chemistry of the particle since the chemistry of a particle is represented by the number of pixels having a gray value in the red, green, or mixture gray-scale ranges. This criterion was performed by a simple summation of the pixels comprising a label. If this summation was less than 500 then this

label was eliminated by turning all pixels in the label to zero. A value of 500 was determined iteratively until satisfactory results were obtained. Figure 42 illustrates Search Criterion 3.

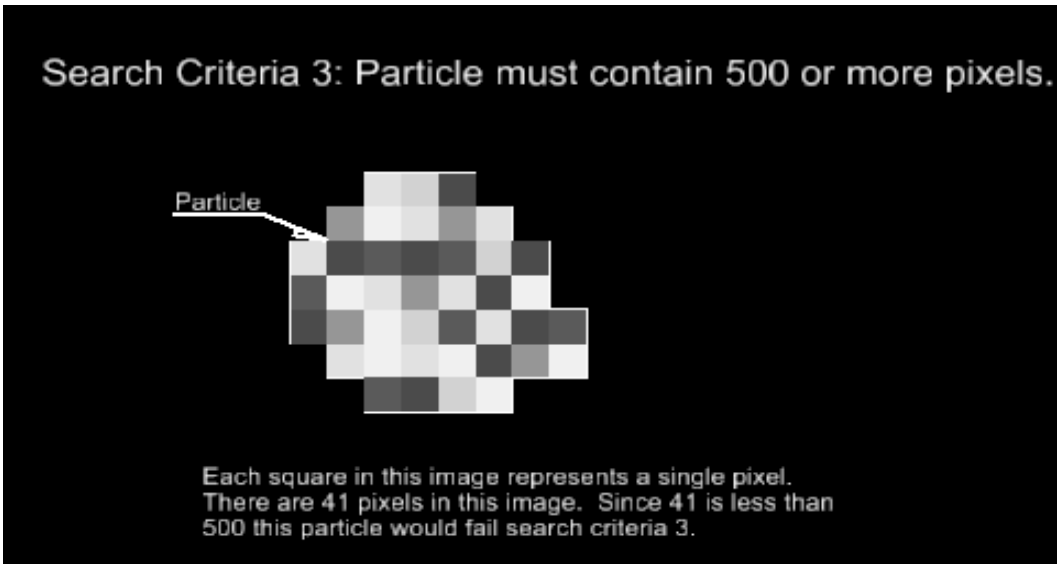

Figure 42: Search Criterion 3, no particle can be comprised of less than 500 pixels.

Search Criterion 4 acts to restrict the analysis to particles approaching approximately circular. Fly ash is a fine grained material consisting of mostly spherical, glassy particles (Malhotra & Ramezanianpour, 1994). An eginvalue problem used in linear algebra was performed to develop a ratio that represents the relationship between the major and minor axis of the particle using Principal Component Analysis (PCA). PCA calculates orthoganal eigenvectors that represent the major and minor axes of the particle. Eigenvalues represent the magnitude of its corresponding eigenvector; therefore, the ratio of the largest eigenvalue to the smallest will represent the particles deviation from circular. All labels with eigenvalue ratios greater than 1.5 are eliminated from the analysis. Figure 43 illustrates the goal of search criterion 4.

Search Criterion 5 is an extension to Criterion 4 as it acts to control the irregularity of the shape of the particle so that only particles approximatley circular and without anomalies are analyzed. If Search Criterion 4 is passed then the remainng label is saved as an image with a boarder size just fitting the label (Figure 44). This particel specific image is furthur analyzed

with Criterion 5. Search Criterion 5 says that each feature must occupy, at a minimum, 65% of the particle specific image. This value was determined iteratively until satisfactory results were obtained. This criterion is accomplished by summing all of the pixles in the particle and dividing this result by the total number of pixels in the particle specific image. The resulting ratio is then examined. Figure 45 illustrates Search Criterion 5.

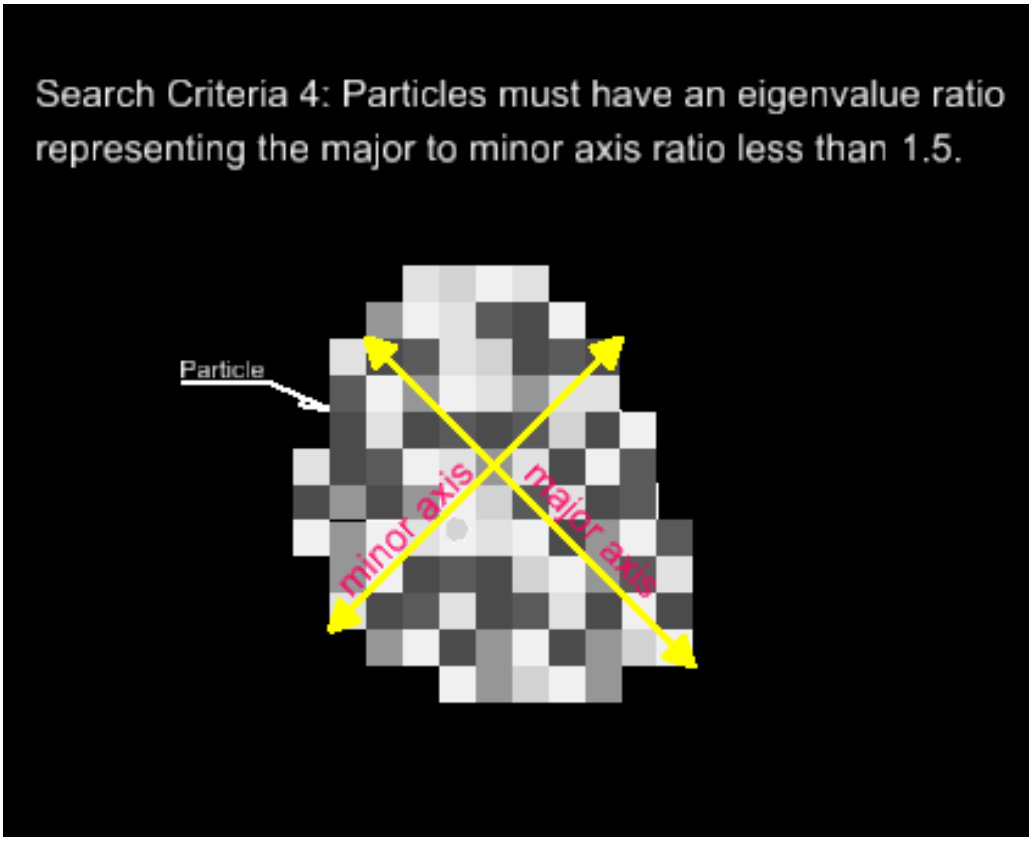

Figure 43: Illustration representing the goal of search criterion 4.

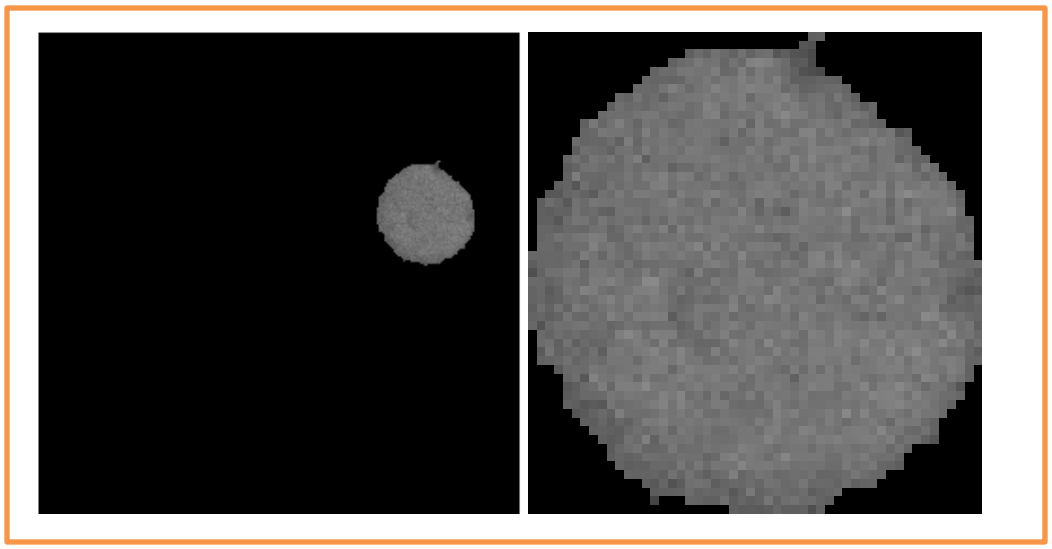

Figure 44: Particles remaining in AFA stage field image after Search Criterion 4 (Left). Particle specific image with a boarder just fitting the particle (Right).

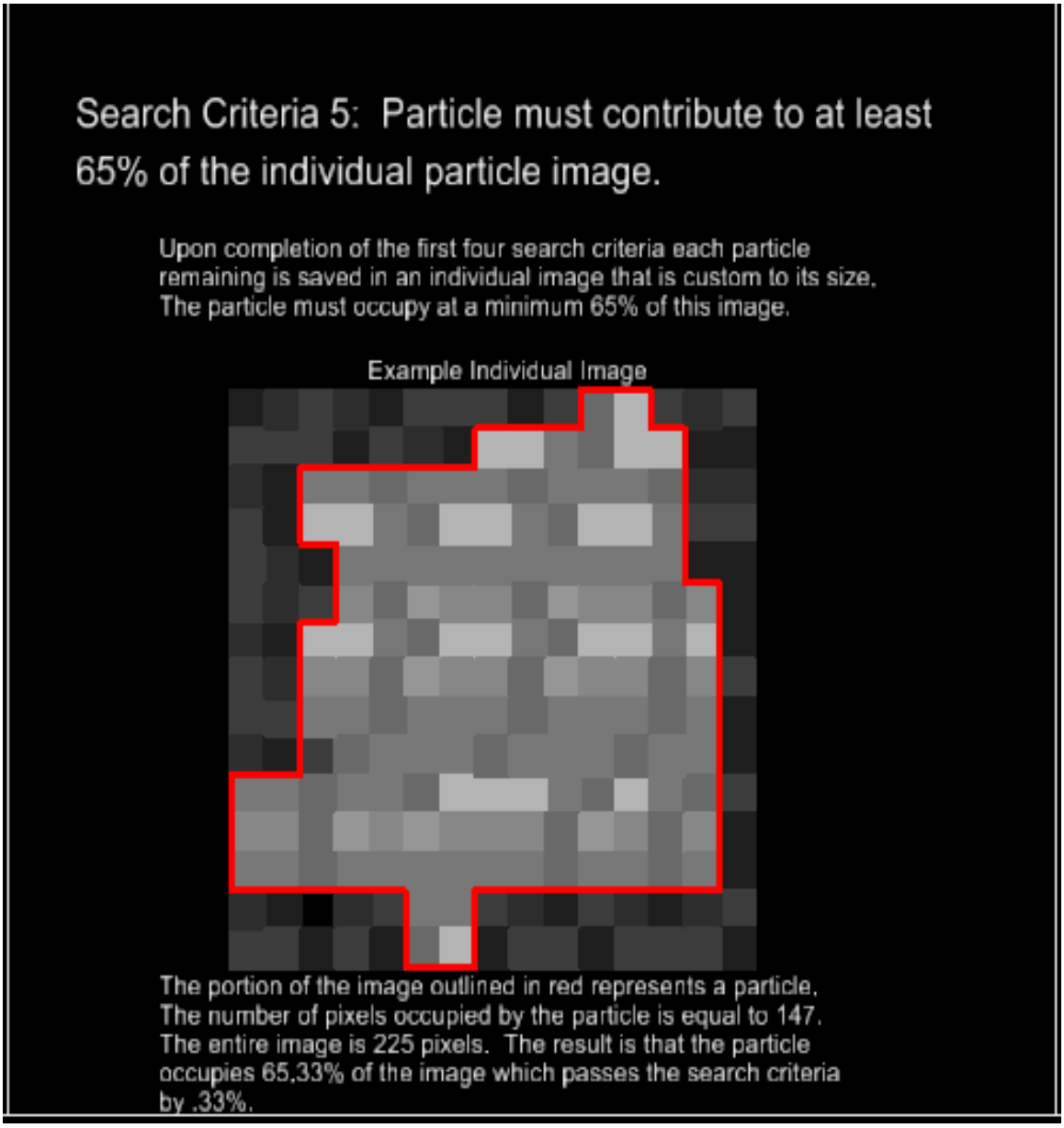

Figure 45: Illustration of Search Criterion 5.

Search Criterion 6 is another filter for particles that may not be circular. This criterion compares the number of pixels comprising the particles boarder to the number of pixels comprising the particles custom image boarder. This ratio has a maximum value of 80% which

was determined by calculating the ratio of a perfect circle contained in a square with side lengths equal to the diameter of the circle. For instance if a circle of radius R= 2.5, units not important if consistent, were contained in an L x L square, where L=5, the ratio of the circle's circumference to the squares perimeter would be $2 \times \pi \times R \div 4 \times L$ and equal .785. This is the perfect scenario and the ratio as a percentage would be 78.5%. This research allowed 1.5% deviation from this ideal situation. Figure 46 illustrates Search Criterion 6.

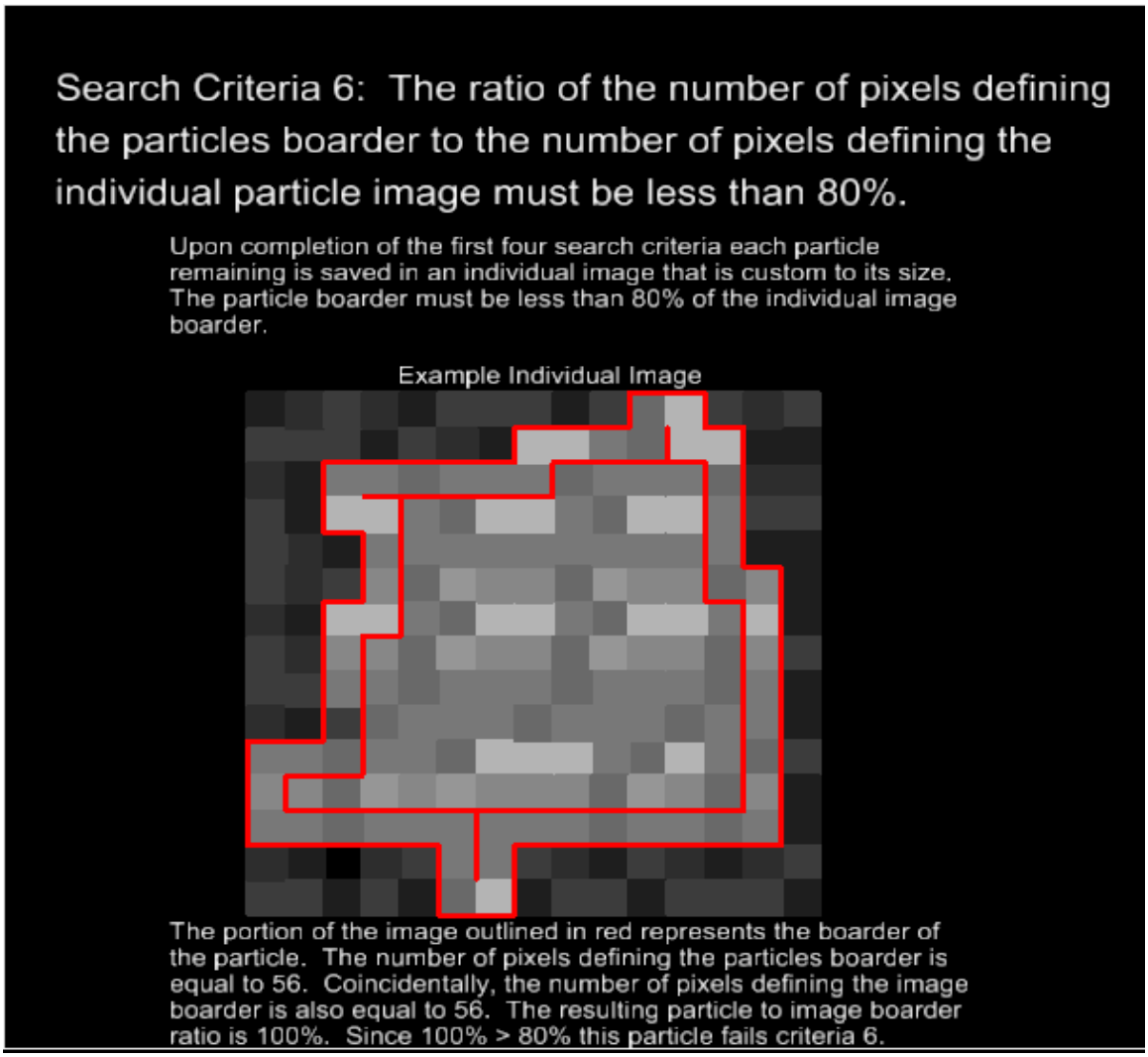

Figure 46: Illustration of Search Criterion 6.

The previously described search criteria act to eliminate all features, which are specified as labels in the analysis, that are not particles or that do not provide useful information about the particles. Once these six criteria have been performed on the original BSE AFA stage field image the remaining particles can be analyzed with confidence. Figure 47 demonstrates the process of analyzing a BSE AFA stage field image containing a usable particle and Figure 48 demonstrates

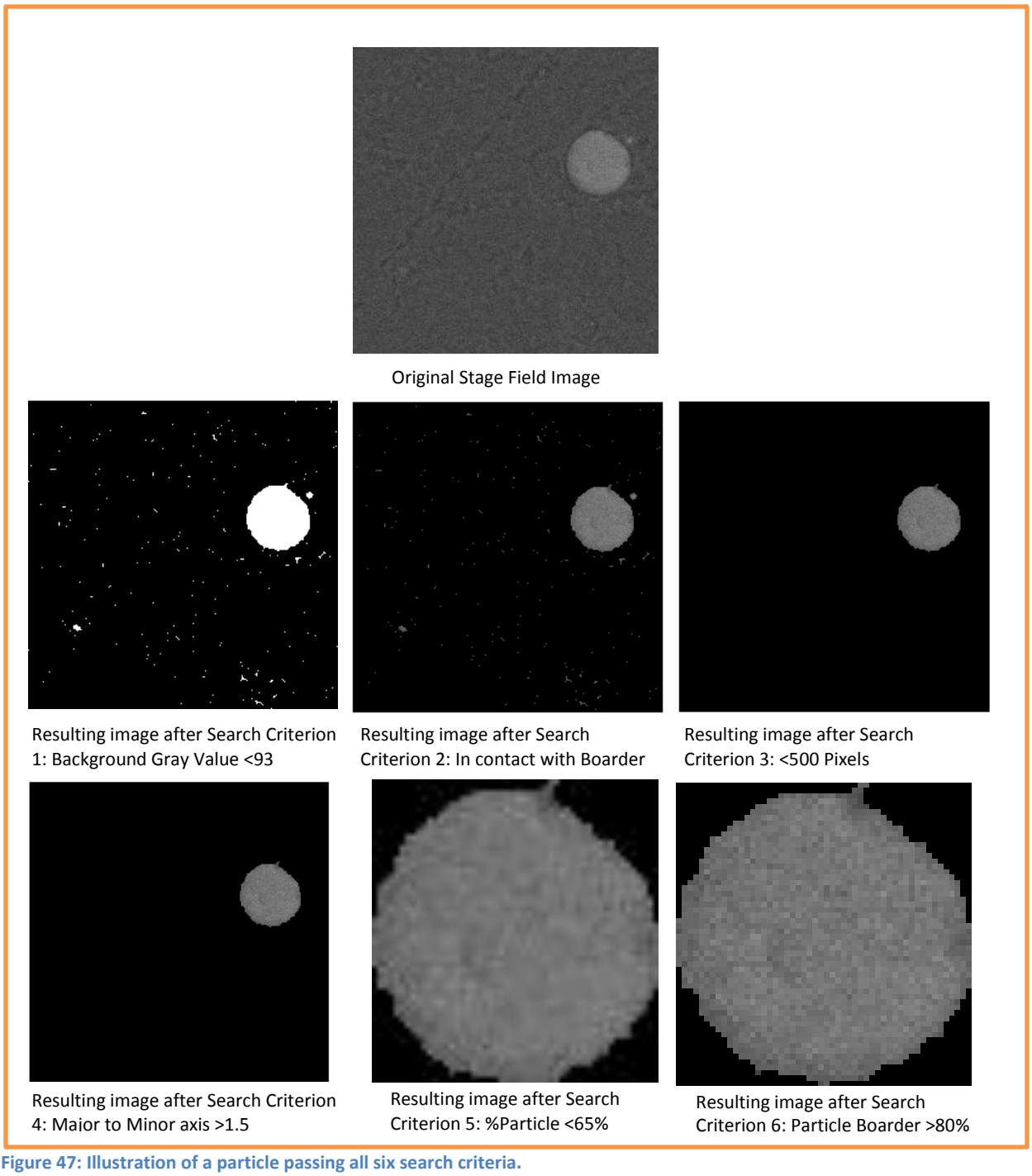

Figure 47: Illustration of a particle passing all six search criteria.

the process of analyzing a stage field image that does not contain a usable particle.

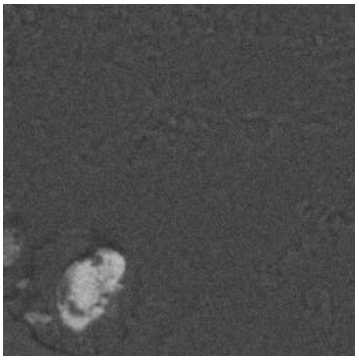

Original AFA stage field image.

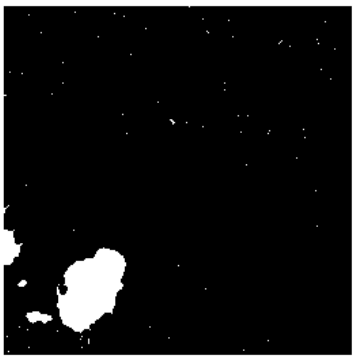

Resulting image after Search Criterion 1: Background Gray Value <93.

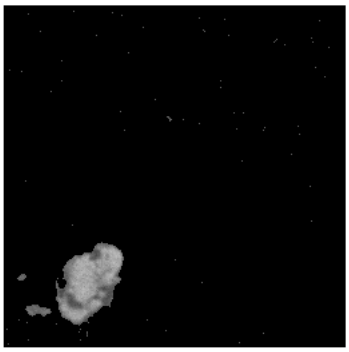

Resulting image after Search Criterion 2: In contact with Boarder.

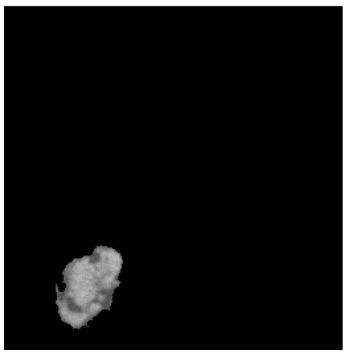

Resulting image after Search Criterion 3: <500 Pixel.

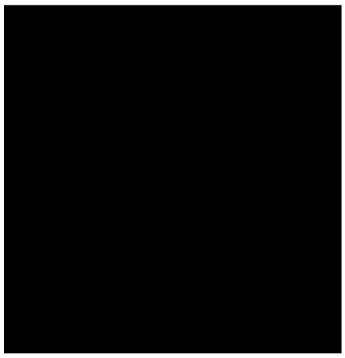

Resulting image after Search Criterion 4: Axis ratio >1.5 (No Particles Remain).

Figure 48: Illustration of a particle failing a search criterion.

Once a BSE AFA stage field image has been analyzed and particles are found the gray-scale histograms for the discovered particles are calculated and compared to the gray-scale

chemical thresholds developed during color segmentation. The percent on cross-section of the red, green, and mixture chemical phases comprising each particle are calculated by the summation of the pixels having gray values in these respective ranges. The diameter of each particle's cross-section is also calculated by taking the average of the size of the custom individual particle image saved after search criterion 4 is passed. The pixel size must also be obtained by viewing the properties of the BSE AFA stage field images and then entered in the program for the diameter to be calculated accurately. Once the pixel size in the AFA images has been determined the program multiplies this value by the average size of the custom image. For example, if the custom image were 50 pixels by 52 pixels the average size would be 51 pixels and if each pixel were 0.30 µm then the cross-section diameter would be $51 \times 0.30 = 15.3$ µm. Figure 49 shows an example of the final results of analyzing a BSE image. Each BSE AFA stage field image is individually analyzed using the previously described search and analyze technique and the results are presented in a table.

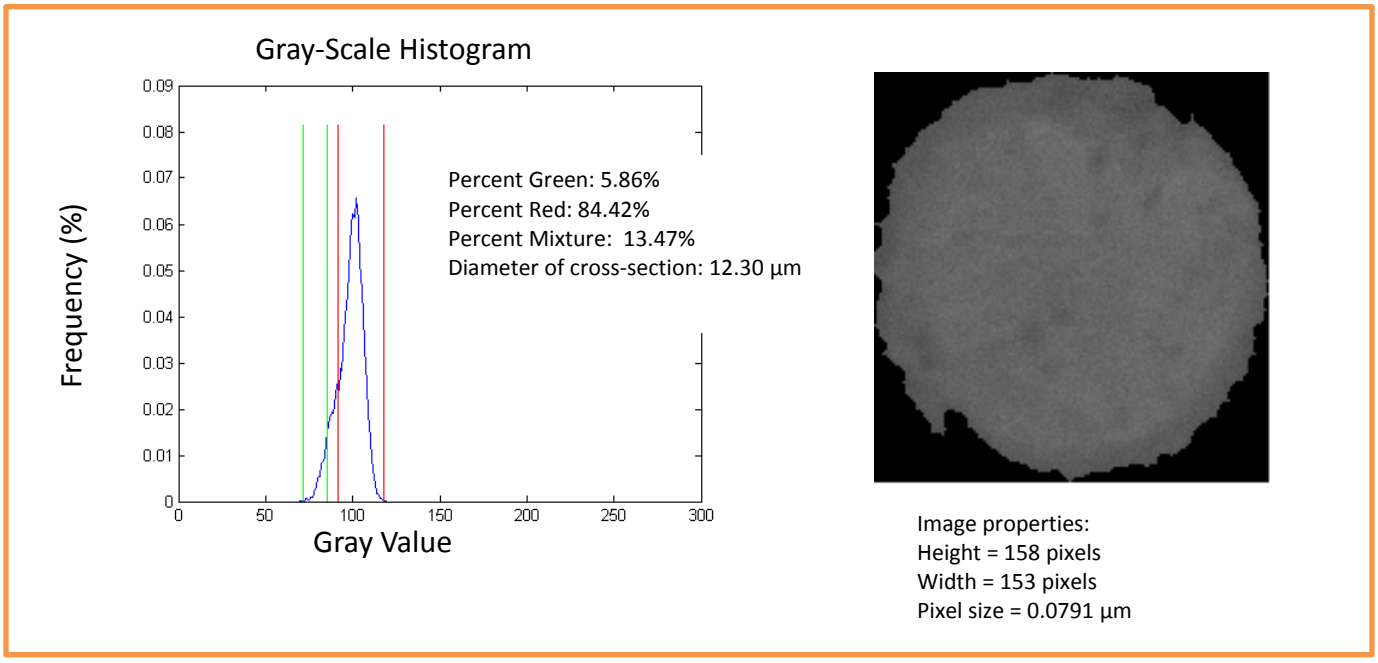

Figure 49: Gray-scale histogram with red and green gray-scale chemical thresholds shown by vertical lines (Left). Particle having the gray-scale histogram shown (Right).

Thus far the process of creating gray-scale chemical thresholds by way of transformation and color segmentation, finding particles present in BSE AFA stage field images, and analyzing the discovered particles to reveal the primary chemical phases present by comparing their gray-scale histograms to the calculated chemical thresholds has been described in detail. In the next chapter, Chapter 6, the chemical composition of the red and green phases as determined by SEDS Analysis will be presented. This information is fundamental to the interpretation of the results of this automated rapid particle investigation technique.

METHODOLOGY - SUMMARY

Now that the complete process of Automated Rapid Particle Investigation (ARPI) has been described in detail a brief summary of this process will be presented. The goal of this research is to rapidly evaluate particles to reveal the primary chemical composition of these particles. The first step in this process is to provide flat polished surfaces of particles so that they can be imaged with an SEM to produce BSE images. This is done by embedding particles in an epoxy puck, polishing this puck with diamond slurry until smooth cross-sections of the embedded particles are revealed, and then running AFA on the polished puck. AFA produces a data set of BSE stage field images that are then analyzed with a Matlab program to reveal the chemical composition of the embedded particles. The Matlab algorithm can be found in Appendix B. This program creates gray-scale chemical thresholds based on the results from a SEDS Analysis performed at NIST. Once gray-scale chemical thresholds are determined each AFA stage field image is individually searched and all usable particles are discovered. The gray values of the discovered particles are compared to the previously developed thresholds and the area percent on cross-section of each chemical phase present in each particle as well as the cross-section diameter of each particle is calculated and presented.

CHAPTER VI

RESULTS

CHEMISTRY IDENTIFICATION

ASTM Class C fly ash acquired from Harrington coal-fired power plant was used exclusively in this research. All samples and the reference particle were Harrington Class C ash. The results of analyzing five manual BSE images are presented here; however, quality images produced by AFA could be analyzed as well. Table 2 shows the settings used in the analysis. These settings include the SEM beam and imaging settings, reference particle transformation settings used in the image analysis procedure, the gray-scale chemical threshold value determination settings, and the AFA stage field search criteria settings. Search criteria 2, 3, 4, 5, and 6 are constant values never changing from the analysis of one BSE data set to another. The SEM beam settings, all background clipping values, the green shelf modification factor, and the gray-scale chemical thresholds may vary from one analysis to another. Trial analyses of sample BSE images and the reference particle BSE image should be performed prior to the Automated Rapid Particle Investigation analysis to confirm all values used.

In order to ensure that only quality particles are found in the analysis process it is necessary to use stringent search criteria to filter the potential particles. Due to the strict search criteria particles are rejected that could be considered a fly ash particle but do not produce usable information. It was deemed necessary to use strict criteria in order to

eliminate particles with anomalies that would result in erroneous results. Five sample BSE images thought to contain a fly ash particle were analyzed using the developed program. The results of the analysis are shown in Table 3. Figure 50 and Figure 51 show the gray-scale histogram of each discovered particle with the red and green gray-scale chemical threshold lines shown vertically. The percent of each particle's cross section comprised of the red, green, and mixture chemical phases as determined by the developed rapid technique is also shown in these figures. Figure 52 shows the diameter distribution for Harrington fly ash (Aboustait, 2013).

Table 2: Automated Rapid Particle Investigation settings.

SEM BEAM SETTINGS					
BEAM ENERGY	FILAMENT	SPOT SIZE	BRIGHTNESS	CONTRAST	WORKING DISTANCE
11 keV	70%	38%	3.27%	100%	11.3 mm
TRANSFORMATION SETTINGS					
BACKGROUND CLIPPING VALUE FOR OSU BSE			BACKGROUND CLIPPING VLAUE FOR NIST BSE		
Gray Value = 67			Gray Value = 0		
GRAY-SCALE CHEMICAL THRESHOLD SETTINGS					
GREEN PHASE GRAY-SCALE RANGE (Green Shelf Modification Factor = 92)			RED PHASE GRAY SCALE RANGE		
Mean gray-scale value +/- 1 standard deviation = 72 to 86			Mean gray-scale value +/- 1 standard deviation = 91 to 118		
AFA STAGE FIELD SEARCH AND ANALYZE SETTINGS					
CRITERION 1	CRITERION 2	CRITERION 3	CRITERION 4	CRITERION 5	CRITERION 6
85	-	500	1.5	65%	80%

Table 3: Automated Rapid Particle Investigation results for 5 BSE images. The area percent on cross-section for each phase comprising each particle is shown.

ARPI Results - Area % on cross-section					
	Green	Red	Mixture	Undefined	Diamter (µm)
P1	5.86	84.42	13.47	0.00	12.30
P2	4.75	69.47	9.04	16.74	14.27
P3	3.87	66.44	5.40	24.29	7.96
P4	5.71	83.93	8.17	2.18	13.73

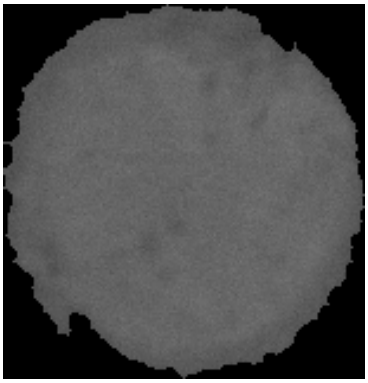

P1

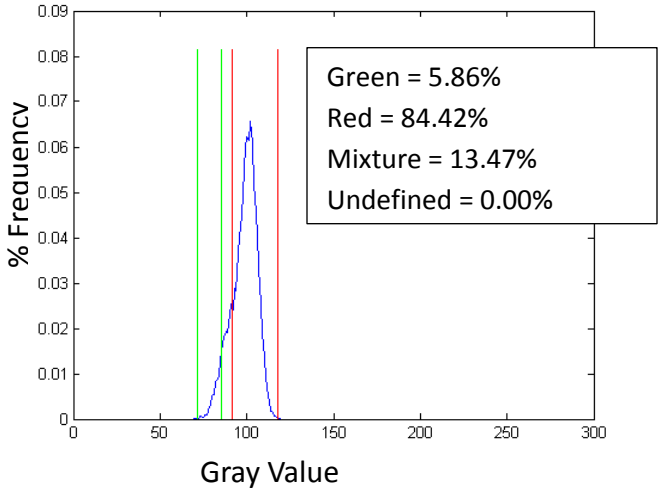

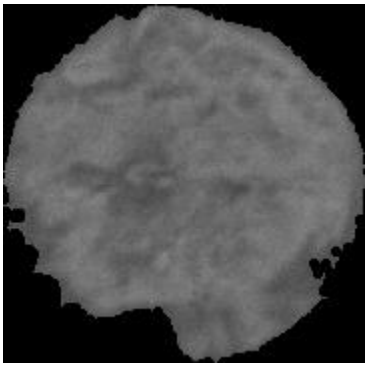

P2

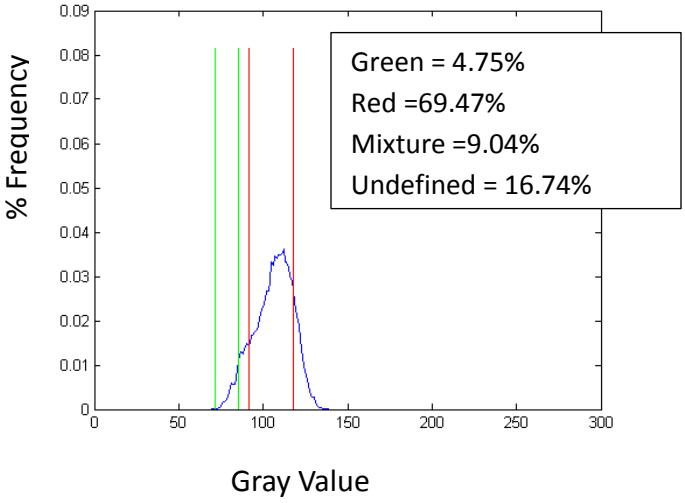

Figure 50: Particles 1 and 2 discovered in the Automated Rapid Particle Investigation analysis.

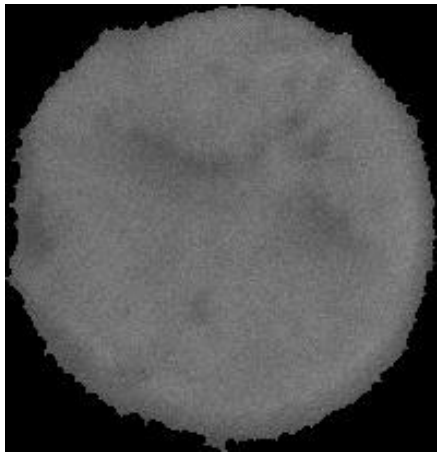

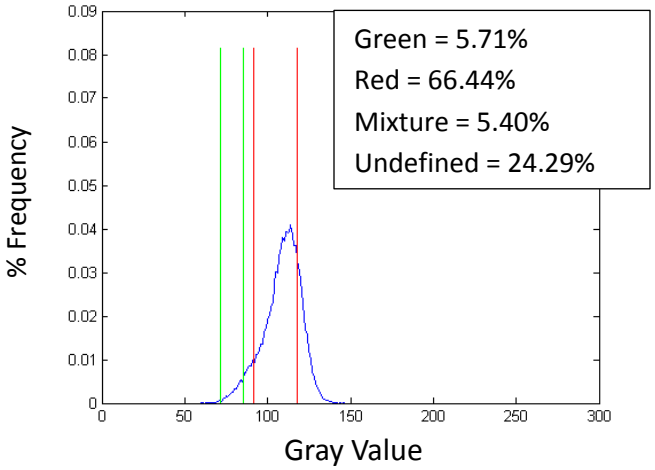

P3

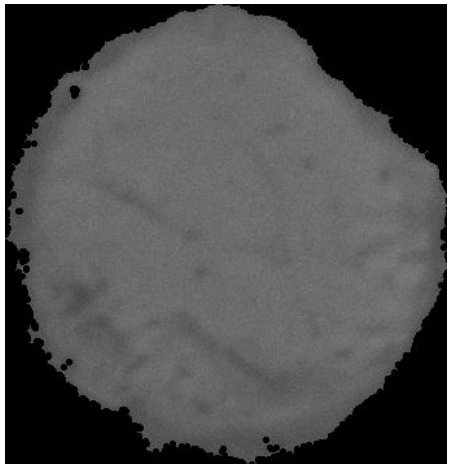

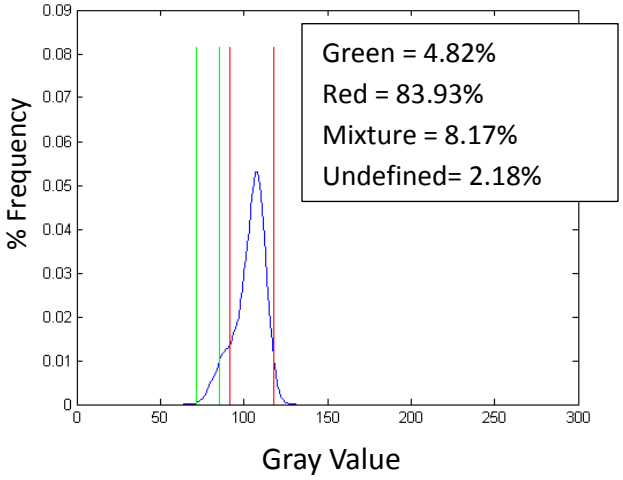

P4

Figure 51: Particles 3 and 4 discovered in the Automated Rapid Particle Investigation analysis.

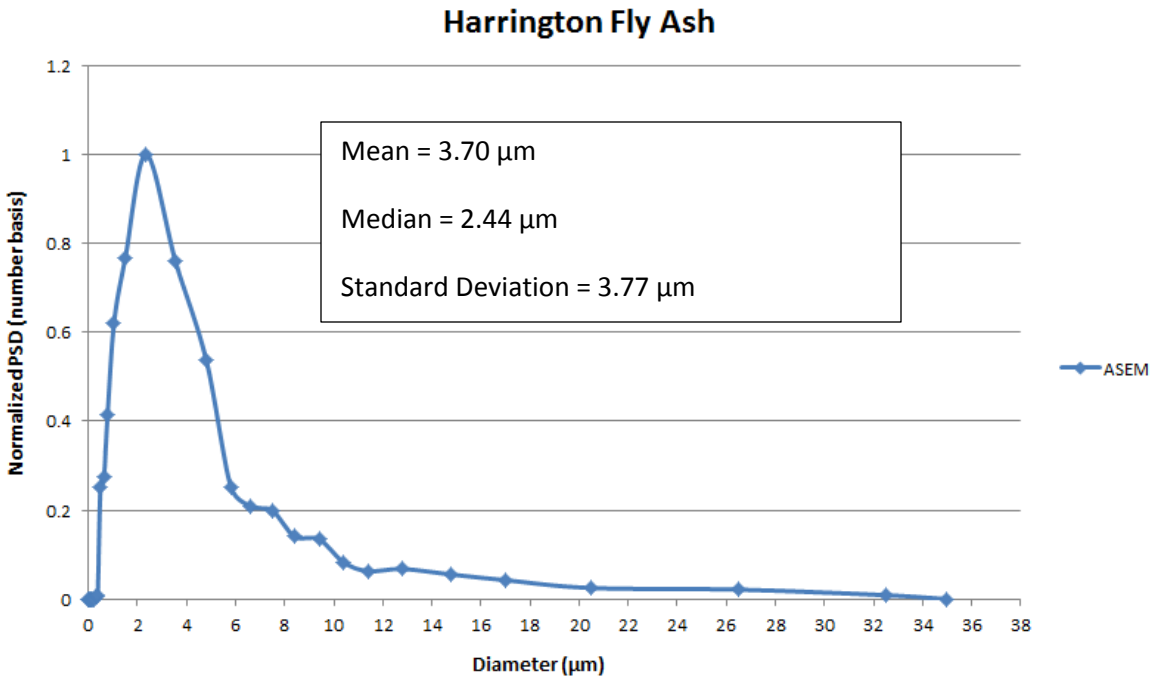

Figure 52: Diameter distribution for Harrington Fly Ash (Aboustait 2013).

Once particles have been discovered and the percent of the green, red, mixture, and undefined chemical phases have been determined for the particles it is necessary to qualitatively describe these phases. Results from the Segmented EDS (SEDS) Analysis at NIST for particle 2C, the reference particle, are used to achieve this. Table 4 shows the results of the SEDS Analysis. The weight percent of all elements comprising the red and green chemical phases as well as one standard deviation are presented in this table. Also, the percent of the cross-sectional area occupied by each phase is shown and is the value that the ARPI results are compared to.

Table 4: Qualitative chemical results for particle 2C in the NIST Segmented EDS Analysis (Hu et al., 2013).

Element		Ca	Si	Al	Fe	O	K	Mg	S	Ti	area % on cross-section
Particle 2C - 427 µm											
red	weight %	24.99	19.94	11.69	12.67	24.00	0.69	3.15	0.99	1.88	83.51
	1σ	6.56	4.87	2.78	5.26	10.01	0.59	1.07	1.11	1.06	
green	weight %	3.47	58.98	1.81	3.58	30.43	0.34	0.42	0.35	0.62	4.44
	1σ	3.88	9.99	1.93	4.46	8.91	0.55	0.50	0.74	1.15	
Magenta	weight %	12.54	32.83	12.27	8.25	26.97	3.47	1.47	0.42	1.78	5.23
	1σ	5.40	9.78	5.99	6.87	9.88	2.02	0.93	0.63	2.10	
Yellow	weight %	15.24	11.50	14.12	28.64	21.05	0.63	6.00	1.39	1.43	6.09
	1σ	4.99	4.83	4.89	13.20	10.42	0.61	2.71	1.37	1.06	
Blue	weight %	21.02	13.33	24.50	10.22	20.72	0.82	2.12	5.82	1.44	0.73
	1σ	14.34	9.90	14.26	7.74	13.33	0.82	1.86	8.35	1.66	

VERIFICATION OF RESULTS - OVERVIEW

In order to verify that the technique presented in this research produces accurate results the ARPI defined red and green regions of particle 2C were analyzed using EDS to determine the percent concentration of the elements present in these regions. These results were compared to the results from the NIST SEDS analysis for particle 2C for the corresponding chemical phase. To further verify the accuracy of this technique the green and red regions as defined by Automated Rapid Particle Investigation were investigated for five sample particles present in the epoxy puck sample using EDS to determine the percent concentration of the elements in these regions. The results were compared to the results from the NIST SEDS analysis. The goal is to compare the chemistry in the regions defined by Automated Rapid Particle Investigation as being the green and red chemical phases to the chemistry of the green and red phases in the NIST SEDS Analysis.

BSE images were taken of particle 2C and the five sample particles. These images were evaluated with Automated Rapid Particle Investigation and gray-scale chemical threshold values for the green and red phases were determined. Once these gray-scale thresholds were found the green and red phases in the BSE images were viewed exclusively to provide guidance in the

location selection for EDS. An example of the resulting green phase exclusive BSE image as well as the resulting red phase exclusive BSE image as determined by the thresholds produced by Automated Rapid Particle Investigation is shown in Figure 53.

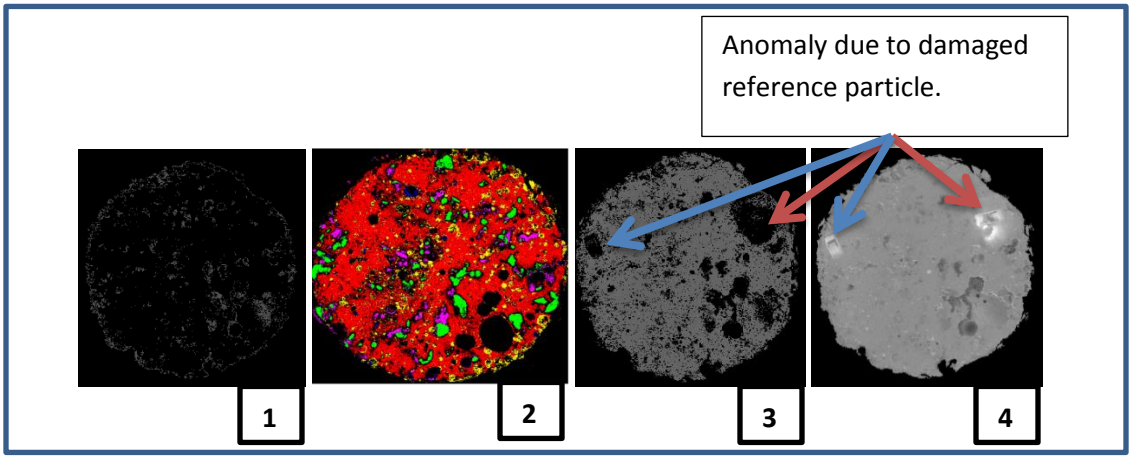

Figure 53: Chemical regions as determined by Automated Rapid Particle Investigation. The green phase (Image 1), red phase (Image 3), color segmented map from NIST SEDS (Image 2), and the complete BSE image of particle 2C taken at OSU (Image 4) are shown.

Once these phase exclusive images have been generated three points defined as the phase of interest were selected to be investigated with EDS and the results of the three point analyses were averaged. The initial output from EDS is a spectrum that represents the counts of a specific element. These spectrums were analyzed using the program DTSA II from NIST to convert the counts into elemental intensities. An elemental intensity is the area under the EDS spectrum peak for a range of energies defining an element. Nine elemental standards were also analyzed in this manner including Na, Mg, Al, Si, S, K, Ca, Ti, and Fe. It should be noted that the oxygen standard was not available for this analysis and since this is a normalized calculation and the NIST SEDS results included oxygen at a high concentration our results will differ slightly from those of SEDS. This will be discussed in further detail later. The calculated elemental intensities from DTSA II were further analyzed by the program CalcZAF. CalcZAF uses elemental standards to calculate k-rations of the elements involved in the investigation. K-rations are the calculated intensities of the elements investigated in a sample divided by the calculated intensities of the corresponding elemental standard. The results of running this analysis are the normalized

elemental concentrations of the elements present in the investigation. Figure 54 illustrates the process of converting EDS counts to elemental concentrations using DTSA II and CalcZAF.

Once the average normalized elemental concentrations have been determined for the three points in regions defined by ARPI as being a specific phase (i.e. green or red) they are compared to the SEDS Analysis results from Table 4. For ease of data comparison the elemental concentrations for the elements present in the analysis are presented in the form of scatter plots. Figure 55 shows the results of the NIST SEDS Analysis for particle 2C, which are presented in Table 4 as well, as scatter plots.

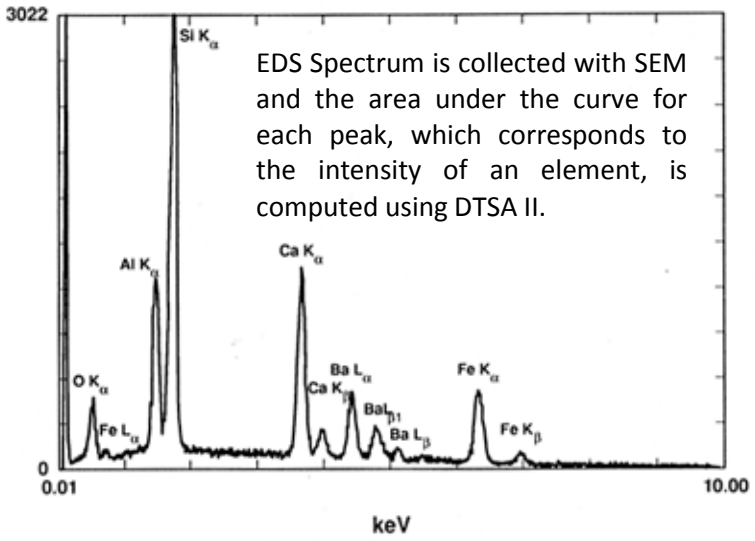

EDS Spectrum is collected with SEM and the area under the curve for each peak, which corresponds to the intensity of an element, is computed using DTSA II.

Intensities are converted to elemental concentration using CalcZAF. K-rations are computed for element i:

$$\frac{I_i}{I_i^{std}} = k_i$$

The uncorrected concentration of a given element i would be:

$$C_i^{unk} = K_i * C_i^{std}$$

Where C_i^{unk} is the desired concentration of element i, K_i is the K-ratio of element i, and C_i^{std} is the concentration of the corresponding standard. Certain interferences such as x-ray absorption need to be corrected for using ZAF correction factors. The Phi-Rho-Z analysis takes into account that the x-ray emissions and absorption occur over the entire interaction volume.

These K- values are inputted into a Geometrically-modified $\phi(\rho z)$ method to give the corrected elemental weight concentration.

Figure 54: The process of elemental converting counts to normalized elemental concentrations.

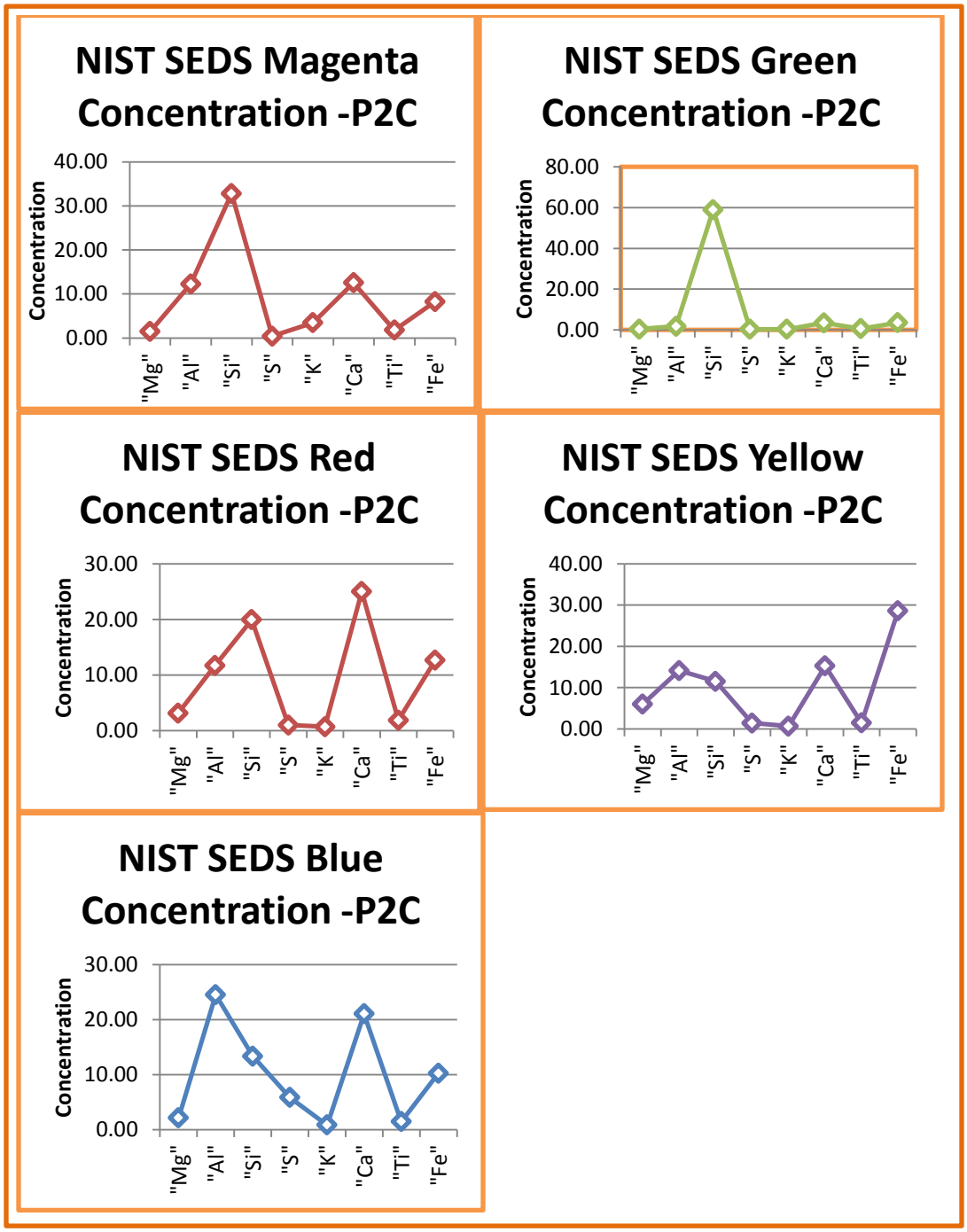

Figure 55: NIST SEDS results shown as scatter plots.

VERIFICATION OF RESULTS – PATICLE 2C RED PHASE

Using the previously described method the normalized elemental concentrations for the red regions as defined by Automated Rapid Particle Investigation (ARPI) for particle 2C were determined and compared to the SEDS results from Table 4. Figure 56 shows the red region of particle 2C as defined by ARPI and the locations of EDS analysis. The results are presented in Table 5 as well as in the form of a scatter plot in Figure 57.

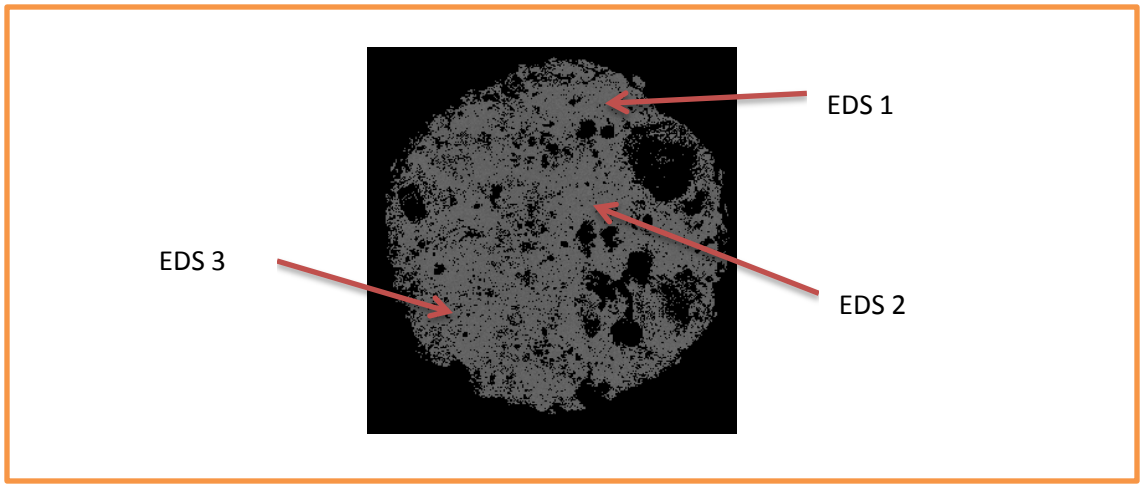

Figure 56: Red phase regions as determined by ARPI and corresponding EDS analysis location.

Table 5: Results of analyzing red regions of particle 2C as defined by Automated Rapid Particle Investigation.

Red phase as determined by ARPI; Normalized elemental concentrations for particle 2C								
	"Mg"	"Al"	"Si"	"S"	"K"	"Ca"	"Ti"	"Fe"
%Weight	3.90	23.46	22.98	4.23	2.78	31.53	3.60	7.86
1σ	3.68	6.46	9.45	1.23	1.86	12.51	4.64	2.70
NIST SEDS Results for the red phase; Normalized elemental concentrations for Particle 2C								
	"Mg"	"Al"	"Si"	"S"	"K"	"Ca"	"Ti"	"Fe"
weight %	3.15	11.69	19.94	0.99	0.69	24.99	1.88	12.67
1σ	1.07	2.78	4.87	1.11	0.59	6.56	1.06	5.26

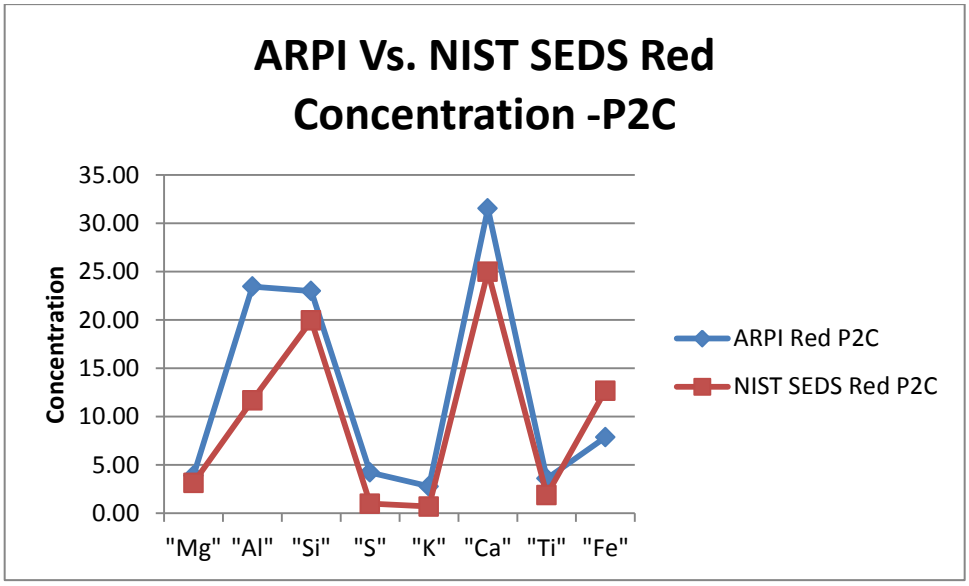

Figure 57: ARPI Vs. SEDS red phase elemental concentration.

The comparison between the normalized elemental concentrations in the ARPI defined red regions and the NIST SEDS results correlate well. Magnesium, silicon, calcium, and iron all fall within one standard deviation of the SEDS results. Aluminum, sulfur, potassium, and titanium do not fall within one standard deviation; in fact, they are all higher in concentration than the SEDS results. There is a trend of an upward shift in the concentrations calculated for regions defined as red according to ARPI. This is likely due to the absence of oxygen in the calculation for the normalized elemental concentrations. Recall that nine standards were available at OSU when verifying the results relative to the NIST SEDS results and oxygen was not among the available standards. Table 4 shows that the concentration of oxygen in the SEDS analysis was 24.00% for the red phase. Since this is a normalized concentration calculation this causes the concentrations calculated at OSU to increase due to the redistribution of the missing 24.00% occupied by oxygen. Taking this into consideration it is not unreasonable to assume that sulfur, potassium, and titanium would fall in the range of one standard deviation of the NIST

SEDS results if oxygen were included in the normalized concentration calculations for ARPI accuracy confirmation. The upward shift of aluminum concentration did not seem to follow the overall trend of the other elements; therefore, it is believed that the absence of oxygen in the analysis may not have been the only contributor. Another contributor may be the presence of the neglected phases such as yellow, blue, and magenta. Recall that the red and green phases were assumed to be the dominant phases present in the fly ash under investigation due to their relatively high frequency of occurrence and so all other phases were neglected in the ARPI analysis. The presence of these neglected phases may appear when EDS is performed due to the large interaction volume of the beam. When the electron beam interacts with the sample it excites a volume much larger than the beam diameter itself, as shown in Figure 4, and information from this larger region is collected. Figure 58 shows the EDS analysis locations on the color segmented map of particle 2C. Notice how dispersed the yellow, blue, and magenta phases are around the analysis locations and in particle 2C in general.

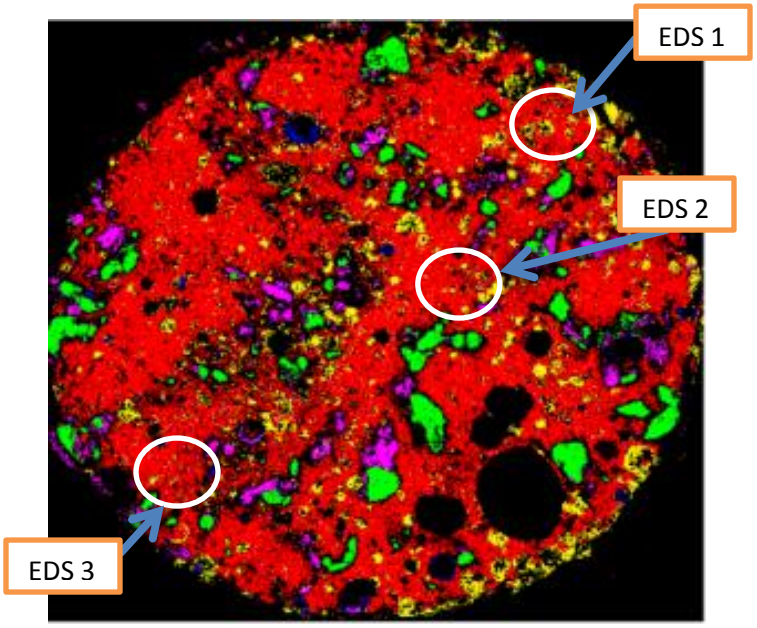

Figure 58: EDS locations for red phase for ARPI and SEDS correlation.

VERIFICATION OF RESULTS – PARTICLE 2C GREEN PHASE

Using the previously described method the normalized elemental concentrations for the ARPI defined green regions of particle 2C were determined and compared to the NIST SEDS results. Figure 59 shows the green region of particle 2C as defined by ARPI and the locations of EDS analysis. The results are presented in Table 6. The results are also presented as a scatter plot in Figure 60.

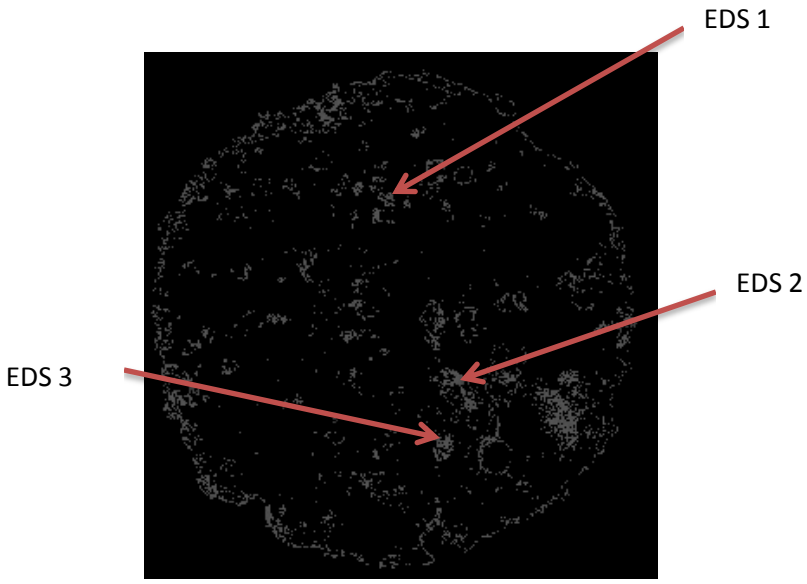

Figure 59: EDS location for ARPI defined green phase regions in 2C.

Table 6: Results of analyzing ARPI defined green regions of particle 2C.

Normalized Elemental Concentration For Green Regions As Determined By ARPI								
	"Mg"	"Al"	"Si"	"S"	"K"	"Ca"	"Ti"	"Fe"
%Weight	2.43	9.25	67.24	0.93	1.69	7.24	3.55	2.73
1σ	3.79	12.29	26.32	0.35	1.24	7.93	2.64	2.17
SEDS Results for the Green Phase in Particle 2C								
	"Mg"	"Al"	"Si"	"S"	"K"	"Ca"	"Ti"	"Fe"
weight %	0.42	1.81	58.98	0.35	0.34	3.47	0.62	3.58
1σ	0.50	1.93	9.99	0.74	0.55	3.88	1.15	4.46

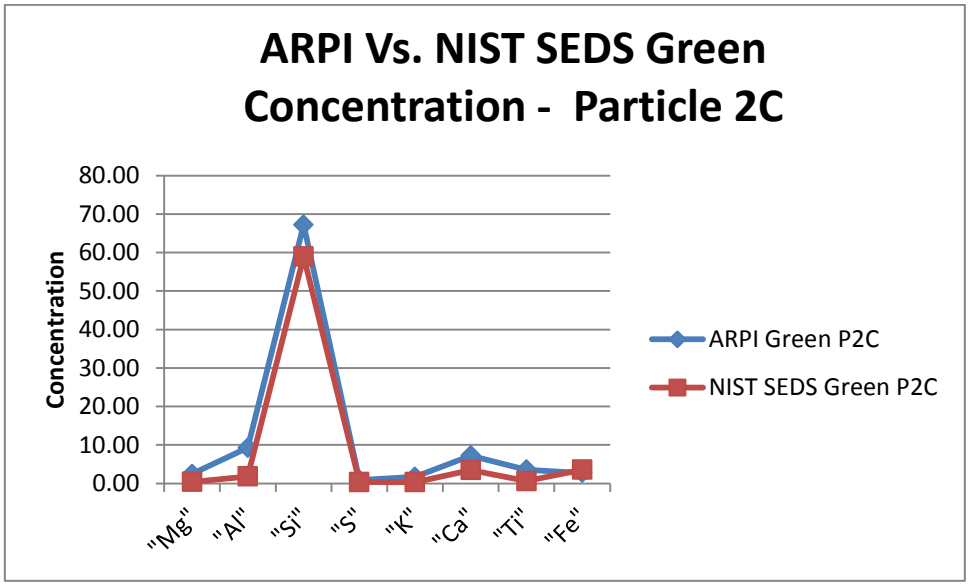

Figure 60: ARPI vs. SEDS Elemental Concentrations.

The normalized elemental concentrations for the regions defined as the green phase by ARPI correlate well with the results of the SEDS analysis. The uniform shift seen in the red phase is noticed yet again for the green phase. The absence of 30.43% oxygen in the normalized elemental concentration calculations is thought to have caused this. The results of the ARPI defined green region elemental concentration analysis for silicon, sulfur, calcium, and iron all fall within one standard deviation of the NIST SEDS results. Aluminum yet again showed a more significant increase in concentration. The relatively large interaction volume exciting surrounding phases that may not be characteristic to the green phase chemistry may have been the cause of this.

VERIFICATION OF RESULTS – SAMPLE PARTICLES RED PHASE

To further verify the accuracy of the technique developed in this research five particles were analyzed and the red regions were discovered using the red phase gray-scale threshold outputs from ARPI. These thresholds were used to view the red regions in each particle as defined by ARPI exclusively. Three points were analyzed for each particle for a total of fifteen points. The normalized elemental concentrations were calculated by averaging the results of all fifteen point analyses. Table 7 presents the results of the analysis and compares the data to the NIST SEDS results for particle 2C. Figure 61 illustrates the results as a scatter plot.

Table 7: Results of analyzing red regions as defined by Automated Rapid Particle Investigation of 5 sample particles.

Normalized Elemental Concentration For ARPI Defined Red Phase Regions of Sample Particles								
	"Mg"	"Al"	"Si"	"S"	"K"	"Ca"	"Ti"	"Fe"
weight %	4.23	14.35	24.20	0.75	1.47	39.42	4.59	9.36
1σ	2.27	7.12	17.39	0.40	1.04	16.35	1.96	5.07
SEDS Results for the Red Phase in Particle 2C								
	"Mg"	"Al"	"Si"	"S"	"K"	"Ca"	"Ti"	"Fe"
weight %	3.15	11.69	19.94	0.99	0.69	24.99	1.88	12.67
1σ	1.07	2.78	4.87	1.11	0.59	6.56	1.06	5.26

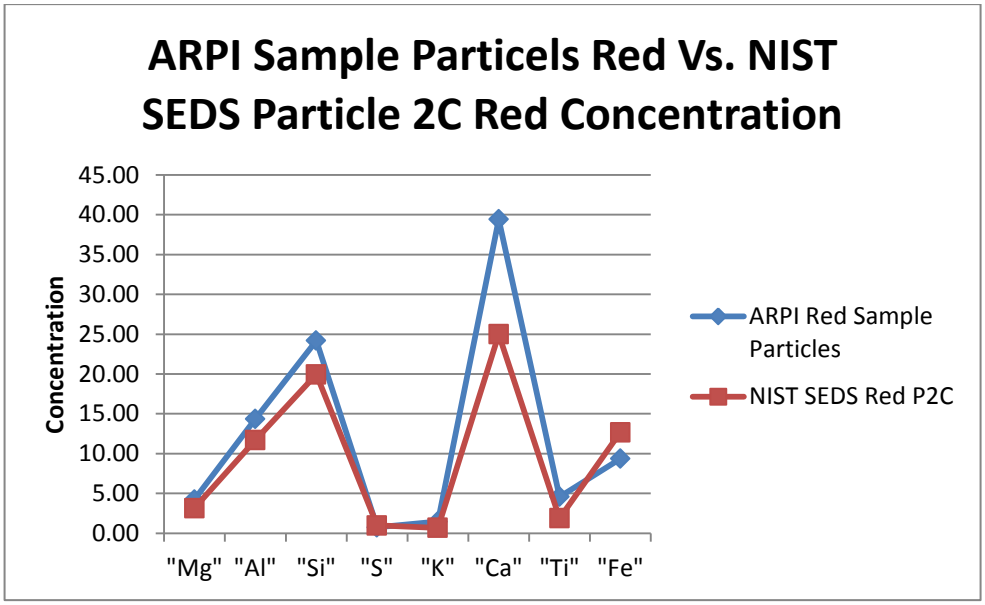

Figure 61: ARPI vs. NSIT SEDS for the red phase of sample particles.

The normalized elemental concentrations resulting from analyzing the ARPI defined red regions of five sample particles correlates well with the results from the NIST SEDS analysis of the red phase in particle 2C. Once again a fairly uniform upward shift is seen which is attributed to the redistribution of 24.00% oxygen content. The normalized elemental concentration of magnesium, aluminum, silicon, sulfur, and iron for ARPI defined red regions all fall within one standard deviation of the SEDS results for the red regions in particle 2C. The normalized elemental concentration for potassium, calcium, and titanium fall just outside of one standard deviation in the upward direction. It is believed that if the oxygen standard was available and included in the analysis these values would decrease and ultimately fall within the range of the NIST SEDS results.

VERIFICATION OF RESULTS – SAMPLE PARTICLES GREEN REGIONS

In order to further confirm the accuracy of the results of ARPI an attempt was made to investigate the ARPI defined green regions of the five sample particles. Due to the relatively small sized of the sample particles, diameter approximately equal to 12 µm, and resulting small regions defined as green no usable data could be collected by EDS. The large interaction volume of the electron beam with the sample caused the regions around the suspected green regions to emit information. This resulted in normalized elemental concentrations that strongly resembled the NIST SEDS red phase results due to the high presence of the red phase in the fly ash under investigation.

A discovery was made when investigating the ARPI defied green regions of particle 2C and the five sample particles. In all ARPI defined green region evaluations the boarder of the particle was defined as green. This seemed odd as this did not match the results of the NIST SEDS analysis for particle 2C. Figure 62 shows the green regions defined by NIST SEDS, the color segmented map, and the ARPI defined green regions for particle 2C.

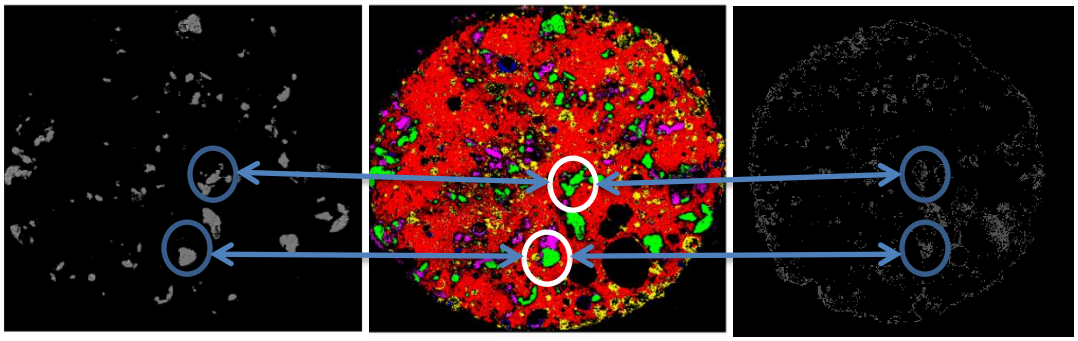

Figure 62: Green regions of particle 2C as defined by NIST SEDS analysis (Left), NIST SEDS color segmented map of particle 2C (center), ARPI defined green regions of particle 2C (Right).

Notice how the ARPI defined green regions of particle 2C included the boundary of the particle and is obviously incorrect in comparison to the NIST SEDS results. The cause of this is

the effect of pixel averaging. When transitioning from low gray-values as those of the epoxy background in the samples examined by this research to high gray-values as those of the red phase there is a transition between the two levels of gray values. This transition inevitably passes through the green range gray-scale chemical thresholds and produces an erroneous green phase shell around the particle. This is an issue that must be considered in the green phase results of this technique; however, it is thought that as the concentration of the green phase increases in a particle the effects of pixel averaging on the green phase results decreases. Figure 63 illustrates the concept of pixel averaging.

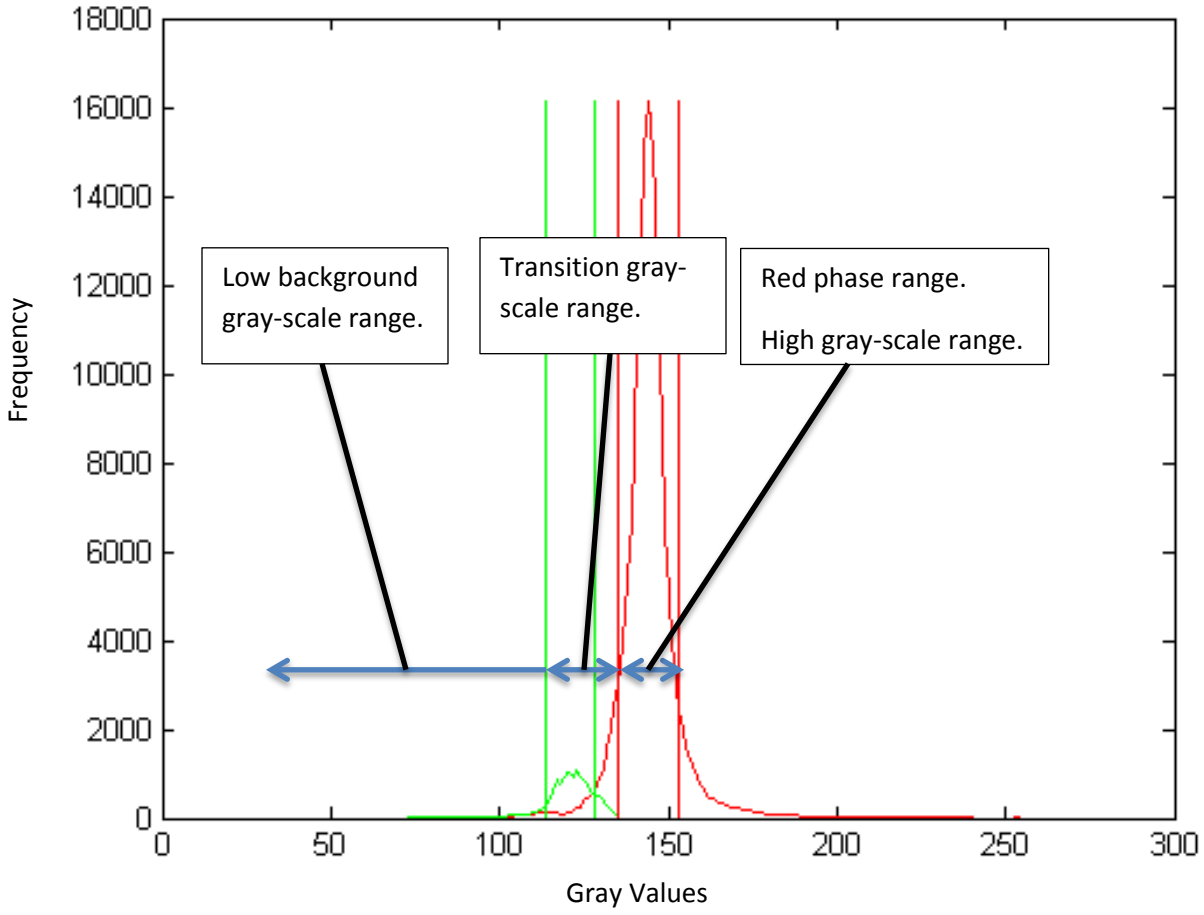

Figure 63: Illustration of the effects of pixel averaging.

VERIFICATION OF RESULTS – CONCLUSION

The fly ash under investigation is classified as an ASTM Class C fly ash and is dominated by the red chemical phase in the NIST SEDS analysis. The results of ARPI showed a strong correlation to the results of the red and green chemical phases' area percent on cross-section calculation from NIST SEDS analysis. The chemistry investigation verified that the regions defined by ARPI as having the red and green chemical characteristics were indeed the correct regions. The green regions of the sample particles provided no usable information as their cross-section diameters and corresponding green regions were too small to produce usable data due to the relatively large interaction volume of the electron beam. Pixel averaging was seen to be an issue in the results of the green phase as defined by ARPI.

CHAPTER VII

CONCLUSION

A method of rapid particle investigation of individual fly ash particles using scanning electron microscopy and image analysis has been described in detail. This method was referred to as Automated Rapid Particle Investigation (ARPI). A procedure for embedding fly ash particles in an epoxy puck, polishing the epoxy puck to reveal cross-sections of the embedded particles, creating BSE images of the particles using scanning electron microscopy, and analyzing the BSE images through image analysis to search for quality particles and further analyze these particles to quantitatively and qualitatively reveal the primary chemical composition of these particles has been developed. The accuracy of this technique was verified using EDS spot analysis and the results of ARPI were determined feasible.

ARPI was performed on a sample of BSE images and the results reflected the results of NIST SEDS analysis for the primary chemical phases present. The analysis of the sample BSE images proved this method reasonable. This is an initial attempt to qualitatively and quantitatively describe the chemical composition of individual fly ash particles in an automated rapid technique and some concerns were discovered. The effects of pixel averaging cause the results for the green phase in a red phase dominated particle to contain a certain amount of error. Further research on this topic needs to be conducted to develop a way to correct for the effects of pixel averaging. Future work should also consist of investigating a larger quantity of fly ash

particles both by ARPI and chemically to verify that ARPI produces accurate and repeatable results.

REFERENCES

Aboustait, M. (2013). Harrington Fly Ash Diameter Distribution. Unpublished Data.

ASPEX. (2007). Automated Feature Analysis for Perception: User Documentation. United States of America: ASPEX, LLC.

ASTM Standard C618. (2012). Standard Specification for Coal Fly Ash and Raw or Calcined Natural Pozzolan for Use in Concrete. Annual Book of ASTM Standards. West Conshohocken, PA: ASTM International.

ASTM Standard C114. (2011). Standard Test Methods for Chemical Analysis of Hydraulic Cement. Annual Book of ASTM Standards. West Conshohocken, PA: ASTM International.

Chancey, R. T. (2008). Characterization of Crystalline and Amorphous Phases and Respective Reactivities in a Class F Fly Ash. (Unpublished doctoral dissertation). University of Texas, Austin Texas.

Goldstein, J.,, Newbury, D., Joy, D., Lyman, C., Echlin, P., Lifshin, E., . . .Michael, J. (2003). *Scanning Electron Microscopy and X-Ray Microanalysis*. 3rd ed. United States of America: Springer Science+Business Media, Inc.

Gonzalez, R. C., & Woods, R. E. (2008). *Digital Image Processing*. 3rd Edition. Upper Saddle River, New Jersey: Pearson Prentice Hall.

Helmuth, R. (1987). *Fly Ash in Cement and Concrete* .United States of America: Portland Cement Association.

Hu, Q., Ley, M. T., Davis, J., Hanan, J. C., Frazier, R., & Zhang. (2013). 3D chemical segmentation of fly ash particles with X-ray computed tomography and electron probe microanalysis. Fuel, 116, 229-236.

Kosmatka, S. H., Kerkhoff, B., Panarese W.C.(2008). *Design and Control of Concrete Mixtures*. United States of America: Portland Cement Association.

Malhotra, M. (2001). *Seventh CANMET/ACI International Conference on Fly Ash, Silica Fume, Slag and Natural Pozzolans in Concrete*. V ed. Vol. 2.

Malhotra, M. (2004). *Eighth CANMET/ACI International Conference on Fly Ash, Silica Fume, Slag and Natural Pozzolans in Concret*. V. ed.

Malhotra, M. (1989). *Fly Ash, Silica Fume, Slag and Natural Pozzolans in Concrete*, Proceedings Third International Conference Tron`dheim. Normway. V. ed.

Malhotra, V. M., Ramezanianpour, A. A. (1994). *Fly Ash in Concrete*. 2nd Edition. Canada: Minister of Supply and Services.

Mehta, P. K., Monteiro, P. J. (2006). *Concrete: Microstructure, Properties, and Materials.* 3rd Edition. United States of America: The McGraw-Hill Companies.

Thomas, M. (2007). Optimizing the Use of Fly Ash in Concrete. Concrete. Portland Cement Association.

APPENDICES

APPENDIX A

Segmented EDS (SEDS) Analysis

SEGMENTED EDS ANALYSIS

Figure 8 shows the BSE and raw elemental maps, derived based on raw elemental counts, produced by Electron Probe Microanalysis (EPMA) which uses the same technology as Scanning Electron Microscopes (SEM). Once this initial data set has been produced with EPMA it is desired to analyze the data to find compositionally distinct regions within the particle. In order to do this the x-ray spectral data collected by EPMA is converted into compositional data using DTSA II and a suite of pure elemental and mixed compositional standards. An unsupervised clustering technique known as ISO Means is used to perform multivariable statistics on the data set to find these distinct regions. Multivariable statistics is the idea of simultaneously observing and analyzing multiple outcomes and variables. ISO Means identifies compositionally distinct areas by the use of principle components and k-means clustering as well as in-class statistical controls. K-means acts to portion information into "k" clusters by assigning observations to clusters with the nearest mean value. An in-class statistical control is the technique of separating out the effects of one component from the effects of all other components and is used in multivariable analyses. Once all compositionally distinct areas are found each region is assigned a color as in the top right image of Figure 8.

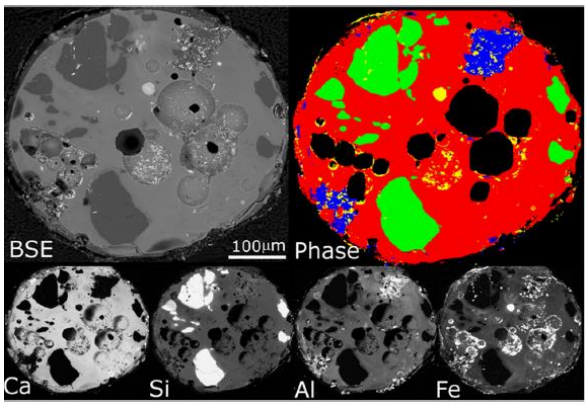

Figure 8: BSE image of particle 1C used for the Segmented EDS Analysis (Top Left). Gray-scale x-ray map images for particle 1C used for Segmented EDS Analysis (Bottom). Color segmentation of particle 1C produce by Segmented EDS Analysis (Top Right) (Hu et al., 2013).

APPENDIX B

(Matlab algorithm)

```
%Automated Rapid Particle Investigation
%1) Transform NIST BSE gray-scale histogram to OSU BSE gray-scale
histogram
a=imread('NIST.BMP'); %Particle to be transformed_NIST'.
AA=a; %Rename image a to AA.
b=imread('OSU.tif'); %Particle to be matched_OSU.
particle_a=a>0;%Background clipping value for NIST BSE.
[L num]=bwlabel(particle_a);%Labels disconnected features.
L(L~=L(round(size(L,1)/2),round(size(L,2)/2)))=0;%Sets all but largest
%label to 0.
particle_a(L==0)=0;%Sets all regions in image particle_a to 0 if label
is 0
particle_a=imfill(particle_a,'holes');%restores gray values in largest
%particle.
a(particle_a==0)=0;%Set regions to 0 in image a that are 0 in
particle_a.

ao=a;%Renames image a to ao which is NIST bakcground clipped.
particle_b=b>110;%Background clipping value for OSU BSE.
[L num]=bwlabel(particle_b);
L(L~=L(round(size(L,1)/2),round(size(L,2)/2)))=0;
particle_b(L==0)=0;
particle_b=imfill(particle_b,'holes');
b(particle_b==0)=0;

apixel=a(particle_a>0);%Rename image a to apixel.
bpixel=b(particle_b>0);%Rename image b to bpixel.
apixel_match=histeq(apixel,imhist(bpixel));%Equilize histograms
a(particle_a>0)=apixel_match;%Trnasform histogram a.

%2) Find the gray-scale range for each color in the segmented EDS
%(Color Segmentation Program)
bse=a;%NIST transformed image from transformation.
eds=imread('EDS.BMP');%Open NIST Segmented EDS color map.
eds=eds(:,:,1:3);%Chose first three color layers
rlay=eds(:,:,1); %Red layer in eds image
glay=eds(:,:,2); %Green layer in eds image
blay=eds(:,:,3); %Blue layer in eds image
mag=rlay>150 & blay>150;%Magenta is a combo of red and blue
yel=rlay>150 & glay>150;%Yellow is a combo of red and green
red=((rlay>150)-(mag>0)-(yel>0));%Red is the red layer minus mag and
yellow
green=((glay>150)-(yel>0));%Green is the green layer minus yellow
blue=((blay>150)-(mag>0));%Blue is the blue layer minus magenta
b_mag=bse;%(!)Rename the transformed NIST BSE image as b_mag
b_mag(mag==0)=0;%($)Set all gray values to 0 in the b_mag BSE image
that
%are 0 in the magenta EDS image
b_yel=bse;                              % (!)
b_yel(yel==0)=0;                        % ($)
b_red=bse;                              % (!)
b_red(red==0)=0;                        % ($)
b_green=bse;                            % (!)
b_green(green==0)=0;                    % ($)
```

```
b_blue=bse;                                % (!)
b_blue(blue==0)=0;                         % ($)

%Normalized Histograms
hred=imhist(b_red);hred(1)=0;%Create histogram of red phase
hred=smooth(hred/sum(hred));%Normalize red histogram
mean_red=find(b_red>0);%The following five line create one std dev
mean_red=b_red(mean_red);
var_red=var(double(mean_red));
std_red=sqrt(var_red);
mean_red=mean(mean_red);

%Green Shelf Evaluation (Clip the shelf in the green histogram)
C=133%Gray value clip (Must be reevaluated if the transformation
particles
%change)
right=b_green%Rename b_green to right
right=b_green>C%Create an image of the green layer that only shows gray
%values >C
b_right=bse%Rename BSE image to b_right
b_right(right==0)=0;%Set all areas in BSE = 0 that are zero in previous
%b_right image
b_left=b_green-b_right;%Creat gray value image less than the cut off
hgreen=imhist(b_left);hgreen(1)=0;%Create histogram of green phase
hgreen=smooth(hgreen/sum(hgreen))%Normalize green histogram
mean_green=find(b_left>0);%The following lines create one std dev
mean_green=b_left(mean_green);
var_green=var(double(mean_green));
std_green=sqrt(var_green);
mean_green=mean(mean_green);

hyel=imhist(b_yel);hyel(1)=0;%Creat yellow histogram
hyel=smooth(hyel/sum(hyel));%Normalize yellow histogram
mean_yel=find(b_yel>0);%The following five line create one std dev
mean_yel=b_yel(mean_yel);
var_yel=var(double(mean_yel));
std_yel=sqrt(var_yel);
mean_yel=mean(mean_yel);


hmag=imhist(b_mag);hmag(1)=0;%Create magenta histogram
hmag=smooth(hmag/sum(hmag));%Normalize magenta histogram
mean_mag=find(b_mag>0);%The following five line create one std dev
mean_mag=b_mag(mean_mag);
var_mag=var(double(mean_mag));
std_mag=sqrt(var_mag);
mean_mag=mean(mean_mag);


hblue=imhist(b_blue);hblue(1)=0;%Create blue histogram
hblue=smooth(hblue/sum(hblue));%Normalize Blue histogram
mean_blue=find(b_blue>0);%The following five line create one std dev
mean_blue=b_blue(mean_blue);
var_blue=var(double(mean_blue));
```

```
std_blue=sqrt(var_blue);
mean_blue=mean(mean_blue);

%3)Start of finding particles in a data set (Run through all fiild
images
%and analyze the data)

t=1;%Operator used to name each individual particle found
PS=.316396%Pixels size in micron - value found in details of AFA stage
%field properties
Allhistogram=[];%Create blank matrix file to store all hitograms for
%individual particles
for Part=678:727%Open each filed image individually
gg=strcat('Field',num2str(Part),'.TIF');%Rename the field image to "gg"
%for ease of programming
a=imread(gg);%Open the field image as image "a"
A=a>93;%Turn all regions with gray value <=93 black in the original
image
%(Reevaluate per data set)
e=fspecial('disk',2)>0;%Sets up a parameter used to clean up the labels
bound=zeros(size(a));%The next 5 line define a boarder of the image
bound(1,:)=1;
bound(end,:)=1;
bound(:,1)=1;
bound(:,end)=1;
A=imclose(A,e);%This causes pixels within 2 pixels of one another to
%combine. (Cleans up the disconnected regions)
[L num]=bwlabel(A);%Labels all disconneted regions
AA=uint8(zeros(size(A)));
for i=1:num%Loop through all labels
    C=L==i;%Name label i to C
    overlay=C & bound;%Define a variable that is a combinations of
label C
    %and the boundary
    if sum(overlay(:))>0;%Add up the pixels that are a combination of C
and
        %the boundary and see if it exist
        L(L==i)=0;%If the combination of C and the boundary exist then
turn
        %lable C to black
    elseif sum(C(:))<500%If label C has less than 500 pixels then turn
        %label C black (Next line turns it black)
        L(L==i)=0;
    else
        [I J]=find(C>0);%The next 10 lines set up the eigen value
problem
        %that allows us to compare the major axis to the minor axis in
        %order to check if circular
        Coord=[I,J];
        Cen=sum(Coord,1)/size(Coord,1);
        Coord(:,1)=Coord(:,1)-Cen(1);
        Coord(:,2)=Coord(:,2)-Cen(2);
        S=Coord'*Coord;
        S=S/size(Coord,1);
        [V D]=eig(S);
        D=diag(D);
```

```
        Rat=D(2)/D(1);
        if Rat>1.5;%If the major to minor axis eigenvalue is greater
than
            %1.5 than turn black (The next line turns the label black)
              L(L==i)=0;

        end
    end
end
            aa=a;%Rename image "a" to "aa"
            aa(L==0)=0;%Turn all regions in the original image black
that
            %were turned black through the preceeding filtering process
            [I J]=find(L>0);%Create a matrice image of remaining labels
            gg=strcat('p',num2str(t),'.bmp');%Number each individual
            %particle image
            Win=aa(min(I):max(I),min(J):max(J));%Create window of size
            %custom to each individual label.
            Sw=size(Win);%Stores the height and width of the custom
image
            Aw=Win>0;%Views each particle in the custom images
            ratiow=sum(Aw(:))/(Sw(1)*Sw(2));%Percent the particle
occupies
            %in the custom image.
            S1=Sw(1)%Number of pixles horizontally
            S2=Sw(2)%Number of pixles vertivally
            Diameter(t)=(S1+S2)/2*PS %Diameter of the particle cross-
sect
            %calculated by the average size of the custom image
            SF=2*S1+2*S2-4 %The total number of pixles that make up the
            %image boarder
            Border=zeros(size(Win));%creat a blank image Border with
the
            %same size as a,we start to fill in border pixel in this
image.
            for i=1:Sw(1)%check each row for every column, next line
                C=find(Aw(i,:)>0);
                if ~isempty(C)%if C is not empty
                Max=max(C);Min=min(C);%find the border pixels in row i
                Border(i,Max)=1;%far side pixel
                Border(i,Min)=1;%near side pixel
                end
            end
            for j=1:Sw(2)%Same procedure as previous 8 lines but for
column
                C=find(Aw(:,j)>0);
                if ~isempty(C)
                Max=max(C);Min=min(C);
                Border(Max,j)=1;
                Border(Min,j)=1;
                end
            end
            b=Border%Create an image b that just shows the boarder
            hb=imhist(b);hb(1)=0;%Create a histogram of image b
            Sum_Boarder=sum(hb)%Find the number of pixles in image b
with
```

```
            %gray value > 0
            Boarder_Ratio=Sum_Boarder/SF %Ratio of particle boarder
pixles
            %to image boarder pixles


                if ratiow>0.65%If particle occupies greater than 65% of
                    %custom image then continue
                    if Boarder_Ratio<0.80%If particle boarder is less
than
                        %80% of the custom image boarder than continue.
                    h=imhist(Win);h(1)=0;%Create histogram of
Individual
                    %particle
                    h=h/sum(h);%Normalize individual particle histogram
                    Allhistogram=[Allhistogram;h'];%Fill in each row
with
                    %frequency values for individual particle
                    mean_h=find(Win>0);%The following 23 lines create
one
                    %std dev for individual particle histograms and
plots
                    %the color segmentation histograms as a comparison
                    mean_h=Win(mean_h);
                    var_h=var(double(mean_h));
                    std_h=sqrt(var_h);
                    mean_h=mean(mean_h);

                figure,plot(h(2:255));%The following 19 lines of code
Plot
                %individual particle histogram w/ the color
segmentation
                line([mean_red-std_red mean_red-std_red],[0
max(hred(2:end))],'color','red');
                line([mean_red+2*std_red mean_red+2*std_red],[0
max(hred(2:end))],'color','red');
                line([mean_green-std_green mean_green-std_green],[0
max(hred(2:end))],'color','green');
                line([mean_green+std_green mean_green+std_green],[0
max(hred(2:end))],'color','green');

                    AA(min(I):max(I),min(J):max(J))=Win;
                    imwrite(Win,gg);%Save individual images of each
                    %accepted particle
                    t=t+1;%Increse the particle number by one in order
to
                    %prepare to save the next particle found
                    end
                end

if sum(AA(:))==0;%If no particles in field image then delete image
delete(gg)
end
end
%%%%
```

```
red_range=[mean_red-std_red,mean_red+2*std_red];%Define red range
green_range=[mean_green-std_green,mean_green+std_green]%Define green
range
if red_range(1)<green_range(2)%Check for overlaping ranges
    R=red_range(1);
    red_range(1)=green_range(2);
    green_range(2)=R;
    mix_range=[green_range(2) red_range(1)];
else
    mix_range=[green_range(2) red_range(1)];
end
if floor(green_range(2))==floor(red_range(1))
    red_range(1)=red_range(1)+1;
end
green=sum(Allhistogram(:,floor(green_range(1)):floor(green_range(2))),2
);
%Percent of green phase in individual particle
red=sum(Allhistogram(:,floor(red_range(1)):floor(red_range(2))),2);
%Percent of red phase in individual particle
if (mix_range(2)-mix_range(1))>1;
mix=sum(Allhistogram(:,floor(mix_range(1)):floor(mix_range(2))),2);
%Percent of mixture in individual particle
else
mix=zeros(size(Allhistogram,1),1);
%If no mix then 0% mixture in individual particle
end
RESULT=[green,red,mix];%Plot results
```

VITA

Jerod Laurence Wilkins

Candidate for the Degree of

Master of Science

Thesis: AUTOMATED RAPID PARTICLE INVESTIGATION USING SCANNING ELECTRON MICROSCOPY

Major Field: Civil Engineering

Biographical:

Education:

Completed the requirements for the Master of Science in Civil Engineering, Magna Cum Lade, at Oklahoma State University, Stillwater, Oklahoma in December, 2013.

Completed the requirements for the Bachelor of Science in Civil Engineering, Magna Cum Lade, at Oklahoma State University, Stillwater, Oklahoma in December, 2013.

Experience: Employed by the Oklahoma Department of Transportation as Roadway Designer, Bridge Designer, and Construction inspector, July 2006 to Present. Employed by Oklahoma State University, College of Engineering Architecture and Technology as Teaching Assistant, 2011. Employed by Oklahoma State University, College of Civil Engineering as Teaching Assistant, 2011. Employed by Oklahoma State University College of Civil Engineering as Research Assistant, 2011 to 2013.

Professional Membership: American Institute of Steel Construction, American Concrete Institute, Institute of Transportation Engineers, Golden Key National Honor Society, Chi Epsilon Honor Society, and Phi Kappa Phi National Honor Society.